



HAL
open science

The specificity of pectate lyase VdPelB from *Verticillium dahliae* is highlighted by structural, dynamical and biochemical characterizations

Josip Safran, Vanessa Ung, Julie Bouckaert, Olivier Habrylo, Roland Molinié, Jean-Xavier Fontaine, Adrien Lemaire, Aline Voxeur, Serge Pilard, Corinne Pau-Roblot, et al.

► To cite this version:

Josip Safran, Vanessa Ung, Julie Bouckaert, Olivier Habrylo, Roland Molinié, et al.. The specificity of pectate lyase VdPelB from *Verticillium dahliae* is highlighted by structural, dynamical and biochemical characterizations. *International Journal of Biological Macromolecules*, 2023, pp.123137. 10.1016/j.ijbiomac.2023.123137 . hal-03947228v1

HAL Id: hal-03947228

<https://u-picardie.hal.science/hal-03947228v1>

Submitted on 2 Nov 2023 (v1), last revised 6 Nov 2023 (v2)

HAL is a multi-disciplinary open access archive for the deposit and dissemination of scientific research documents, whether they are published or not. The documents may come from teaching and research institutions in France or abroad, or from public or private research centers.

L'archive ouverte pluridisciplinaire **HAL**, est destinée au dépôt et à la diffusion de documents scientifiques de niveau recherche, publiés ou non, émanant des établissements d'enseignement et de recherche français ou étrangers, des laboratoires publics ou privés.



Distributed under a Creative Commons Attribution 4.0 International License

International Journal of Biological Macromolecules

The specificity of pectate lyase VdPelB from *Verticillium dahliae* is highlighted by structural, dynamical and biochemical characterizations

--Manuscript Draft--

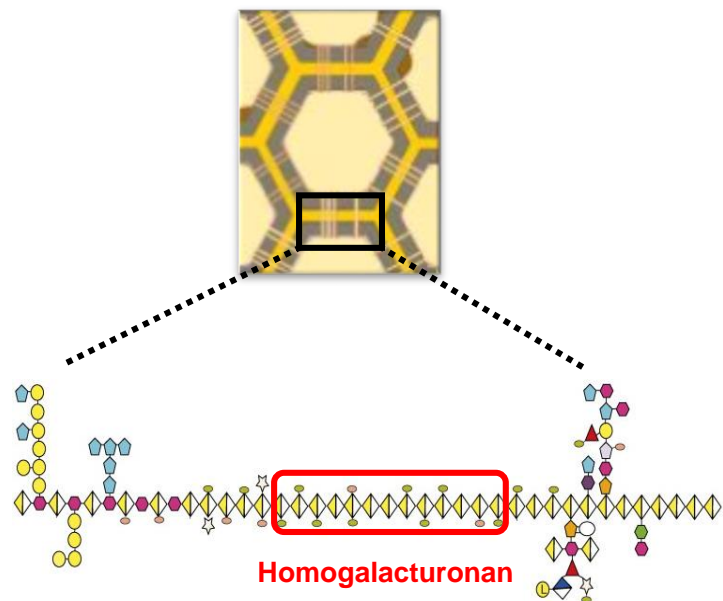
Manuscript Number:	IJBIMAC-D-22-10686R1
Article Type:	Research Paper
Section/Category:	Proteins and Nucleic acids
Keywords:	pectins; pectate lyase; <i>Verticillium dahliae</i>
Corresponding Author:	Fabien Sénéchal, Ph.D UMR1158: Transfrontaliere BioEcoAgro Amiens, FRANCE
First Author:	Josip Safran, Ph.D
Order of Authors:	Josip Safran, Ph.D Vanessa Ung Julie Bouckaert, Ph.D Olivier Habrylo, Ph.D Roland Molinié, Ph.D Jean-Xavier Fontaine, Ph.D Adrien Lemaire Aline Voxeur, Ph.D Serge Pilard, Ph.D Corinne Pau-Roblot, Ph.D Davide Mercadante, Ph.D Jérôme Pelloux, Pr. Fabien Sénéchal, Ph.D
Abstract:	<p>Pectins, complex polysaccharides and major components of the plant primary cell wall, can be degraded by pectate lyases (PLs). PLs cleave glycosidic bonds of homogalacturonans (HG), the main pectic domain, by β-elimination, releasing unsaturated oligogalacturonides (OGs). To understand the catalytic mechanism and structure/function of these enzymes, we characterized VdPelB from <i>Verticillium dahliae</i>. We first solved the crystal structure of VdPelB at 1.2Å resolution showing that it is a right-handed parallel β-helix structure. Molecular dynamics (MD) simulations further highlighted the dynamics of the enzyme in complex with substrates that vary in their degree of methylesterification, identifying amino acids involved in substrate binding and cleavage of non-methylesterified pectins. We then biochemically characterized wild type and mutated forms of VdPelB. Pectate lyase VdPelB was most active on non-methylesterified pectins, at pH8.0 in presence of Ca²⁺ ions. The VdPelB-G125R mutant was most active at pH9.0 and showed higher relative activity compared to native enzyme. The OGs released by VdPelB differed to that of previously characterized PLs, showing its peculiar specificity in relation to its structure. OGs released from <i>Verticillium</i>-partially tolerant and sensitive flax cultivars differed which could facilitate the identification VdPelB-mediated elicitors of defence responses.</p>
Suggested Reviewers:	Mirjam Czjzek Biological Research Station Roscoff czjzek@sb-roscoff.fr Estelle Bonnin Biopolymers Interactions Assemblies Research Unit estelle.bonnin@inrae.fr

	Suzanna Saez-Aguayo Andrés Bello University susana.saez@unab.cl
Opposed Reviewers:	
Response to Reviewers:	

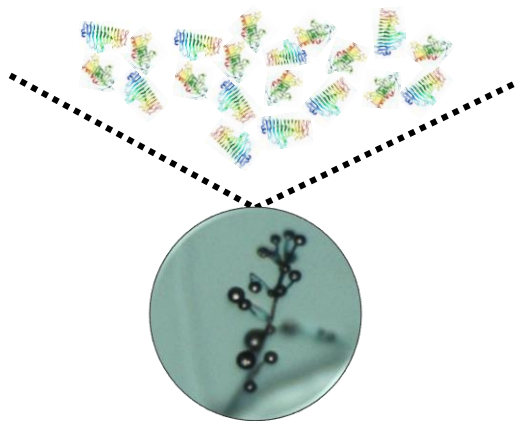
Highlights

- First crystallographic structure of *Verticillium* pectate lyase.
- Identification of key amino-acids for the activity
- Biochemical characterization of the enzyme and LC-MS/MS analysis of the oligogalacturonides (OG) produced
- Susceptible or partially resistant flax cultivars differ in OGs produced

PRIMARY CELL WALL

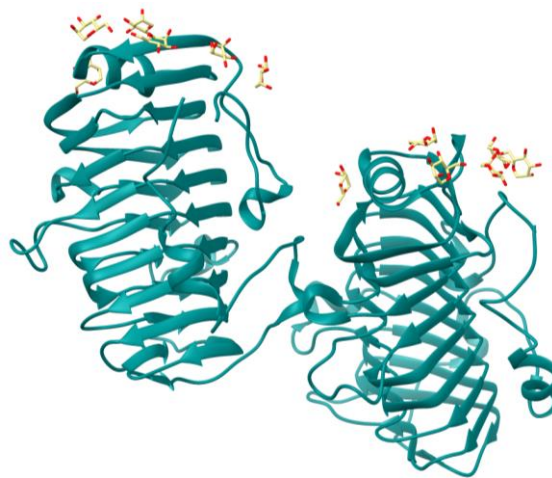


Pectate lyase like (PLLs) degrading enzymes

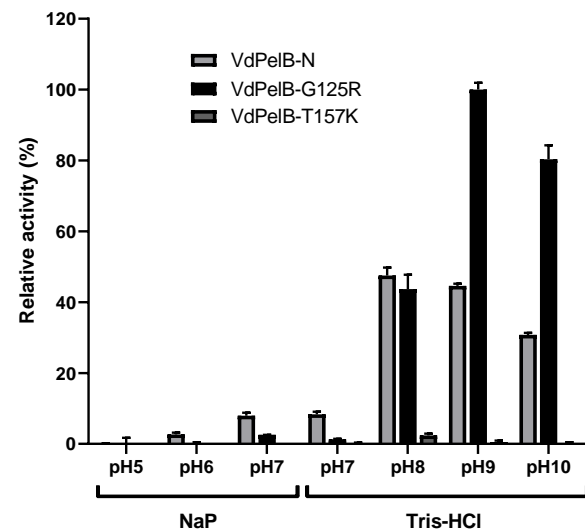


VERTICILLIUM DAHLIAE

VdPeIB CRYSTAL STRUCTURE

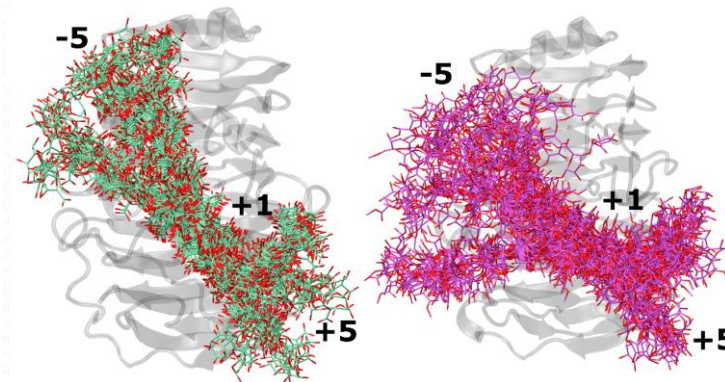


BIOCHEMICAL CHARACTERIZATION

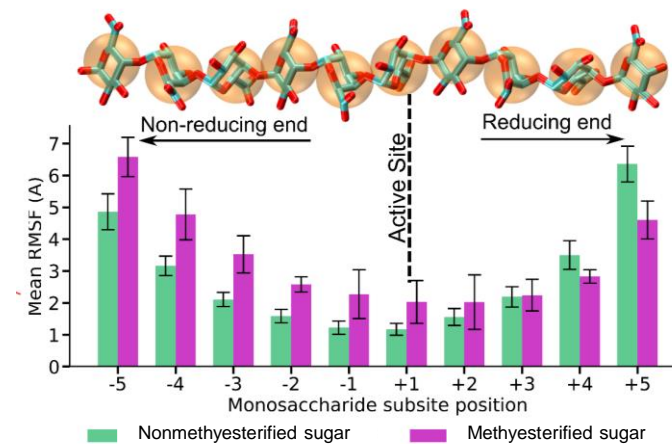


MD SIMULATIONS

VdPeIB substrate dynamics



RMSF analysis



Declaration of interests

The authors declare that they have no known competing financial interests or personal relationships that could have appeared to influence the work reported in this paper.

The authors declare the following financial interests/personal relationships which may be considered as potential competing interests:

Safran Josip reports financial support was provided by Conseil Régional Hauts-de-France. Safran Josip reports financial support was provided by Fonds européen de développement régional.

Abstract

Pectins, complex polysaccharides and major components of the plant primary cell wall, can be degraded by pectate lyases (PLs). PLs cleave glycosidic bonds of homogalacturonans (HG), the main pectic domain, by β -elimination, releasing unsaturated oligogalacturonides (OGs). To understand the catalytic mechanism and structure/function of these enzymes, we characterized VdPelB from *Verticillium dahliae*. We first solved the crystal structure of VdPelB at 1.2Å resolution showing that it is a right-handed parallel β -helix structure. Molecular dynamics (MD) simulations further highlighted the dynamics of the enzyme in complex with substrates that vary in their degree of methylesterification, identifying amino acids involved in substrate binding and cleavage of non-methylesterified pectins. We then biochemically characterized wild type and mutated forms of VdPelB. Pectate lyase VdPelB was most active on non-methylesterified pectins, at pH8.0 in presence of Ca^{2+} ions. The VdPelB-G125R mutant was most active at pH9.0 and showed higher relative activity compared to native enzyme. The OGs released by VdPelB differed to that of previously characterized PLs, showing its peculiar specificity in relation to its structure. OGs released from *Verticillium*-partially tolerant and sensitive flax cultivars differed which could facilitate the identification VdPelB-mediated elicitors of defence responses.

Keywords: Pectate lyase, pectins, homogalacturonan, oligogalacturonides, *Verticillium dahliae*.

1 **The specificity of pectate lyase VdPelB from *Verticillium dahliae* is highlighted by**
2 **structural, dynamical and biochemical characterizations**

3

4 Josip Safran¹, Vanessa Ung², Julie Bouckaert³, Olivier Habrylo¹, Roland Molinié¹, Jean-Xavier
5 Fontaine¹, Adrien Lemaire¹, Aline Voxeur⁴, Serge Pilard⁵, Corinne Pau-Roblot¹, Davide
6 Mercadante², Jérôme Pelloux^{1*}, Fabien Sénéchal^{1*}

7

8

9 ¹ : UMRT INRAE 1158 BioEcoAgro – BIOPI Biologie des Plantes et Innovation, Université
10 de Picardie, 33 Rue St Leu, 80039 Amiens, France. ² : School of Chemical Sciences, The
11 University of Auckland, Private Bag 92019, Auckland 1142, New Zealand. ³ : UMR 8576
12 Unité de Glycobiologie Structurale et Fonctionnelle (UGSF) IRI50, Avenue de Halley, 59658
13 Villeneuve d'Ascq, France. ⁴ : Université Paris-Saclay, INRAE, AgroParisTech, Institut Jean-
14 Pierre Bourgin (IJPB), 78000, Versailles, France. ⁵ : Plateforme Analytique, Université de
15 Picardie, 33, Rue St Leu, 80039 Amiens, France.

16 *contributed equally as last authors

17 **Corresponding author:** Fabien Sénéchal (fabien.senechal@u-picardie.fr) and Jérôme Pelloux
18 (jerome.pelloux@u-picardie.fr)

19 UMR INRAE 1158 BioEcoAgro-Biologie des Plantes et Innovation, Université de Picardie
20 Jules Verne, UFR des Sciences, 33 Rue St Leu, 80039 Amiens, France

21

22 **Abstract**

23 Pectins, complex polysaccharides and major components of the plant primary cell wall, can be
24 degraded by pectate lyases (PLs). PLs cleave glycosidic bonds of homogalacturonans (HG), the
25 main pectic domain, by β -elimination, releasing unsaturated oligogalacturonides (OGs). To
26 understand the catalytic mechanism and structure/function of these enzymes, we characterized
27 VdPelB from *Verticillium dahliae*. We first solved the crystal structure of VdPelB at 1.2Å
28 resolution showing that it is a right-handed parallel β -helix structure. Molecular dynamics (MD)
29 simulations further highlighted the dynamics of the enzyme in complex with substrates that
30 vary in their degree of methylesterification, identifying amino acids involved in substrate
31 binding and cleavage of non-methylesterified pectins. We then biochemically characterized
32 wild type and mutated forms of VdPelB. Pectate lyase VdPelB was most active on non-
33 methylesterified pectins, at pH8.0 in presence of Ca^{2+} ions. The VdPelB-G125R mutant was
34 most active at pH9.0 and showed higher relative activity compared to native enzyme. The OGs
35 released by VdPelB differed to that of previously characterized PLs, showing its peculiar
36 specificity in relation to its structure. OGs released from *Verticillium*-partially tolerant and
37 sensitive flax cultivars differed which could facilitate the identification VdPelB-mediated
38 elicitors of defence responses.

39

40

41

42 **Keywords:** Pectate lyase, pectins, homogalacturonan, oligogalacturonides, *Verticillium*
43 *dahliae*.

44

45 1. Introduction

46 Primary cell wall, a complex structure of proteins and polysaccharides, cellulose and
47 hemicelluloses, is embedded in a pectin matrix. Pectins, are complex polysaccharides
48 composing up to 30% of cell wall dry mass in dicotyledonous species [1]. Pectin is mainly
49 constituted of homogalacturonan (HG), rhamnogalacturonan I (RG-I) and rhamnogalacturonan
50 II (RG-II) domains, but its composition can differ between plant organs and among species.
51 The most abundant pectic domain is HG, a linear homopolymer of α -1,4-linked galacturonic
52 acids (GalA), which represents up to 65% of pectins [2]. During synthesis, HG can be O-
53 acetylated at O-2 or O-3 and/or methylesterified at C-6 carboxyl, before being exported at the
54 cell wall with a degree of methylesterification (DM) of ~80% and a degree of acetylation (DA)
55 of ~5-10%, depending on species [3]. At the wall, HG chains can be modified by different
56 enzyme families, including pectin acetyltransferase (PAEs; EC 3.1.1.6), pectin methylesterases
57 (PMEs; CE8, EC 3.1.1.11), polygalacturonases (PGs; GH28, EC 3.2.1.15, EC 3.2.1.67, EC
58 3.2.1.82), and pectin lyases-like (PLLs), which comprise pectate lyases (PLs; EC 4.2.2.2) and
59 pectin lyase (PNLs, EC 4.2.2.10). All these enzymes are produced by plants to fine-tune pectin
60 during development [4–8], but they are also secreted by most phytopathogenic bacteria and
61 fungi during plant infection [9–13]. PMEs and PAE hydrolyse the O6-ester and O2-acetylated
62 linkages, respectively, leading to a higher susceptibility of HG to PG- and PLL-mediated
63 degradation [14]. PLL are pectolytic enzymes that cleave HG via a β -elimination mechanism
64 leading to the formation of an unsaturated C4-C5 bond [15], and can be divided into two
65 subfamilies depending on their biochemical specificities: i) PLs have a high affinity for non- or
66 low-methylesterified pectins and an optimal pH near 8.5. Their activity requires Ca^{2+} ions. ii)
67 PNLs are most active on high-DM pectins at acidic pH values [16]. Both type of enzymes can
68 degrade HG chains, and release oligogalacturonides (OGs), but their mode of action can differ.
69 For PLs both endo and exo modes of action have been described, while only endo-PNL have
70 been characterised so far [17]. For the latter, it was notably shown that endo-PNLs from *B.*
71 *fuckeliana*, *A. parasiticus* and *Aspergillus* sp., can first release OGs with degrees of
72 polymerisation (DP) 5–7, that are subsequently used as substrates, generating OGs of DP3 and
73 DP4 as end-products [9,18,19]. Despite having the same DP, the final products can differ in
74 their degrees and patterns of methylesterification and acetylation (DM/DA) depending on the
75 enzymes' specificities; implying potential differences in substrate binding, and therefore in
76 PLLs fine structures. Several crystallographic structures of bacterial and fungal PLL have been
77 reported [15,20–24]. Overall, the PLL fold resemble that of published PME, PGs and

78 rhamnogalacturonan lyases [25–27], and is composed of three parallel β -sheets forming a right-
79 handed parallel β -helix. The three β -sheets are called PB1, PB2 and PB3 and the turns
80 connecting them T1, T2 and T3 [28]. The active site features three Asp, localized on the PB1
81 β -sheet and, in the case of PLs, accommodates Ca^{2+} [29]. In PNLs, Ca^{2+} is, on the other hand,
82 replaced by Asp [15]. Additionally, the PL binding site is dominated by charged acidic and
83 basic residues (Gln, Lys, Arg) which can accommodate negatively charged pectate substrates.
84 In contrast, the PNL binding site is dominated by aromatic residues [15,29], which have less
85 affinity for lowly methylesterified pectins. These differences in structure could translate into
86 distinct enzyme dynamics when in complex with substrates of varying degrees of
87 methylesterification.

88 In fungi, PLLs are encoded by large multigenic families which are expressed during
89 infection. *Verticillium dahliae* Kleb., a soil-borne vascular fungus, targets a large number of
90 plant species, causing Verticillium wilt disease to become widespread among fiber flax, with
91 detrimental effects to fiber quality [30–32]. *V. dahliae* infects plants by piercing the root surface
92 using hyphae. When Verticillium reaches the vascular tissue, hyphae start to bud and form
93 conidia which progress in xylem vessels before germinating and penetrating adjacent vessel
94 elements to start another infection cycle. [33,34]. During its colonization and proliferation
95 Verticillium produces and secretes a number of pectinolytic enzymes, including thirteen PLLs.
96 Considering the role of PLLs in determining pathogenicity, it is of paramount importance to
97 determine their biochemical and structural properties [30,35,36]. This could allow engineering
98 novel strategies to control or inhibit, the pathogen's pectinolytic arsenal. For this purpose, we
99 characterized, via combined experimental and computational approaches, one *V. dahliae* PLL
100 (VdPelB, VDAG_04718) after its heterologous expression in *P. pastoris*. The obtention of the
101 3D structure of VdPelB after X-ray diffraction and the analysis of enzyme dynamics when in
102 complex with substrates of distinct DM, allowed the identification of the residues favouring
103 pectate lyase (PL) activity. Experiments confirmed the importance of these residues in
104 mediating PL activity showing that VdPelB is a *bona fide* PL, that releases peculiar OG as
105 compared to previously characterized PLs. More importantly, the OGs released from roots of
106 *Verticillium*-partially tolerant and sensitive flax cultivars differed, paving the way for the
107 identification of VdPelB-mediated OGs that can trigger plant defence mechanisms.

108

109 **2. Material and methods**

110 **2.1. Bioinformatical analysis**

111 *Verticillium dahliae* PLL sequences were retrieved using available genome database
112 (ftp.broadinstitute.org). SignalP-5.0 Server (<http://www.cbs.dtu.dk/services/SignalP/>) was
113 used for identifying putative signal peptide and putative glycosylation sites were predicted
114 using NetOGlyc 4.0 Server (<http://www.cbs.dtu.dk/services/NetOGlyc/>). Sequences were
115 aligned and phylogenetic analysis was carried out using MEGA multiple sequence alignment
116 program (<https://www.megasoftware.net/>). Homology models used for molecular replacement
117 were created using I-TASSER structure prediction software
118 (<https://zhanglab.ccmb.med.umich.edu/I-TASSER/>) and UCSF Chimera
119 (<http://www.cgl.ucsf.edu/chimera/>) was used for creation of graphics.

120 **2.2. Fungal strain and growth**

121 *V.dahliae* was isolated from CALIRA company flax test fields (Martainneville, France) and
122 was kindly provided by Linéa-Semences company (Grandvilliers, France). Fungus was grown
123 as described in Safran et al. [37]. Briefly, fungus was grown in polygalacturonic acid sodium
124 salt (PGA, P3850, Sigma) at 10 g.L⁻¹ and in pectin methylesterified potassium salt from citrus
125 fruit (55–70% DM, P9436, Sigma) solutions to induce expression of *PLLs*. After 15 days of
126 growth in dark conditions at 25°C and 80 rpm shaking, mycelium was collected and filtered
127 under vacuum using Buchner flask. Collected mycelium was frozen in liquid nitrogen,
128 lyophilized and ground. Isolation of RNA and cDNA synthesis was realized as previously
129 described in Lemaire et al.[38].

130 **2.3. Cloning, heterologous expression and purification of VdPelB**

131 *V. dahliae* PelB gene (VdPelB, UNIPROT: G2X3Y1, GenBank: EGY23280.1,
132 *VDAG_04718*) consists of 1 single exon of 1002 bp length. The coding sequence, minus the
133 nucleotides encoding signal peptide, was PCR-amplified using cDNA and gene-specific
134 primers while VdPelB mutants were generated by PCR mutagenesis, a method for generating
135 site-directed mutagenesis, using specific primers carrying mutations (Table S1). Cloning of the
136 PCR-amplified sequences in pPICZαB, sequencing and expression in *P. pastoris* heterologous
137 expression system as well as purification steps were done as previously described in Safran et
138 al. [37].

139 **2.4. Crystallization of VdPelB**

140 Pectate lyase VdPelB was concentrated at 10 mg.mL⁻¹ in Tris-HCl pH-7.5 buffer.
141 Crystallization conditions were screened using the sitting-drop vapor-diffusion method. Pectate

142 lyase VdPelB (100 nL) was mixed with an equal volume of precipitant (1:1) using Mosquito
143 robot (STP Labtech). The crystals that resulted in best diffraction data were obtained with 0.1
144 M MIB (Malonic acid, Imidazole, Boric acid system) at pH8.0, with 25 % PEG 1500 as the
145 precipitant (condition B5 from the PACT premier kit, Molecular Dimensions, Sheffield, UK)
146 after 1 month. Optimization was realized using the hanging drop vapor-diffusion method
147 forming the drop by mixing 1 μ L of precipitant solution with 1 μ L of the enzyme. The crystals
148 (120 μ m x 30 μ m) were cryo-protected by increasing PEG 1500 concentration to 35%, before
149 mounting them in a loop and flash-cooling them in liquid nitrogen.

150 **2.5. VdPelB X-ray data collection and processing**

151 X-ray diffraction data were collected at the PROXIMA-2a beamline of the Soleil
152 synchrotron (Saint Aubin, France), at a temperature of -173°C using an EIGER 9M detector
153 (Dectris). Upon a first data collection to 1.3 Å resolution, three more data sets were collected
154 from the same crystal in order to obtain a complete data set. Thereby the kappa angle was tilted
155 once to 30°, once to 60° and finally a helical data set was collected at 1.2 Å resolution. The
156 reflections of each data set were indexed and integrated using XDS [39], scaled and merged
157 using XSCALE [40]. The VdPelB crystal has a primitive monoclinic lattice in the P 1 2₁ 1 space
158 group, with two molecules contained in asymmetric unit [41].

159 **2.6. Structure solution and refinement**

160 The structure of VdPelB was solved by molecular replacement using *Phaser* [42]. The data
161 were phased using pectate lyase BsPelA (PDB: 3VMV, Uniprot D0VP31), as a search model
162 [43]. Model was build using *Autobuild* and refined using *Refine* from PHENIX suite [44]. The
163 model was iteratively improved with *Coot* [45] and *Refine*. The final structure for VdPelB has
164 been deposited in the Protein Data Bank (PDB) as entry 7BBV.

165 **2.7. VdPelB biochemical characterization**

166 Pierce BCA Protein Assay Kit (Thermo Fisher Scientific, Waltham, Massachusetts, United
167 States) was used to determine the protein concentration, with Bovine Serum Albumin (A7906,
168 Sigma) as a standard. Deglycosylation was performed using Peptide-N-Glycosidase F (PNGase
169 F) at 37 °C for one hour according to the supplier's protocol (New England Biolabs, Hitchin,
170 UK). Enzyme purity and molecular weight were estimated using a 12% SDS-PAGE and mini-
171 PROTEAN 3 system (BioRad, Hercules, California, United States). Gels were stained using

172 PageBlue Protein Staining Solution (Thermo Fisher Scientific) according to the manufacturer's
173 protocol.

174 The substrate specificity of VdPelB was determined using PGA (81325, Sigma) and citrus
175 pectin of various DM: 20–34% (P9311, Sigma), 55–70% (P9436, Sigma) and >85% (P9561,
176 Sigma), with 0.5 μM CaCl_2 or 5 μM EDTA (Sigma) final concentrations. Enzyme activity was
177 measured by monitoring the increase in optical density at 235 nm due to formation of
178 unsaturated uronide product using UV/VIS Spectrophotometer (PowerWave Xs2, BioTek,
179 France) during 60 min. The optimum temperature was determined by incubating the enzymatic
180 reaction between 20 and 70°C for 12 min using PGA as a substrate (0.4%, w/v). The optimum
181 pH was determined between pH5.0 and 10.0 using sodium phosphate (NaP, pH5.0 to 7.0) and
182 Tris-HCl buffer (pH7.0 to 10.0) and 0.4% (w/v) PGA as a substrate. VdPelB and VdPelB-
183 G125R kinetic parameters, K_m , V_{\max} and k_{cat} , were calculated using GraphPad Prism (8.4.2).
184 The reactions were performed using 0.75 to 15 $\text{mg}\cdot\text{mL}^{-1}$ PGA concentrations at 50 mM Tris-
185 HCl pH8.0 (native) and 9.0 (G125R) during 12 min at 35°C. All experiments were realized in
186 triplicate. The statistical analysis was done using the Welch's t-test.

187 **2.8. Digestion of commercial pectins and released OGs profiling**

188 OGs released after digestions by recombinant VdPelB or commercially available
189 Aspergillus PL (named AsPel) were identified as described in Voxeur et al., 2019 [9], using a
190 novel in-house OGs library. Briefly, DM 20–34% (P9311, Sigma) and sugar beet pectin with
191 DM 42% and degree of acetylation (DA) 31% (CP Kelco, Atlanta, United States) were prepared
192 at 0.4 % (w/v) final concentration diluted in 50 mM Tris-HCl buffer (pH8.0) and incubated
193 with either VdPelB or AsPel (E-PCLYAN, Megazyme). For each substrate, enzyme
194 concentrations were adjusted to have enzymes at iso-activities (Table S2). For each substrate
195 two dilutions, were used for analysing OGs released in early, VdPelB-2 and AsPel-2, and late
196 phase, VdPelB-1 and AsPel-1, of digestions. Digestions were performed overnight. Non-
197 digested pectins were pelleted by centrifugation and the supernatant dried in a speed vacuum
198 concentrator (Concentrator plus, Eppendorf, Hamburg, Germany). Separation of OGs was done
199 as previously described using an ACQUITY UPLC Protein BEH SEC column (125Å, 1.7 μm ,
200 4.6 mm x 300 mm) at a flow rate of 0.4 $\text{ml}\cdot\text{min}^{-1}$. MS detection was performed using an
201 ACQUITY UPLC H-Class system coupled to a SYNAPT G2-Si-Q-TOF hybrid quadrupole
202 time-of-flight instrument (Waters) equipped with an electrospray ionization (ESI) source (Z-
203 spray) and an additional sprayer for the reference compound (lock spray). Samples were
204 analysed by ESI-high-resolution MS (HRMS) and MS/MS in negative ionization mode. Data

205 acquisition and processing were performed with MASSLYNX software (v.4.1; Waters).
206 [9,37,46].

207 The intensities were defined as the area under the curve, for each OG. Peak areas were clustered
208 by hierarchical clustering with complete linkage on the euclidian distance matrix and visualized
209 in the heatmap-package using R version 3.6.0. The statistical analysis was done using the
210 Welch's t-test.

211 **2.9. Molecular Dynamics simulations**

212 Two sets of molecular dynamics (MD) simulations were conducted on the VdPelB protein:
213 one in complex with a fully non-methylesterified polygalacturonate decaaccharide, and the
214 other with a fully methylesterified polygalacturonate decaaccharide. Parameters specified by
215 the AMBER14SB_parmbsc1 forcefield [47] were used to create the molecular topologies of
216 the complexes. Each complex was set up in a cubic box with solute-box distances of 1.0 nm
217 and solvated with water molecules specific to the TIP3P water model [48]. Na⁺ and Cl⁻ ions
218 were added to neutralise the system's net charge and reach a salt concentration of 0.165 M.
219 Using a steep-descent algorithm with a step size of 0.01, energy minimisation was performed
220 to resolve clashes between particles, with convergence being established at a particle-particle
221 force of 1000 kJ mol⁻¹ nm⁻¹. Particle-particle forces were calculated by considering van der
222 Waals and electrostatic interactions occurring up to 1.0 nm, as well as long-range electrostatics
223 treated in the Fourier space using the Particle Mesh Ewald (PME) summation method. Solvent
224 equilibration was attained post minimisation in two stages: through the NVT and NPT
225 ensembles, to reach constant temperature and pressure, respectively. Equilibration of the
226 solvent under the NVT ensemble was conducted for 1 ns, integrating the equation of motion at
227 a time step of 2 fs. The target reference temperature was 310.15 K, coupled every 0.1 ps using
228 the V-rescale thermostat3. Based on the Maxwell-Boltzmann distribution [49] at 310.15 K,
229 random velocities were then assigned to each particle in the system. Finally, solvent
230 equilibration under the NPT ensemble was conducted for 1 ns, continuing from the last step of
231 the previous equilibration, in terms of particle coordinates and velocities, at a reference
232 temperature of 310.15 K, coupled every 0.1 ps using the V-rescale thermostat [50]. Here,
233 pressure coupling was isotropically coupled every 2.0 ps, at 1 bar, using the Parrinello-Rahman
234 barostat [51]. Particle-particle interactions were computed by constructing pair lists using the
235 Verlet scheme. Short-range van der Waals and electrostatic interactions sampled through a
236 Coulomb potential, were calculated at a cutoff of 1.0 nm. The PME algorithm [52] was used to
237 compute long-range electrostatic interactions beyond this cut-off in the Fourier space, utilising

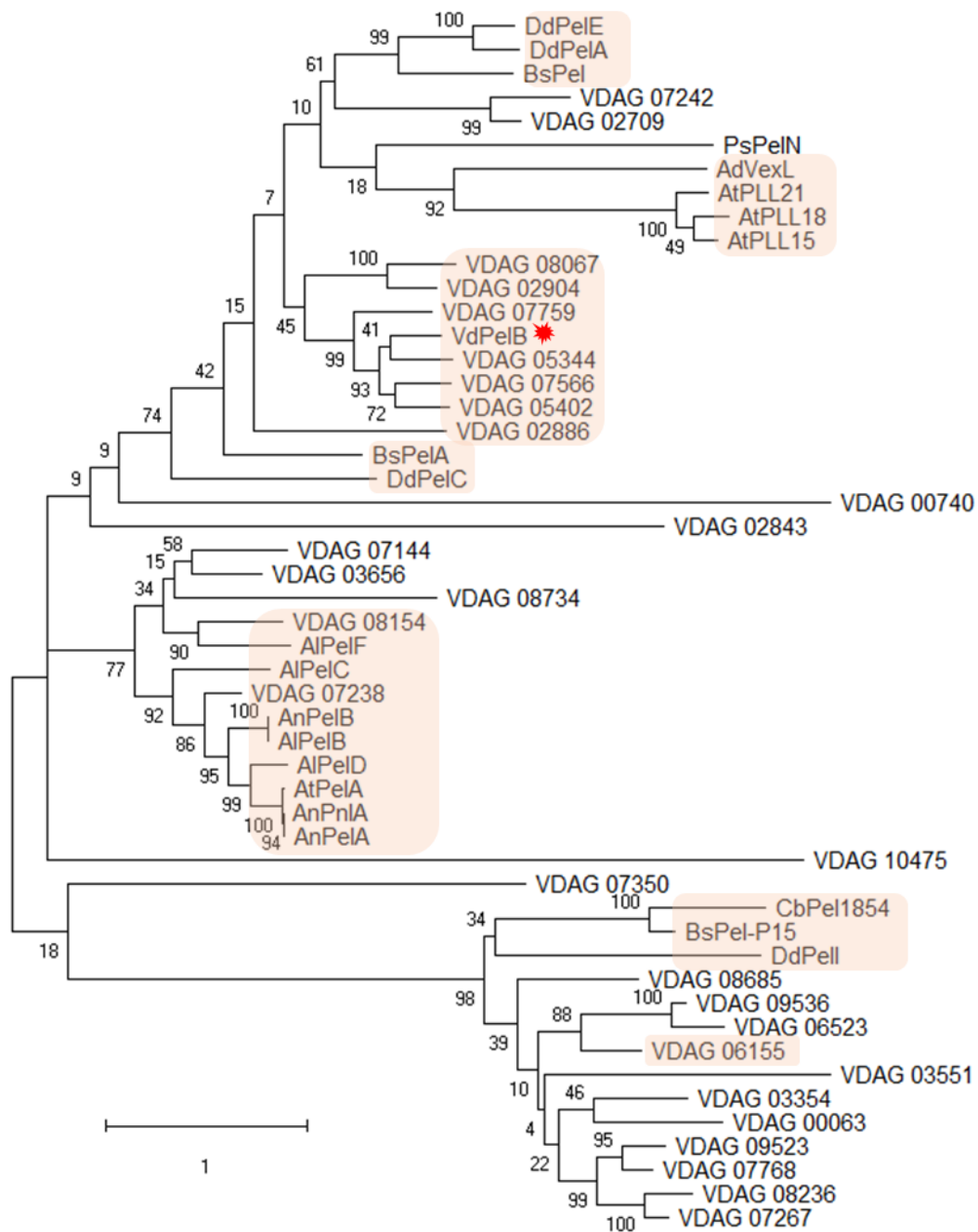
238 a Fourier grid spacing of 0.16 and a cubic B-spline interpolation level at 4. The simulations
239 were then performed on in-house machines, using GROMACS (Groningen Machine for
240 Chemical Simulations) version 2021.37. Each set of simulations were run for 150 ns each, at a
241 time step of 2 fs, with molecular dynamics trajectories written out every 10 ps. Simulations
242 were replicated 7 times for a total production run time of 1.05 μ s per complex. Replicates
243 differed with respect to the random particle velocity sets computed under the NVT ensemble.
244 For analysis, the first 50 ns of each production run were discarded as equilibration time. In-
245 house Python 3 scripts implemented using Jupyter notebooks [53] were used to carry out
246 analyses. Figures were created and rendered with Matplotlib [54] and VMD (Visual Molecular
247 Dynamics)[55].

248

249 **3. Results and Discussion**

250 **3.1. Sequence and phylogeny analysis**

251 In addition to 9 polygalacturonases (PGs) and 4 pectin methylesterases (PMEs), *V.*
252 *dahliae* encodes 30 putative endo-pectate lyases (EC 4.2.2.2), exo-pectate lyases (EC 4.2.2.9),
253 endo-pectin lyases (EC 4.2.2.10), belonging to PL1-PL3 and PL9 families, respectively [56].
254 For hierarchical clustering of *Verticilium*'s sequences with other PLLs, fifty-one amino acid
255 sequences encoding putative PLLs, belonging to bacteria, fungi and plants were aligned and a
256 phylogenetic tree was built. Different clades can be distinguished. (**Fig. 1**). *V. dahliae* PelB
257 (VdPelB, VDAG_04718) clustered with VDAG_05344 (59.68% sequence identity) with close
258 relations to VDAG_05402 (57.19% sequence identity) and VDAG_07566 (56.95% sequence
259 identity). VDAG_05402 and VDAG_05344, that are found in the protein secretome, have
260 orthologs in *V. alfalfa* (VDBG_07839 and VDBG_10041), which were shown to possess
261 putative lyase activity [36,57]. Plant PLLs from *A. thaliana* (AtPLL21, AtPLL15 and AtPLL18)
262 formed a separate clade with close connections to *A. denitrificans* (AdVexL), a PLL homologue
263 [58]. *D. dadanti* (DdPelI), *Bacillus Sp.* KSM-P15 (BsPel-P15) and *C. bescii* (CbPel1854)
264 formed separate clades similarly to *B. subtilis* and *D. dadantii* PLs (BsPel, DdPelA and
265 DdPelC). The clade corresponding to PNLs consisting of *A. tubingensis* PelA (AtPelA), *A.*
266 *niger* (AnPelA, AnPnlA and AnPelB), *A. luchuensis* AlPelB was closely related to
267 VDAG_07238 and VDAG_08154 which were indeed annotated as putative PNLs [18,56].
268 VDAG_06155 was previously named VdPel1 and previously characterized as a pectate lyase
269 [35].



270

271 **Fig. 1. Phylogenetic analysis of *V. dahliae* pectate lyase VdPelB with selected PLLs**

272 Phylogenetic tree representing *V. dahliae* VdPelB (VDAG_04718, G2X3Y1, red star) amino acid sequence in
 273 comparison with PLLs from *Verticillium* [VDAG_00740 (G2WQU8), VDAG_02904 (G2WXC5), VDAG_05344
 274 (G2X628), VDAG_07242 (G2XBA4), VDAG_07759 (G2XC77), VDAG_02709 (G2WWT0), VDAG_02843
 275 (G2WX64), VDAG_02886 (G2WXA7), VDAG_03656 (G2X1P5), VDAG_05402 (G2X597), VDAG_07144
 276 (G2X9U9), VDAG_07238 (G2XBA0), VDAG_07566 (G2XBY8), VDAG_08067 (G2XD35), VDAG_08154
 277 (G2XDC2), VDAG_08734 (G2XF02), VDAG_10475 (G2XJZ3), VDAG_03354 (G2WZB2), VDAG_03551
 278 (G2WZV9), VDAG_07267 (G2XBC9), VDAG_07768 (G2XC86), VDAG_08236 (G2XDK4), VDAG_06155
 279 (G2X8L4), VDAG_06523 (G2X7R5), VDAG_08685 (G2XEV0), VDAG_09523 (G2XH91), VDAG_09536
 280 (G2XHA4), VDAG_00063 (G2WR80), VDAG_07350 (G2XGG7)], *Arabidopsis thaliana* [AtPLL15
 281 (At5g63180), AtPLL18 (At3g27400), AtPLL21 (At5g48900)], *Dickeya dadanti* [DdPelA (P0C1A2), DdPelC

282 (P11073), DdPelE (P04960), DdPelI (O50325)], *Bacillus subtilis* [BsPel (P39116)], *Bacillus Sp.* KSM-P15
283 [BsPel-P15 (Q9RHW0)], *Bacillus sp.* N16-5 [BsPelA (D0VP31)], *Aspergillus niger* AnPelA [(Q01172), AnPelB
284 (Q00205), AnPn1A (A2R3I1)], *Achromobacter denitrificans* [AdVexL (A0A160EBC2)], *Aspergillus tubingensis*
285 [AtPelA (A0A100IK89)], *Aspergillus luchuensis* [AlPelB (G7Y0I4)], *Acidovorax citrulli* [AcPel343, (A1TSQ3)],
286 *Paenibacillus sp.* 0602 [PsPelN (W8CR80)], *Caldicellulosiruptor bescii* [CbPel1854 (B9MKT4)]. Maximum
287 likelihood tree was constructed with 1000 bootstrap replicates. Most important clades are indicated in orange
288 squares while VdPelB is marked by red star. Amino acids sequences were retrieved from Uniprot and TAIR.

289 **3.2. Expression and purification of VdPelB**

290 Since the expression was performed using the pPICZ α B vector with the yeast alpha-factor
291 directing VdPelB secretion in the culture media, the protein could be easily recovered and
292 purified. The protein is composed of 343 amino acids, including the 6xHIS tag at the C-terminus
293 used for affinity chromatography purification. After purification, VdPelB purity was assessed
294 using SDS-PAGE with an apparent molecular mass of ~38 kDa (**Fig. S1**), higher than what was
295 predicted on the basis of the amino acid sequence (33.8 kDa). However, this shift is likely to
296 correspond to the two tags that are fused to the protein (His and C-myc) and to the presence of
297 19 putative O-glycosylation sites, as predicted by NetOGlyc 4.0 Server.

298 **3.3. VdPelB has a right-handed parallel β -helix fold**

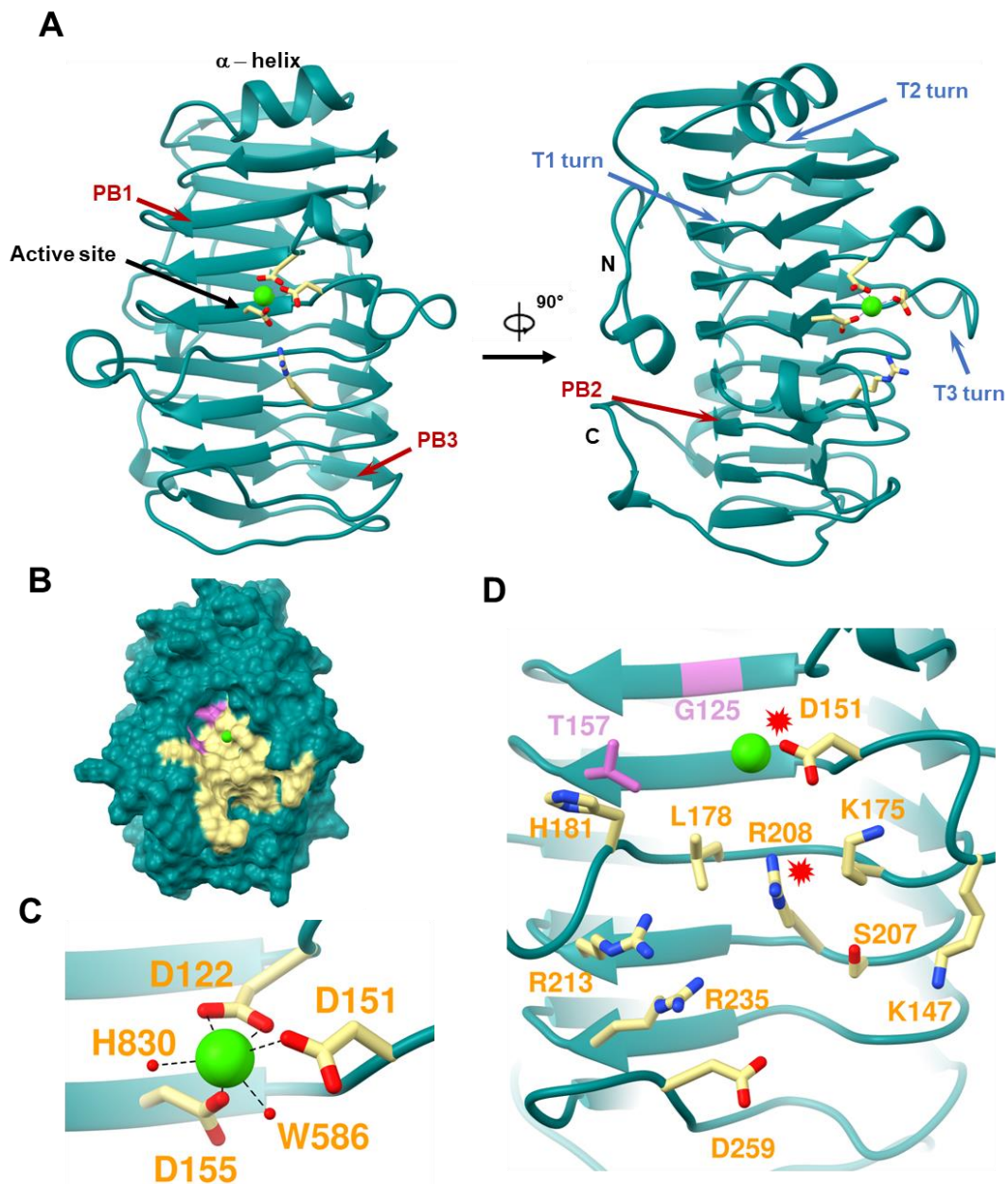
299 Pectate lyase VdPelB was crystallized and its 3D structure was determined using X-ray
300 diffraction. VdPelB crystallized in monoclinic P 1 2₁ 1 asymmetric unit. Four data sets,
301 collected from the same crystal at 1.2 Å resolution, were integrated, scaled and merged. There
302 are two molecules in the asymmetric units: chains A and B are highly similar with a C α root
303 mean square deviation (rmsd) value of 0.227 Å (**Fig. S2A**). The VdPelB structure consists of
304 298 amino acids with 18 at the N-terminus and 27 amino acids at the C-terminus that were not
305 resolved because of poor electron densities, while overall electron densities were well defined.
306 While no N-glycosylation sites could be revealed on the VdPelB structure, six O-glycosylation
307 sites carrying mannose are visible for each molecule: T22, T44, T45, T46, S48 and T54, in
308 accordance with the shift in size previously observed (**Fig. S2A**). During data acquisition no
309 heating of the crystal was observed, as shown by low B factors and good occupancies (**Fig. S3A**
310 **and B**). The final models' geometry, processing and refinement statistics are summarized
311 (**Table 1**). The VdPelB's structure has been deposited in the Protein Data Bank as entry 7BBV.

312 **Table 1. Data collection, processing and refinement for VdPelB**

Characteristics	VdPeIB
Data collection	
Diffraction source	PROXIMA2
Wavelength (Å)	0.980
Temperature (°C)	-100.15
Detector	DECTRIS EIGER X 9M
Crystal-to-detector distance (mm)	115.02
Rotation range per image (°)	0.1
Total rotation range (°)	360
Crystal data	
Space group	P1 21 1
<i>a, b, c</i> (Å)	60.89, 59.69, 93.87
α, β, γ (°)	90.00, 96.35, 90.00
Subunits per asymmetric unit	2
Data statistics	
Resolution range (Å)	60.52-1.2 (1.243 - 1.2)
Total No. of reflection	8536161 (112943)
No. of unique reflection	207497 (19983)
No. of reflections, test set	10362 (1003)
R_{merge} (%)	0.1036 (4.709)
Completeness (%)	99.30 (96.11)
$\langle I/\sigma(I) \rangle$	18.03 (0.22)
Multiplicity	41.1 (5.6)
$CC_{1/2}$ (%)	1 (0.116)
Refinement	
$R_{\text{crys}}/R_{\text{free}}$ (%)	17.3 / 19.7
Average B – factor (Å ²)	33.18
No. of non-H atoms	
Protein	9097
Ion	2
Ligand	234
Water	1052
Total	10385
R.m.s. deviations	
Bonds (Å)	0.013
Angles (°)	1.39
Ramachandran plot	
Most favoured (%)	95.1
Allowed (%)	4.90
Outlier (%)	-

314 The VdPelB has a right-handed parallel β -helix fold which is common in pectinases
315 [59]. The β -helix is formed by three parallel β -sheets - PB1, PB2 and PB3 which contain 7, 10
316 and 8 β -strands, respectively. Turns connecting the PB1-PB2, PB2-PB3 and PB3-PB1 β -sheets
317 are named T1-turns, T2-turns and T3-turns, respectively, according to Yoder and Jurnak (**Fig.**
318 **2A, S4A and B**) [60]. T1-turns consist of 2-14 amino acids and builds the loop around the
319 active site on the C-terminus. T2 turns mostly consist of 2 amino acids with Asn being one of
320 the predominant amino acid, forming an N-ladder with the exception of an N245T mutation in
321 VdPelB [15,20]. Pectate lyase VdPelB has a α -helix on N-terminus end that shields the
322 hydrophobic core and is commonly conserved in PLs and PGs [15,61], while the C-terminus
323 end is also protected by tail-like structure carrying one α -helix. Interestingly N- and C- terminus
324 tails pack against PB2 (**Fig. 2A**). There are only two Cys (C25 and C137) that do not form a
325 disulphide bridge.

326 Sequence and structural alignments show that VdPelB belong to the PL1 family. The
327 VdPelB shares the highest structural similarity with BsPelA (PDB: 3VMV), with 30.06%
328 sequence identity and C α rmsd of 1.202 Å. The second-best structural alignment was with
329 DdPelC (PDB: 1AIR) with 24.20% identity and C α rmsd of 1.453 Å [43,62]. Both of these
330 structures lack the long T3 loop described in *A.niger* pectate lyase (AnPelA, PDB: 1IDJ, **Fig.**
331 **S2B and S5**) [15]. The putative active site is positioned between the T3 and T2 loops (**Fig. 2A**
332 **and B**).



333

334 **Fig. 2. Structure determination of VdPelB**

335 A) Ribbon diagram of VdPelB crystalized in P1 21 1 space group. VdPelB is a right-handed parallel β helical
 336 structure consisting of β strands (red arrows) and turns (blue arrows). VdPelB active site's amino acids are yellow-
 337 colored while Ca atom is green. B) Surface representation of VdPelB binding groove. C) Active site of VdPelB
 338 highlighting conserved amino acids and atoms interacting with Ca. D) Structure of VdPelB binding groove
 339 highlighting amino acids involved in the interaction (yellow) and amino acids not of previously characterized in
 340 PLs (plum). Red stars indicate amino acids from the active site.

341 **3.4. Active site harbours Ca^{2+} that is involved in catalysis**

342 The VdPelB active site is well conserved, harbouring strictly conserved acidic and basic
 343 amino acids that are required for Ca^{2+} binding. Previously reported structures showed that two
 344 Asp (D122 and D155) and one Arg (R208) in VdPelB, are conserved, while D151 can be

345 mutated to Glu, or Arg in PNLs (**Fig. 2C and D**, Mayans et al., 1997). Other conserved amino
346 acids in VdPelB include K175 and R213, with K175 being responsible for binding the carboxyl
347 oxygen while R213 hydrogen bonds to C-2 and C-3 of GalA (**Fig. 2D**) [29,63]. Mutating any
348 of these amino acids leads to decreased enzyme activity [64]. In VdPelB, Ca²⁺ ion is directly
349 coordinated by D122, two carboxyl oxygen, D151, D155 and two water molecules (W568 and
350 W830, **Fig. 2C**). In addition, mutation of D122T (VdPelB numbering) in BsPelA, is responsible
351 for reduced affinity for Ca²⁺ [43]. In the catalytic mechanism, Ca²⁺ is directly involved in
352 acidification of the proton absorption from C5 and elimination of group from C4, generating an
353 unsaturated product. R208 act as a base, similarly to the hydrolysis in the reaction mechanism
354 of the GH28 family [65,66].

355 **3.5. Structural analysis of VdPelB suggests a PL activity mediated by peculiar** 356 **specificities**

357 The VdPelB binding groove comprises a number of basic and acidic amino acids
358 including K147, D151, K175 L178, H181, S207, R208, R213 and R235 and D259 (**Fig. 2C**
359 **and D**), that have previously been shown to be characteristics of PLs. This would suggest an
360 enzyme activity on low DM pectins as amino acids positioned at the binding groove were
361 indeed shown to differ between PNL and PL [15,21,24,29]. These amino acids are indeed
362 mutated in Arg, Trp, Tyr, Gln and Gly in PNLs, which, by reducing their charge, would favour
363 higher affinity for highly methylesterified pectins [15,29]. In VdPelB, as the T3 loop is missing,
364 there are no equivalent to PNL specific W66, W81, W85, W151 amino acids (**Fig. S2B**, AnPelA
365 numbering) and, moreover, W212 and W215 are replaced by K175 and L178 in VdPelB. In
366 BsPelA and DdPelC, these amino acids are replaced by K177/K190 and L180/L193,
367 highlighting the high conservation of amino acids in VdPelB/BsPelA/DdPelC and subsequently
368 in PLs. When a DP4 ligand from DdPelC crystal structure is superimposed to VdPelB, hydrogen
369 bonds and van der Waals interactions are visible with the above-mentioned amino acids (**Fig.**
370 **S6**) [15,21,29,43].

371 Interestingly, despite this rather conserved PL-related binding groove, VdPelB harbors,
372 in the vicinity of the active site, G125 and T157 that are not present in the well characterized
373 DdPelC [62]. At these positions, DdPelC, which was shown to be a *bona fide* PL with a high
374 activity on polygalacturonic acid and alkaline pH with Ca²⁺-dependency, harbours Arg and Lys
375 [15,63,67]. In that respect, the presence of G125 and T157 in VdPelB is similar to that identified
376 in *Bacillus sp.* Pel-22, Pel-66, and Pel-90 and *Bacillus sp.* which showed activity on both PGA
377 and high methylesterified pectins (**Fig. 2B and D**) [22,68,69]. The DdPelC amino acids being

378 overall positively charged, could explain the binding preference towards non-methylesterified,
379 negatively charged substrates in the vicinity of the active site. In contrast, considering the size
380 of Gly and Thr, they would sterically accommodate the increased size of methylesterified
381 substrate. G125 and T157 could therefore account for a potential dual activity of VdPelB.
382 Moreover, in previously characterized PLs and PNLs there is the presence of a small amino
383 acids, Ser or Ala that replace H181. While H181 interacts directly with the substrate these
384 amino acids do not provide this interaction instead the primary Ca^{2+} in the active site induce a
385 substrate conformation that could be recognized by PLs [43]. Finally, L178 is positioned in-
386 between the catalytic Ca^{2+} and R208 and is involved in substrate binding making it a perfect
387 candidate to assess its importance (**Fig. 2D**).

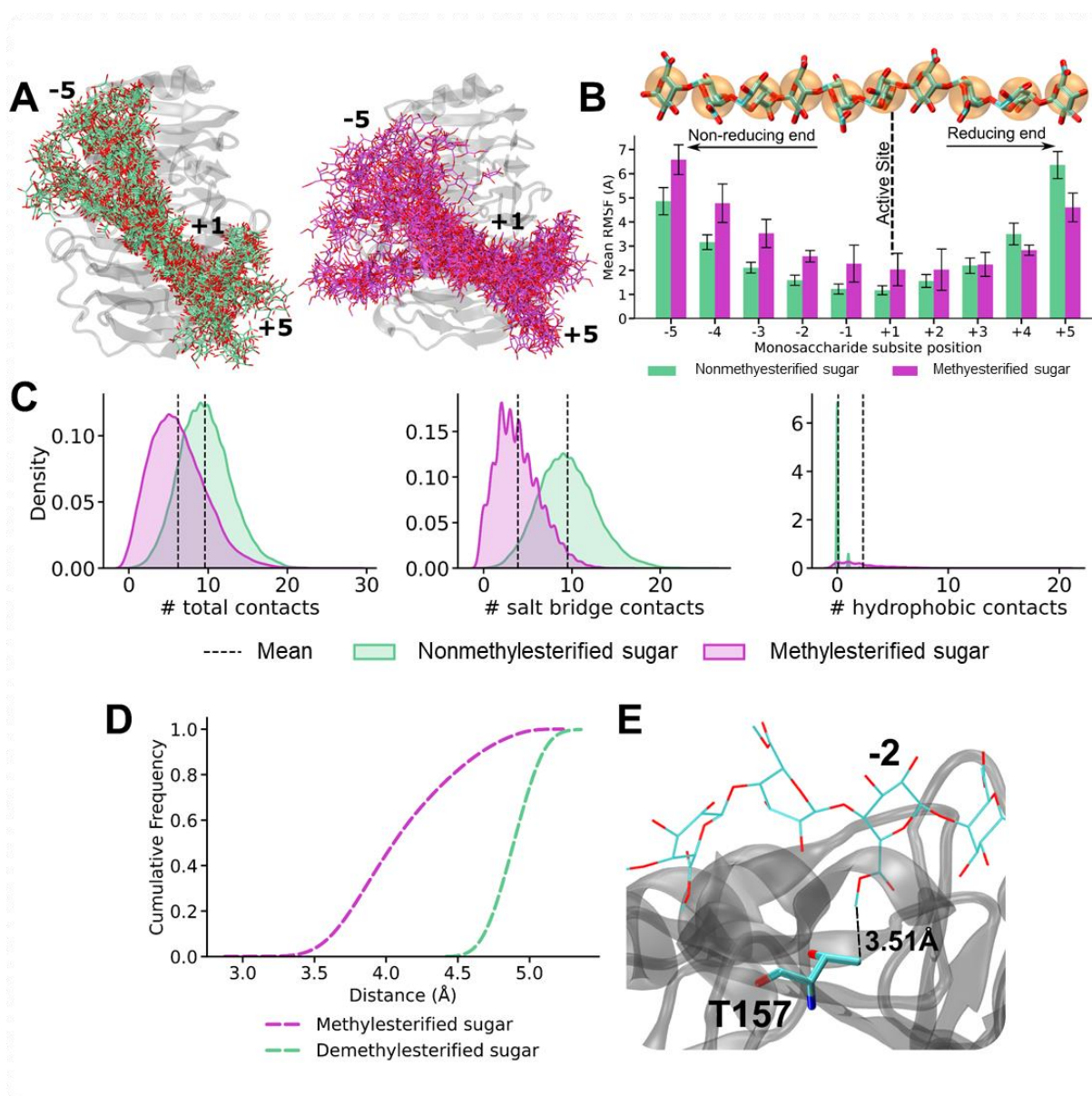
388 **3.6. Molecular dynamic simulations show higher dynamics of VdPelB in complex with** 389 **methylesterified substrates**

390 To determine how the structure of VdPelB and the observed differences in amino-acidic
391 composition might influence the affinity with differently methylated substrates, we performed
392 MD simulations on VdPelB in complex with either a non-methylesterified or fully
393 methylesterified deca-saccharides, which are able to occupy the entire binding groove (**Fig. 3**).
394 MD simulations show substantially differential dynamic profiles for oligosaccharides with and
395 without methylesterification. Expectedly, the dynamics is lowest in proximity of the catalytic
396 subsite (+1) and increases consistently towards both the reducing and non-reducing ends of the
397 substrate: with the highest dynamics found at the non-reducing end (**Fig. 3A**).

398 A quantitative estimation of the substrate dynamics was obtained by monitoring the root
399 square mean fluctuations (RMSF) of each sugar residue and shows that a polygalacturonate
400 substrate associates more stably in the subsites of the binding groove placed towards the sugar's
401 reducing end (subsites -1 to -5), with differences between methylesterified and non-
402 methylesterified substrates approaching the obtained standard deviation. In some cases, the
403 dynamics reversed for non-methylesterified sugars, with a higher RMSF for de-methylesterified
404 sugars towards the saccharide's reducing end (**Fig. 3B**). Moreover, and in line with an observed
405 positively charged binding groove, non-methylesterified substrates retain a higher number of
406 contacts than methylesterified sugars, with salt-bridges contributing the most to the observed
407 differences (**Fig. 3C**).

408 We then additionally and specifically focused on the analysis of the interactions made by
409 T157, which is nested with the -2 subsite of the binding groove. Simulations sample consistently

410 higher contacts formation between a methylesterified sugar docked in subsite -2 and T157, with
 411 distances shifted to lower values when compared to a non-methylesterified sugar (**Fig. 3D**),
 412 even the RMSF of non-methylesterified monosaccharides docked in subsite -2 experience on
 413 average, significantly lower dynamics. Altogether, the formation of a larger number of contacts
 414 between methylesterified saccharides docked in the -2 subsite suggests an active role of T157
 415 in the binding of methylesterified chains: with the butanoic moiety of T157 engaging in
 416 hydrophobic interactions with the methyl-ester presented by methylesterified sugar units (**Fig.**
 417 **3E**). While T157 is seen to have an active role in engaging with the substrate's hydrophobic
 418 moieties, an active role of G125, also in the same subsite, was not observed but it is plausible
 419 that the minimal size of G125 would increase the accommodability of methylesterified sugars
 420 in that position.



421

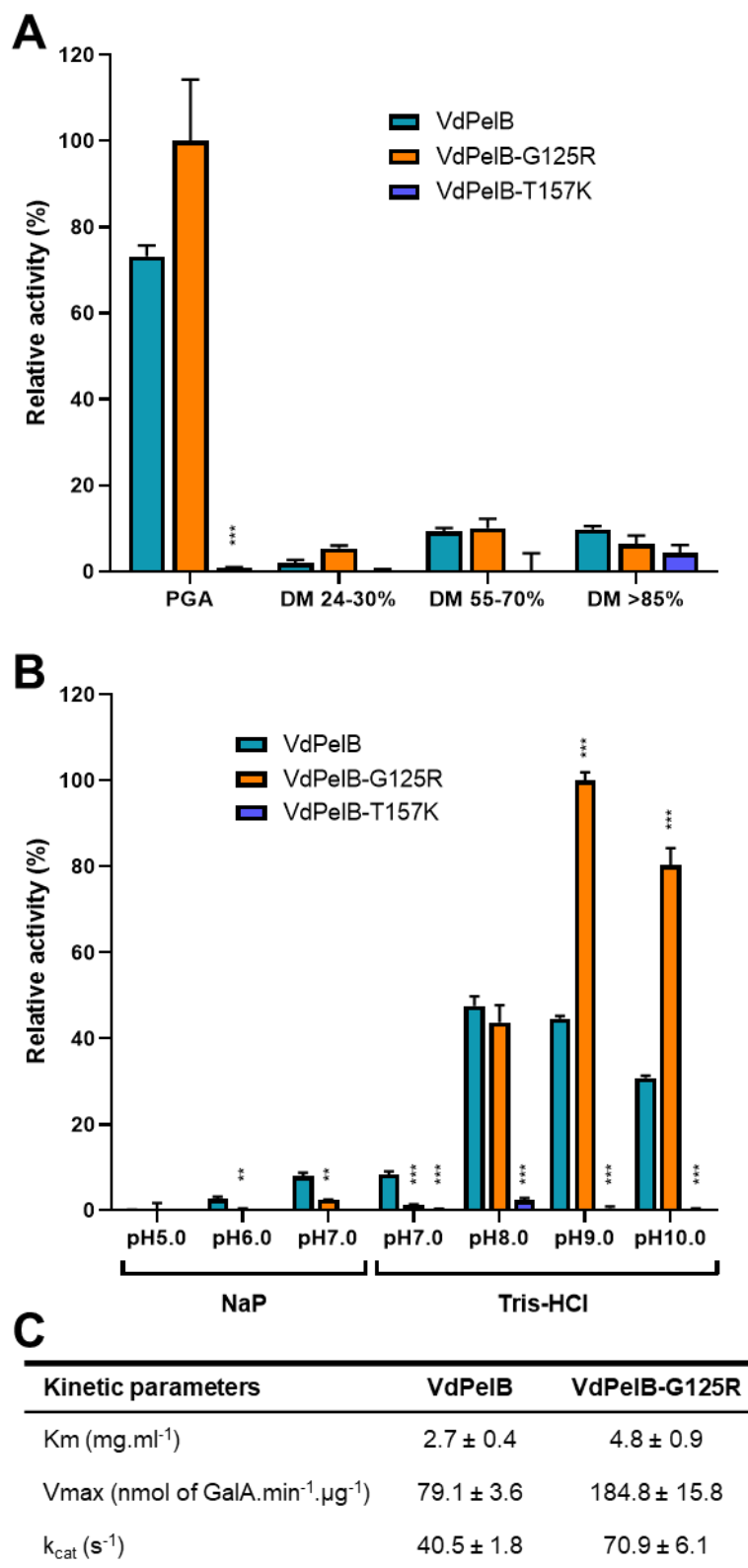
422 **Fig. 3. VdPelB substrate dynamics in complex with fully de-methylesterified and methylesterified complex**

423 A) Ensembles of non-methylesterified (green, left panel) and methylesterified (pink, right panel) HG
424 decasaccharide at every 100 frames for the simulated VdPelB complexes. Substrate within the enzymes' binding
425 grooves are labelled from -5 (HG-non-reducing end) to +5 (HG-reducing end) B) RMSF of non-methylesterified
426 (green) and methylesterified (pink) HG bound across the binding groove of VdPelB. Numbers indicate the beta
427 sheet position from the active site. C) Analysis of the contacts between VdPelB and non-methylesterified (green)
428 and methylesterified substrate (pink). D) Distance between T157K residue and the substrate residues plotted as
429 cumulative frequency. E) T157 hydrophobic interaction with methyl-ester of methylesterified substrate.

430 **3.7. Biochemical characterization of VdPelB**

431 We first determined the activity of VdPelB by following the release of 4,5-unsaturated
432 bonds which can be detected at 235 nm using UV spectrophotometer. The VdPelB activity was
433 first tested for its dependency towards Ca^{2+} . Using a standard PL assay, with PGA as a substrate,
434 an increase in the VdPelB activity was measured in presence of calcium. In contrast in presence
435 of EDTA, used as a chelating agent, no activity was detected, confirming the calcium-dependent
436 activity of the enzyme (**Fig. S7A**) [15]. Activity measured in absence of added CaCl_2 reflects
437 the presence of calcium from the culture media that is bound to VdPelB during production, and
438 previously identified in the 3D structure. We tested the effects of increasing CaCl_2
439 concentrations and showed that the maximum activity was already reached when using as low
440 as 0.125 μM (**Fig. S7B**). To test the substrate-dependence of VdPelB, four substrates of
441 increasing degrees of methyl-esterification were used. The VdPelB showed the highest activity
442 on PGA, with less than 10% of the maximum activity measured on the three others substrates
443 (**Fig. 4A**). This shows that, as inferred from above-mentioned structural and dynamical data,
444 The VdPelB act mainly as a PL although it can still show residual activity on high DM pectins.
445 Considering this, PGA was used as substrate to test the pH-dependence of the enzyme's activity
446 in sodium acetate and Tris-HCl buffers (**Fig. 4A**). Pectate lyase VdPelB was most active at pH
447 8, with only a slight decrease in activity at pH 9 (93%). In contrast, the relative activity at pH
448 5-7 was close to null. The pH optimum for VdPelB was the same as *B. fuckeliana* Pel (pH 8)
449 [70], close to that reported for *D. dadantii* PelN (pH 7.4) [71], but was lower to that measured
450 for *B. clausii* Pel (pH 10.5) [72]. In contrast, the pH optimum was higher compared to five PNLs
451 from *Aspergillus* sp. AaPelA (pH 6.1), AtPelA (pH 4.5), AtPelA (pH 6.4), AtPelD (pH 4.3)
452 [18] and *A. parasiticus* Pel (pH 4) [19]. The optimum temperature assay showed that VdPelB
453 was most active at 35°C (**Fig. S8**). The VdPelB appeared less heat-tolerant as compared to
454 thermophilic PLLs reported from *Bacillus* sp. RN1 90°C [73], *B. clausii* Pel, 70°C [72], *B.*
455 *subtilis* Pel168, 50°C [74]. However, its optimum temperature is in the range of that measured

456 for *X. campestris* Pel [75] and cold-active Pel1 from *M. eurypsychrophila* [76]. The lack of
 457 disulphide bridges previously shown in the structure could be responsible for the lower stability
 458 of the enzyme at high temperatures, in comparison with previously characterized PLs [77].



459

460 **Fig. 4. Biochemical characterization of VdPelB**

461 A) Substrate-dependence of VdPelB, G125R and T157K. The activities were measured after 12 min of incubation
462 with PGA, pectins DM 24-30%, DM 55-70%, DM>85% with addition of Ca²⁺ at 35°C. B) pH-dependence of
463 VdPelB, G125R and T157K activity. The activities were measured after 12 min of incubation with PGA in sodium
464 phosphate (NaP) and Tris-HCl buffer at 35°C. Values correspond to means ± SD of three replicates. Welch t-test
465 comparing native with mutant VdPelB forms was used for statistical analysis. P value ***<0.001 and **<0.01. C)
466 Determination of Km, Vmax and kcat for ADPG2 and PGLR. Activity was assessed using various concentrations
467 of PGA at 35°C and pH8.0 (VdPelB) and pH9.0 (VdPelB-G125R).

468 **3.8. Mutation of specific amino-acids affects VdPelB activity**

469 Considering the structure of VdPelB and our hypothesis related to the role of some
470 amino acids in determining the mode of action of VdPelB, we generated mutated forms of the
471 enzyme for five amino acids that likely to be involved in the catalytic mechanism and/or
472 substrate binding: G125R, D151R, T157K, L178K and H181A. Enzymes were produced in *P.*
473 *pastoris* and purified (**Fig. S1**). If the importance of some of these amino acids (i.e. D151 and
474 H181) in the catalytic mechanism was previously shown for others PL [43,78], our study
475 highlights the key role of some novel amino acids in the catalytic mechanism. The activities of
476 mutants were tested at iso-quantities of wild-type enzyme. Surprisingly, the G125R mutant was
477 25% more active on PGA compared to the native enzyme and a shift in the optimum pH was
478 observed (**Fig. 4A**). While native enzyme was most active at pH8.0 with slight decrease in
479 activity at pH9.0, the activity of G125R mutant was approximately doubled at pH9.0 and
480 pH10.0 (**Fig. 4B**). Both enzymes kept the same activity at pH8.0. Moreover, using PGA as a
481 substrate, at 35°C, VdPelB and VdPelB-G125R differ slightly in their Km (2.7 versus 4.8
482 mg.ml⁻¹), Vmax (79.1 versus 184.8 nmol of GalA.min⁻¹.µg⁻¹) and kcat (40.5 versus 70.9 s⁻¹,
483 **Fig. 4C**). The substitution of Gly with Arg, present in a number of previously characterized
484 PL could facilitate the interaction with the substrate and alkalization of the active site thanks
485 to its physio-chemical properties [62]. Despite not knowing the exact rotamer orientation, the
486 presence of Arg with high pK_a allowing strong hydrogen bonding and complex electrostatic
487 interactions within the active site, could change the optimal pH by acting on the protonation
488 state of amino acids involved in catalysis, as previously reported for a number of different
489 enzymes [65,79–82]. The activity of T157K was closed to null when tested on PGA and
490 different pHs. The introduction of a Lys, a chemically different and larger amino acids is likely
491 to introduce steric clashes notably with H181 and L178 that are important for the activity. The
492 H181A mutant lost much of its activity as there are less interaction/recognition with the
493 substrate. No activity for D151R and L178K mutants were observed in line with the fact that
494 D151 is an active site amino acid that binds the Ca²⁺. Mutation of this amino-acid is negatively

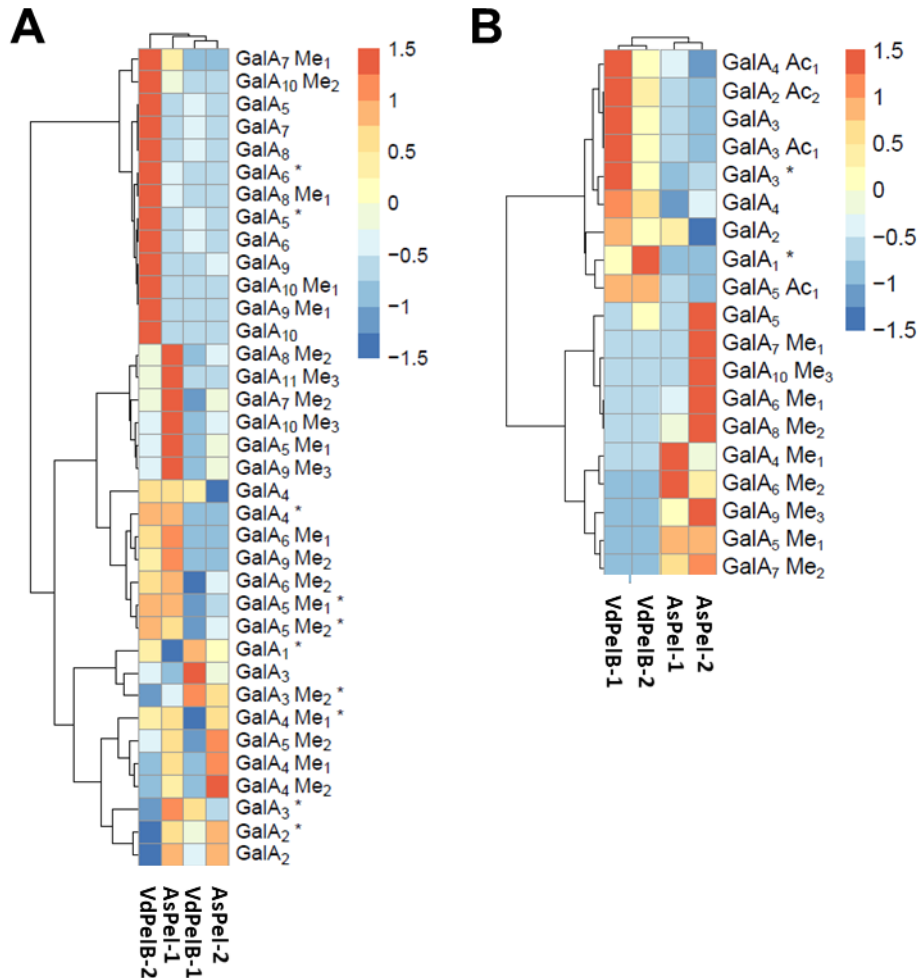
495 impairing the functioning of the enzyme (**Fig. S7A and B**) [43,78]. We can hypothesize that
496 L178K mutation positioned in between Ca²⁺, R208 and the substrate, induces specific substrate
497 conformation that diminishes the direct interaction between the enzyme catalytic centre and the
498 substrate, which translates to loss of activity (**Fig. S9**).

499 **3.9. Identification of the OGs released by VdPelB from commercial and cell wall** 500 **pectins**

501 To further understand the specificity of VdPelB on different substrates, we performed
502 LC-ESI-MS/MS to determine the profiles of digestion products (OGs) and to compare with that
503 of commercially available *Aspergillus sp.* Pel (AsPel, **Fig. S10**). To be fully comparable,
504 digestions were realized, for each substrate, at iso-activities for the two enzymes. On the basis
505 of digestion profiles, we identified 48 OGs and created a dedicated library that was used for
506 identification and integration of peaks (**Table S3**). MS² fragmentation allowed determining the
507 structure of some of the OGs (**Fig. S11 and S12**). The OGs released by either of the enzymes
508 mainly corresponded to 4,5-unsaturated OGs, which is in accordance with β-eliminating action
509 of PLLs. When using pectins DM 20-34% and at low enzyme's concentration (VdPelB-2),
510 VdPelB mainly released non-methylesterified OGs of high DP (GalA₅, GalA₆, GalA₇, GalA₈,
511 GalA₉, GalA₁₀) that were subsequently hydrolysed when using more concentrated VdPelB
512 (VdPelB-1, **Fig. 5A**). These digestion products strikingly differed to that generated by AsPel,
513 that are methylesterified OGs of higher DP (GalA₄Me₁, GalA₄Me₂, GalA₅Me₁, GalA₆Me₂,
514 GalA₁₁Me₃...), thus showing distinct enzymatic specificities. Altogether, these first results
515 unequivocally shows both VdPelB and AsPel act as endo-PLs, but they differ in their
516 processivity [9]. When using sugar beet pectins, that are known to be highly acetylated (DM
517 42%, DA 31%), VdPelB released acetylated OGs (GalA₂Ac₂, GalA₃Ac₁, GalA₄Ac₁,
518 GalA₅Ac₁), while AsPel showed much lower activity and relative abundance of these OGs (**Fig.**
519 **5B**). Previous reports have shown that differences exist between PNL, in particular with regards
520 to acetyl substitutions [18]. In contrast, AsPel released mainly methylesterified OGs (GalA₆Me₁,
521 GalA₈Me₁, GalA₁₀Me₃...).

522

523



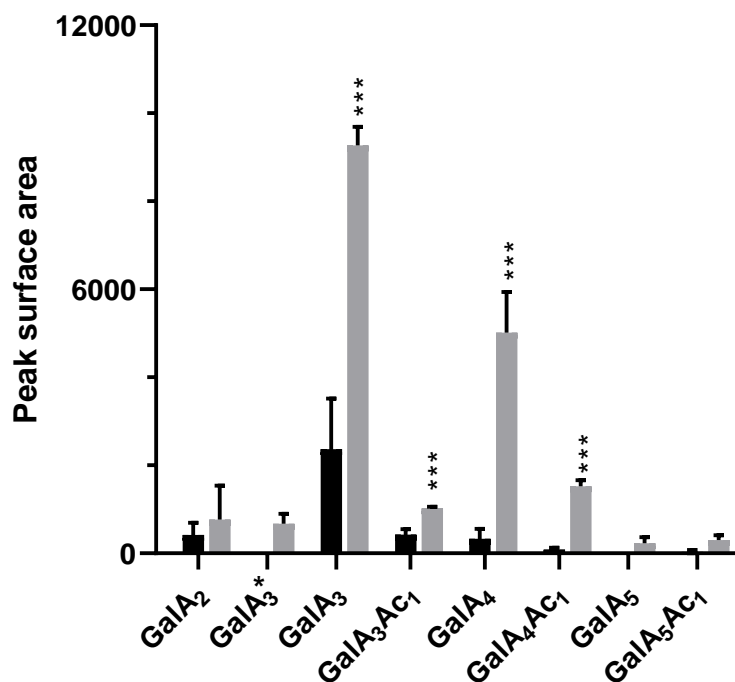
524

525 **Fig. 5. Analysis of OGs produced by the action of VdPelB and AsPeI on pectins of various degrees of**
 526 **methylesterification and acetylation**

527 OGs were separated by SEC and analysed by MS/MS. A) Pectins DM 24-30%. B) Sugar beet pectins (DM 42%
 528 DA 31%). Substrates were digested overnight at 40°C and pH8.0 using isoactivities of VdPelB and AsPeI. Enzyme
 529 concentrations are stated in Table S2. Subscript numbers indicate the DP, DM and DA. * indicate non-unsaturated
 530 OGs. Values correspond to means of three replicates.

531 *V. dahliae* and closely related fungus from the same genus are known flax pathogens,
 532 where they use their enzymatic arsenal, that includes pectin degrading enzymes, for penetrating
 533 the host cell leading to infection [30]. To assess the potential role of VdPelB in flax
 534 pathogenicity we digested root cell walls from two flax cultivars, Evea (Verticillium-partially
 535 resistant), and Violin (Verticillium-susceptible), and we compared the OGs released. On root
 536 cell walls, VdPelB released mainly unsaturated OGs up to DP5 (**Fig. 6**). From similar starting
 537 root material, the OG total peak area detected was five times lower for Evea compared to Violin,
 538 suggesting that it is less susceptible to digestion by VdPelB. OGs released by VdPelB were
 539 mainly non-methylesterified but could be acetylated (GalA₂, GalA₃, GalA₃Ac₁, GalA₄,

540 GalA₄Ac₁ GalA₅, GalA₅Ac₁), and the abundance of GalA₃ and GalA₄ was five and fifteen times
 541 higher in Violin, respectively. These data together with that obtained from sugar beet pectins
 542 strongly suggests that VdPelB preference is for non-methylesterified and acetylated substrates.
 543 Our data suggest that cell wall structure differ between the two cultivars and that VdPelB could
 544 determine *Verticillium* pathogenicity thanks to a better degradation of the cell wall pectins of
 545 sensitive cultivars [37]. Similarly, VdPel1 was previously identified as virulence factor, where
 546 the deletion of this gene decreased virulence in tobacco, as compared with the wild-type
 547 *Verticillium* [35].



548

549 **Fig. 6. Analysis of OGs released by VdPelB from flax roots.**

550 The VdPelB was incubated overnight with roots from Évéa (spring flax, partially resistant to *Verticillium* wilt,
 551 black) and Violin (winter flax, more susceptible to *Verticillium* wilt, grey). Values correspond to means \pm SD of
 552 three replicates. Welch t-test comparing Eevea with Violin was used for statistical analysis. P value ***<0.001.
 553 Subscript numbers indicate the DP, DM and DA.

554

555 4. Conclusion

556 We have characterized, by multidisciplinary approaches, a novel pectinolytic enzyme
 557 from *V.dahliae*, VdPelB, that belongs to the PLL family. The protein was crystallised and its
 558 3D structure determined at a high resolution. Pectate lyase VdPelB showed a conserved

559 structure, with parallel β -sheet topology for PLs and the active site harboured three conserved
560 Asp coordinating Ca^{2+} and Arg involved in the β -elimination mechanism. The binding groove
561 of VdPelB reveals conserved amino acids that are characteristic of PLs, with MD simulations
562 confirming the lower dynamics/higher affinity of the enzyme towards non-methylesterified
563 pectins. As inferred from structural and dynamical analyses, VdPelB showed high activity on
564 non-methylesterified substrates, with a maximum activity at pH8.0 and 35°C. The analysis of
565 the structure led the identification, in the VdPelB, of peculiar amino acids that are normally
566 present in PNL. In particular, G125R mutant increased activity on PGA and switch in pH
567 optimum from 8.0 to 9.0 related to amino acids protonation. The analysis of the digestion
568 products showed that VdPelB act as an endo enzyme and that it can release a large diversity of
569 OGs with a preference for non-methylesterified and acetylated products. The OGs generated by
570 VdPelB from pectins extracted from *Verticillium*-partially tolerant and *Verticillium*-sensitive
571 flax cultivars showed that the enzyme could be a determinant of pathogenicity, since these OGs
572 differ as a function of pectins' structure. Thus, our study now paves the way for generating,
573 using dedicated enzymes, OG pools that could be used for protecting plants against
574 phytopathogens.

575

576 **Funding sources**

577 This work was supported by the Conseil Regional Hauts-de-France and the FEDER
578 (Fonds Européen de Développement Régional) through a PhD grant awarded to J.S.

579

580 **Acknowledgements**

581 We wish to thank Sylvain Lecomte and Mehdi Cherkaoui for providing the *Verticillium*
582 *dahliae* DNA, Martin Savko and the staff at Proxima 2a beamline (Synchrotron SOLEIL, Gif
583 sur Yvette, France) for X-ray diffraction and data collection.

584 **Author's contribution**

585 **Josip Safran**: Conceptualization, Data curation, Formal analysis, Investigation, Methodology,
586 Writing - original draft. **Vanessa Ung**: Data curation, Investigation, Methodology. **Julie**
587 **Bouckaert**: Data curation, Investigation, Methodology. **Olivier Habrylo**: Formal analysis,
588 Investigation, Methodology. **Roland Molinié**: Data curation, Formal analysis, Investigation,
589 Methodology. **Jean-Xavier Fontaine**: Data curation, Formal analysis, Investigation,
590 Methodology. **Adrien Lemaire**: Investigation, Methodology. **Aline Voxeur**: Investigation,
591 Methodology. **Serge Pilard**: Investigation, Methodology. **Corinne Pau-Roblot**
592 Conceptualization, Methodology. **Davide Mercadante**: Data curation, Methodology, Writing
593 - review & editing. **Jérôme Pelloux**: Funding acquisition, Conceptualization, Writing - review
594 & editing. **Fabien Sénéchal**: Conceptualization, Writing - review & editing.

595 **Conflicts of interest**

596 There are no conflicts of interest.

597

598 **References**

- 599 [1] B.L. Ridley, M.A. O'Neill, D. Mohnen, Pectins: structure, biosynthesis, and
600 oligogalacturonide-related signaling, *Phytochemistry*. 57 (2001) 929–967.
601 [https://doi.org/10.1016/S0031-9422\(01\)00113-3](https://doi.org/10.1016/S0031-9422(01)00113-3).
- 602 [2] D. Mohnen, Pectin structure and biosynthesis, *Curr. Opin. Plant Biol.* 11 (2008) 266–
603 277. <https://doi.org/10.1016/j.pbi.2008.03.006>.
- 604 [3] M.A. Atmodjo, Z. Hao, D. Mohnen, Evolving views of pectin biosynthesis, *Annu. Rev.*
605 *Plant Biol.* 64 (2013) 747–779. [https://doi.org/10.1146/annurev-arplant-042811-
606 105534](https://doi.org/10.1146/annurev-arplant-042811-105534).
- 607 [4] Y. Rui, C. Xiao, H. Yi, B. Kandemir, J.Z. Wang, V.M. Puri, C.T. Anderson,
608 POLYGALACTURONASE INVOLVED IN EXPANSION3 functions in seedling
609 development, rosette growth, and stomatal dynamics in *Arabidopsis thaliana*, *Plant*
610 *Cell*. 29 (2017) 2413–2432. <https://doi.org/10.1105/tpc.17.00568>.
- 611 [5] C. Xiao, C. Somerville, C.T. Anderson, POLYGALACTURONASE INVOLVED IN
612 EXPANSION1 functions in cell elongation and flower development in *Arabidopsis*,
613 *Plant Cell*. 26 (2014) 1018–1035. <https://doi.org/10.1105/tpc.114.123968>.
- 614 [6] J. Pelloux, C. Rustérucci, E.J. Mellerowicz, New insights into pectin methylesterase
615 structure and function, *Trends Plant Sci.* 12 (2007) 267–277.
616 <https://doi.org/10.1016/j.tplants.2007.04.001>.
- 617 [7] F. Sénéchal, A. Mareck, P. Marcelo, P. Lerouge, J. Pelloux, *Arabidopsis* PME17
618 Activity can be Controlled by Pectin Methylesterase Inhibitor4, *Plant Signal. Behav.* 10
619 (2015) e983351. <https://doi.org/10.4161/15592324.2014.983351>.
- 620 [8] V.S. Nocker, L. Sun, Analysis of promoter activity of members of the Pectate lyase-
621 like(PLL) gene family in cell separation in *Arabidopsis*, *BMC Plant Biol.* 10 (2010)
622 152. <https://doi.org/10.1186/1471-2229-10-152>.
- 623 [9] A. Voxeur, O. Habrylo, S. Guénin, F. Miart, M.C. Soulié, C. Rihouey, C. Pau-Roblot,
624 J.M. Domon, L. Gutierrez, J. Pelloux, G. Mouille, M. Fagard, H. Höfte, S. Vernhettes,
625 Oligogalacturonide production upon *Arabidopsis thaliana*-*Botrytis cinerea* interaction,
626 *Proc. Natl. Acad. Sci. U. S. A.* 116 (2019) 19743–19752.
627 <https://doi.org/10.1073/pnas.1900317116>.

- 628 [10] I. Kars, G.H. Krooshof, L. Wagemakers, R. Joosten, J.A.E. Benen, J.A.L. Van Kan,
629 Necrotizing activity of five *Botrytis cinerea* endopolygalacturonases produced in *Pichia*
630 *pastoris*, *Plant J.* 43 (2005) 213–225. [https://doi.org/10.1111/j.1365-](https://doi.org/10.1111/j.1365-313X.2005.02436.x)
631 313X.2005.02436.x.
- 632 [11] R.P. Jolie, T. Duvetter, A.M. Van Loey, M.E. Hendrickx, Pectin methylesterase and its
633 proteinaceous inhibitor: A review, *Carbohydr. Res.* 345 (2010) 2583–2595.
634 <https://doi.org/10.1016/j.carres.2010.10.002>.
- 635 [12] R.S. Jayani, S. Saxena, R. Gupta, Microbial pectinolytic enzymes: A review, *Process*
636 *Biochem.* 40 (2005) 2931–2944. <https://doi.org/10.1016/j.procbio.2005.03.026>.
- 637 [13] H. Suzuki, T. Morishima, A. Handa, H. Tsukagoshi, M. Kato, M. Shimizu,
638 Biochemical Characterization of a Pectate Lyase AnPL9 from *Aspergillus nidulans*,
639 *Appl. Biochem. Biotechnol.* (2022). <https://doi.org/10.1007/s12010-022-04036-x>.
- 640 [14] G. Limberg, R. Körner, H.C. Buchholt, T.M.I.E. Christensen, P. Roepstorff, J.D.
641 Mikkelsen, Analysis of different de-esterification mechanisms for pectin by enzymatic
642 fingerprinting using endopectin lyase and endopolygalacturonase II from *A. Niger*,
643 *Carbohydr. Res.* 327 (2000) 293–307. [https://doi.org/10.1016/S0008-6215\(00\)00067-7](https://doi.org/10.1016/S0008-6215(00)00067-7).
- 644 [15] O. Mayans, M. Scott, I. Connerton, T. Gravesen, J. Benen, J. Visser, R. Pickersgill, J.
645 Jenkins, Two crystal structures of pectin lyase A from *Aspergillus* reveal a pH driven
646 conformational change and striking divergence in the substrate-binding clefts of pectin
647 and pectate lyases, *Structure.* 5 (1997) 677–689. [https://doi.org/10.1016/S0969-](https://doi.org/10.1016/S0969-2126(97)00222-0)
648 2126(97)00222-0.
- 649 [16] S. Yadav, P.K. Yadav, D. Yadav, K.D.S. Yadav, Pectin lyase: A review, *Process*
650 *Biochem.* 44 (2009) 1–10. <https://doi.org/10.1016/j.procbio.2008.09.012>.
- 651 [17] F. Sénéchal, C. Wattier, C. Rustérucci, J. Pelloux, Homogalacturonan-modifying
652 enzymes: Structure, expression, and roles in plants, *J. Exp. Bot.* 65 (2014) 5125–5160.
653 <https://doi.org/10.1093/jxb/eru272>.
- 654 [18] B. Zeuner, T.B. Thomsen, M.A. Stringer, K.B.R.M. Krogh, A.S. Meyer, J. Holck,
655 Comparative Characterization of *Aspergillus* Pectin Lyases by Discriminative
656 Substrate Degradation Profiling, *Front. Bioeng. Biotechnol.* 8 (2020).
657 <https://doi.org/10.3389/fbioe.2020.00873>.

- 658 [19] G. Yang, W. Chen, H. Tan, K. Li, J. Li, H. Yin, Biochemical characterization and
659 evolutionary analysis of a novel pectate lyase from *Aspergillus parasiticus*, *Int. J. Biol.*
660 *Macromol.* 152 (2020) 180–188. <https://doi.org/10.1016/j.ijbiomac.2020.02.279>.
- 661 [20] M.D. Yoder, S.E. Lietzke, F. Journak, Unusual structural features in the parallel β -helix
662 in pectate lyases, *Structure.* 1 (1993) 241–251. [https://doi.org/10.1016/0969-](https://doi.org/10.1016/0969-2126(93)90013-7)
663 [2126\(93\)90013-7](https://doi.org/10.1016/0969-2126(93)90013-7).
- 664 [21] J. Vitali, B. Schick, H.C.M. Kester, J. Visser, F. Journak, The Three-Dimensional
665 Structure of *Aspergillus niger* Pectin Lyase B at 1.7-Å Resolution, *Plant Physiol.* 116
666 (1998) 69–80. <https://doi.org/10.1104/pp.116.1.69>.
- 667 [22] S.E. Lietzke, R.D. Scavetta, M.D. Yoder, F. Journak, The Refined Three-Dimensional
668 Structure of Pectate Lyase E from *Erwinia chrysanthemi* at 2.2 Å Resolution, *Plant*
669 *Physiol.* 111 (1996) 73–92. <https://doi.org/10.1104/pp.111.1.73>.
- 670 [23] M. Akita, A. Suzuki, T. Kobayashi, S. Ito, T. Yamane, The first structure of pectate
671 lyase belonging to polysaccharide lyase family 3, *Acta Crystallogr. Sect. D Biol.*
672 *Crystallogr.* 57 (2001) 1786–1792. <https://doi.org/10.1107/S0907444901014482>.
- 673 [24] R. Pickersgill, J. Jenkins, G. Harris, W. Nasser, J. Robert Baudouy, The structure of
674 *Bacillus subtilis* pectate lyase in complex with calcium, *Nat. Struct. Biol.* 1 (1994)
675 717–723. <https://doi.org/10.1038/nsb1094-717>.
- 676 [25] A.S. Luis, J. Briggs, X. Zhang, B. Farnell, D. Ndeh, A. Labourel, A. Baslé, A.
677 Cartmell, N. Terrapon, K. Stott, E.C. Lowe, R. McLean, K. Shearer, J. Schückel, I.
678 Venditto, M.C. Ralet, B. Henrissat, E.C. Martens, S.C. Mosimann, D.W. Abbott, H.J.
679 Gilbert, Dietary pectic glycans are degraded by coordinated enzyme pathways in
680 human colonic *Bacteroides*, *Nat. Microbiol.* 3 (2018) 210–219.
681 <https://doi.org/10.1038/s41564-017-0079-1>.
- 682 [26] K. Johansson, M. El-Ahmad, R. Friemann, H. Jörnvall, O. Markovič, H. Eklund,
683 Crystal structure of plant pectin methylesterase, *FEBS Lett.* 514 (2002) 243–249.
684 [https://doi.org/10.1016/S0014-5793\(02\)02372-4](https://doi.org/10.1016/S0014-5793(02)02372-4).
- 685 [27] S.W. Cho, S. Lee, W. Shin, The X-ray structure of *Aspergillus aculeatus*
686 Polygalacturonase and a Modeled structure of the Polygalacturonase-Octagalacturonate
687 Complex, *J. Mol. Biol.* 311 (2001) 863–878. <https://doi.org/10.1006/jmbi.2001.4919>.

- 688 [28] T.N. Petersen, S. Kauppinen, S. Larsen, The crystal structure of rhamnogalacturonase a
689 from *Aspergillus aculeatus*: A right-handed parallel β helix, *Structure*. 5 (1997) 533–
690 544. [https://doi.org/10.1016/S0969-2126\(97\)00209-8](https://doi.org/10.1016/S0969-2126(97)00209-8).
- 691 [29] R.D. Scavetta, S.R. Herron, A.T. Hotchkiss, N. Kita, N.T. Keen, J.A.E. Benen, H.C.M.
692 Kester, J. Visser, F. Journak, Structure of a plant cell wall fragment complexed to
693 pectate lyase C, *Plant Cell*. 11 (1999) 1081–1092.
694 <https://doi.org/10.1105/tpc.11.6.1081>.
- 695 [30] A. Blum, M. Bressan, A. Zahid, I. Trinsoutrot-Gattin, A. Driouich, K. Laval,
696 *Verticillium Wilt on Fiber Flax: Symptoms and Pathogen Development In Planta*, *Plant*
697 *Dis.* 102 (2018) 2421–2429. <https://doi.org/10.1094/PDIS-01-18-0139-RE>.
- 698 [31] K. Zeise, A. Von Tiedemann, Host specialization among vegetative compatibility
699 groups of *Verticillium dahliae* in relation to *Verticillium longisporum*, *J. Phytopathol.*
700 150 (2002) 112–119. <https://doi.org/10.1046/j.1439-0434.2002.00730.x>.
- 701 [32] J. Zhang, X. Yu, C. Zhang, Q. Zhang, Y. Sun, H. Zhu, C. Tang, Pectin lyase enhances
702 cotton resistance to *Verticillium wilt* by inducing cell apoptosis of *Verticillium dahliae*,
703 *J. Hazard. Mater.* 404 (2021) 124029. <https://doi.org/10.1016/j.jhazmat.2020.124029>.
- 704 [33] J.Y. Chen, H.L. Xiao, Y.J. Gui, D.D. Zhang, L. Li, Y.M. Bao, X.F. Dai,
705 Characterization of the *Verticillium dahliae* exoproteome involves in pathogenicity
706 from cotton-containing medium, *Front. Microbiol.* 7 (2016) 1–15.
707 <https://doi.org/10.3389/fmicb.2016.01709>.
- 708 [34] S.J. Klosterman, Z.K. Atallah, G.E. Vallad, K. V. Subbarao, Diversity, Pathogenicity,
709 and Management of *Verticillium* Species, *Annu. Rev. Phytopathol.* 47 (2009) 39–62.
710 <https://doi.org/10.1146/annurev-phyto-080508-081748>.
- 711 [35] Y. Yang, Y. Zhang, B. Li, X. Yang, Y. Dong, D. Qiu, A *Verticillium dahliae* Pectate
712 Lyase Induces Plant Immune Responses and Contributes to Virulence, *Front. Plant Sci.*
713 9 (2018) 1–15. <https://doi.org/10.3389/fpls.2018.01271>.
- 714 [36] D. Duressa, A. Anchieta, D. Chen, A. Klimes, M.D. Garcia-Pedrajas, K.F. Dobinson,
715 S.J. Klosterman, RNA-seq analyses of gene expression in the microsclerotia of
716 *Verticillium dahliae*, *BMC Genomics*. 14 (2013) 5–18. <https://doi.org/10.1186/1471-2164-14-607>.

- 718 [37] J. Safran, O. Habrylo, M. Cherkaoui, S. Lecomte, A. Voxeur, S. Pilard, S. Bassard, C.
719 Pau-Roblot, D. Mercadante, J. Pelloux, F. Sénéchal, New insights into the specificity
720 and processivity of two novel pectinases from *Verticillium dahliae*, *Int. J. Biol.*
721 *Macromol.* 176 (2021) 165–176. <https://doi.org/10.1016/j.ijbiomac.2021.02.035>.
- 722 [38] A. Lemaire, C. Duran Garzon, A. Perrin, O. Habrylo, P. Trezel, S. Bassard, V.
723 Lefebvre, O. Van Wuytswinkel, A. Guillaume, C. Pau-Roblot, J. Pelloux, Three novel
724 rhamnogalacturonan I- pectins degrading enzymes from *Aspergillus aculeatinus*:
725 Biochemical characterization and application potential, *Carbohydr. Polym.* 248 (2020)
726 116752. <https://doi.org/10.1016/j.carbpol.2020.116752>.
- 727 [39] W. Kabsch, Xds., *Acta Crystallogr. D. Biol. Crystallogr.* 66 (2010) 125–32.
728 <https://doi.org/10.1107/S0907444909047337>.
- 729 [40] W. Kabsch, Integration, scaling, space-group assignment and post-refinement, *Acta*
730 *Crystallogr. Sect. D Biol. Crystallogr.* 66 (2010) 133–144.
731 <https://doi.org/10.1107/S0907444909047374>.
- 732 [41] B.W. Matthews, Solvent content of protein crystals., *J. Mol. Biol.* 33 (1968) 491–497.
733 [https://doi.org/10.1016/0022-2836\(68\)90205-2](https://doi.org/10.1016/0022-2836(68)90205-2).
- 734 [42] A.J. McCoy, R.W. Grosse-Kunstleve, P.D. Adams, M.D. Winn, L.C. Storoni, R.J.
735 Read, Phaser crystallographic software, *J. Appl. Crystallogr.* 40 (2007) 658–674.
736 <https://doi.org/10.1107/S0021889807021206>.
- 737 [43] Y. Zheng, C.H. Huang, W. Liu, T.P. Ko, Y. Xue, C. Zhou, R.T. Guo, Y. Ma, Crystal
738 structure and substrate-binding mode of a novel pectate lyase from alkaliphilic *Bacillus*
739 *sp.* N16-5, *Biochem. Biophys. Res. Commun.* 420 (2012) 269–274.
740 <https://doi.org/10.1016/j.bbrc.2012.02.148>.
- 741 [44] D. Liebschner, P. V. Afonine, M.L. Baker, G. Bunkoczi, V.B. Chen, T.I. Croll, B.
742 Hintze, L.W. Hung, S. Jain, A.J. McCoy, N.W. Moriarty, R.D. Oeffner, B.K. Poon,
743 M.G. Prisant, R.J. Read, J.S. Richardson, D.C. Richardson, M.D. Sammito, O. V.
744 Sobolev, D.H. Stockwell, T.C. Terwilliger, A.G. Urzhumtsev, L.L. Videau, C.J.
745 Williams, P.D. Adams, Macromolecular structure determination using X-rays, neutrons
746 and electrons: Recent developments in Phenix, *Acta Crystallogr. Sect. D Struct. Biol.*
747 75 (2019) 861–877. <https://doi.org/10.1107/S2059798319011471>.
- 748 [45] P. Emsley, B. Lohkamp, W.G. Scott, K. Cowtan, Features and development of Coot,

- 749 Acta Crystallogr. Sect. D Biol. Crystallogr. 66 (2010) 486–501.
750 <https://doi.org/10.1107/S0907444910007493>.
- 751 [46] L. Hocq, S. Guinand, O. Habrylo, A. Voxeur, W. Tabi, J. Safran, F. Fournet, J.-M.
752 Domon, J.-C. Mollet, S. Pilard, C. Pau- Roblot, A. Lehner, J. Pelloux, V. Lefebvre,
753 The exogenous application of AtPGLR, an endo - polygalacturonase, triggers pollen
754 tube burst and repair, *Plant J.* 103 (2020) 617–633. <https://doi.org/10.1111/tpj.14753>.
- 755 [47] K. Lindorff-Larsen, S. Piana, K. Palmo, P. Maragakis, J.L. Klepeis, R.O. Dror, D.E.
756 Shaw, Improved side-chain torsion potentials for the Amber ff99SB protein force field,
757 *Proteins Struct. Funct. Bioinforma.* 78 (2010) 1950–1958.
758 <https://doi.org/10.1002/prot.22711>.
- 759 [48] W.L. Jorgensen, J. Chandrasekhar, J.D. Madura, R.W. Impey, M.L. Klein, Comparison
760 of simple potential functions for simulating liquid water, *J. Chem. Phys.* 79 (1983)
761 926–935. <https://doi.org/10.1063/1.445869>.
- 762 [49] J.S. Rowlinson, The Maxwell-boltzmann distribution, *Mol. Phys.* 103 (2005) 2821–
763 2828. <https://doi.org/10.1080/002068970500044749>.
- 764 [50] H.J.C. Berendsen, J.P.M. Postma, W.F. Van Gunsteren, A. Dinola, J.R. Haak,
765 Molecular dynamics with coupling to an external bath, *J. Chem. Phys.* 81 (1984) 3684–
766 3690. <https://doi.org/10.1063/1.448118>.
- 767 [51] M. Parrinello, A. Rahman, Polymorphic transitions in single crystals: A new molecular
768 dynamics method, *J. Appl. Phys.* 52 (1981) 7182–7190.
769 <https://doi.org/10.1063/1.328693>.
- 770 [52] T. Darden, D. York, L. Pedersen, Particle mesh Ewald: An $N \cdot \log(N)$ method for Ewald
771 sums in large systems, *J. Chem. Phys.* 98 (1993) 10089–10092.
772 <https://doi.org/10.1063/1.464397>.
- 773 [53] T. Kluyver, B. Ragan-Kelley, F. Pérez, B. Granger, M. Bussonnier, J. Frederic, K.
774 Kelley, J. Hamrick, J. Grout, S. Corlay, P. Ivanov, D. Avila, S. Abdalla, C. Willing,
775 Jupyter Notebooks—a publishing format for reproducible computational workflows,
776 *Position. Power Acad. Publ. Play. Agents Agendas - Proc. 20th Int. Conf. Electron.*
777 *Publ. ELPUB 2016.* (2016) 87–90. <https://doi.org/10.3233/978-1-61499-649-1-87>.
- 778 [54] J.D. Hunter, Matplotlib: A 2D graphics environment, *Comput. Sci. Eng.* 9 (2007) 90–

- 779 95. <https://doi.org/10.1109/MCSE.2007.55>.
- 780 [55] W. Humphrey, A. Dalke, K. Schulten, VMD: Visual Molecular Dynamics, *J. Mol.*
781 *Graph.* 14 (1996) 33–38.
- 782 [56] S.J. Klosterman, K. V. Subbarao, S. Kang, P. Veronese, S.E. Gold, B.P.H.J. Thomma,
783 Z. Chen, B. Henrissat, Y.-H. Lee, J. Park, M.D. Garcia-Pedrajas, D.J. Barbara, A.
784 Anchieta, R. de Jonge, P. Santhanam, K. Maruthachalam, Z. Atallah, S.G. Amyotte, Z.
785 Paz, P. Inderbitzin, R.J. Hayes, D.I. Heiman, S. Young, Q. Zeng, R. Engels, J. Galagan,
786 C.A. Cuomo, K.F. Dobinson, L.-J. Ma, Comparative Genomics Yields Insights into
787 Niche Adaptation of Plant Vascular Wilt Pathogens, *PLoS Pathog.* 7 (2011) e1002137.
788 <https://doi.org/10.1371/journal.ppat.1002137>.
- 789 [57] S. Mandelc, B. Javornik, The secretome of vascular wilt pathogen *Verticillium albo-*
790 *atrum* in simulated xylem fluid, *Proteomics.* 15 (2015) 787–797.
791 <https://doi.org/10.1002/pmic.201400181>.
- 792 [58] S.D. Liston, S.A. McMahon, A. Le Bas, M.D.L. Suits, J.H. Naismith, C. Whitfield,
793 Periplasmic depolymerase provides insight into ABC transporter-dependent secretion
794 of bacterial capsular polysaccharides, *Proc. Natl. Acad. Sci. U. S. A.* 115 (2018)
795 E4870–E4879. <https://doi.org/10.1073/pnas.1801336115>.
- 796 [59] J. Jenkins, R. Pickersgill, The architecture of parallel β -helices and related folds, *Prog.*
797 *Biophys. Mol. Biol.* 77 (2001) 111–175. [https://doi.org/10.1016/S0079-](https://doi.org/10.1016/S0079-6107(01)00013-X)
798 [6107\(01\)00013-X](https://doi.org/10.1016/S0079-6107(01)00013-X).
- 799 [60] M.D. Yoder, F. Journak, The Refined Three-Dimensional Structure of Pectate Lyase C
800 Implications for an Enzymatic Mechanism, *Plant Physiol.* 107 (1995) 349–364.
- 801 [61] Y. van Santen, J.A.E. Benen, K.H. Schroter, K.H. Kalk, S. Armand, J. Visser, B.W.
802 Dijkstra, 1.68-angstrom crystal structure of endopolygalacturonase II from *Aspergillus*
803 *niger* and identification of active site residues by site-directed mutagenesis, *J. Biol.*
804 *Chem.* 274 (1999) 30474–30480. <https://doi.org/10.1074/JBC.274.43.30474>.
- 805 [62] S.E. Lietzke, R.D. Scavetta, M.D. Yoder, The Refined Three-Dimensional Structure of
806 Pectate Lyase E from, *Plant Physiol.* 111 (1996) 73–92.
- 807 [63] B. Henrissat, S.E. Heffron, M.D. Yoder, S.E. Lietzke, F. Journak, Functional
808 implications of structure-based sequence alignment of proteins in the extracellular

- 809 pectate lyase superfamily., *Plant Physiol.* 107 (1995) 963–76.
810 <https://doi.org/10.1104/pp.107.3.963>.
- 811 [64] N. Kita, C.M. Boyd, M.R. Garrett, F. Jurnak, N.T. Keen, Differential Effect of Site-
812 directed Mutations in *pelC* on Pectate Lyase Activity, Plant Tissue Maceration, and
813 Elicitor Activity, *J. Biol. Chem.* 271 (1996) 26529–26535.
814 <https://doi.org/10.1074/jbc.271.43.26529>.
- 815 [65] S. Ali, C.R. Søndergaard, S. Teixeira, R.W. Pickersgill, Structural insights into the loss
816 of catalytic competence in pectate lyase activity at low pH, *FEBS Lett.* 589 (2015)
817 3242–3246. <https://doi.org/10.1016/j.febslet.2015.09.014>.
- 818 [66] C. Creze, S. Castang, E. Derivery, R. Haser, N. Hugouvieux-Cotte-Pattat, V.E.
819 Shevchik, P. Gouet, The Crystal Structure of Pectate Lyase *PelII* from Soft Rot
820 Pathogen *Erwinia chrysanthemi* in Complex with Its Substrate, *J. Biol. Chem.* 283
821 (2008) 18260–18268. <https://doi.org/10.1074/jbc.M709931200>.
- 822 [67] A. Dubey, S. Yadav, M. Kumar, G. Anand, D. Yadav, Molecular Biology of Microbial
823 Pectate Lyase: A Review, *Br. Biotechnol. J.* 13 (2016) 1–26.
824 <https://doi.org/10.9734/bbj/2016/24893>.
- 825 [68] H.G. Ouattara, S. Reverchon, S.L. Niamke, W. Nasser, Biochemical Properties of
826 Pectate Lyases Produced by Three Different *Bacillus* Strains Isolated from Fermenting
827 Cocoa Beans and Characterization of Their Cloned Genes, *Appl. Environ. Microbiol.*
828 76 (2010) 5214–5220. <https://doi.org/10.1128/AEM.00705-10>.
- 829 [69] M. Soriano, A. Blanco, P. Díaz, F.I.J. Pastor, An unusual pectate lyase from a *Bacillus*
830 sp. with high activity on pectin: Cloning and characterization, *Microbiology.* 146
831 (2000) 89–95. <https://doi.org/10.1099/00221287-146-1-89>.
- 832 [70] G. Chilosi, P. Magro, Pectin lyase and polygalacturonase isoenzyme production by
833 *Botrytis cinerea* during the early stages of infection on different host plants, *J. Plant*
834 *Pathol.* 79 (1997) 61–69. <https://doi.org/10.1080/01904167.2015.1112950>.
- 835 [71] S. Hassan, V.E. Shevchik, X. Robert, N. Hugouvieux-Cotte-Pattat, *PelN* is a new
836 pectate lyase of *dickeya dadantii* with unusual characteristics, *J. Bacteriol.* 195 (2013)
837 2197–2206. <https://doi.org/10.1128/JB.02118-12>.
- 838 [72] C. Zhou, Y. Xue, Y. Ma, Cloning, evaluation, and high-level expression of a thermo-

- 839 alkaline pectate lyase from alkaliphilic *Bacillus clausii* with potential in ramie
840 degumming, *Appl. Microbiol. Biotechnol.* 101 (2017) 3663–3676.
841 <https://doi.org/10.1007/s00253-017-8110-2>.
- 842 [73] W. Sukhumsirchart, S. Kawanishi, W. Deesukon, K. Chansiri, H. Kawasaki, T.
843 Sakamoto, Purification, Characterization, and Overexpression of Thermophilic Pectate
844 Lyase of *Bacillus* sp. RN1 Isolated from a Hot Spring in Thailand, *Biosci. Biotechnol.*
845 *Biochem.* 73 (2009) 268–273. <https://doi.org/10.1271/bbb.80287>.
- 846 [74] C. Zhang, J. Yao, C. Zhou, L. Mao, G. Zhang, Y. Ma, The alkaline pectate lyase
847 PEL168 of *Bacillus subtilis* heterologously expressed in *Pichia pastoris* more stable
848 and efficient for degumming ramie fiber, *BMC Biotechnol.* 13 (2013) 26.
849 <https://doi.org/10.1186/1472-6750-13-26>.
- 850 [75] P. Yuan, K. Meng, Y. Wang, H. Luo, P. Shi, H. Huang, T. Tu, P. Yang, B. Yao, A
851 Low-Temperature-Active Alkaline Pectate Lyase from *Xanthomonas campestris*
852 ACCC 10048 with High Activity over a Wide pH Range, *Appl. Biochem. Biotechnol.*
853 168 (2012) 1489–1500. <https://doi.org/10.1007/s12010-012-9872-8>.
- 854 [76] Y. Tang, P. Wu, S. Jiang, J.N. Selvaraj, S. Yang, G. Zhang, A new cold-active and
855 alkaline pectate lyase from Antarctic bacterium with high catalytic efficiency, *Appl.*
856 *Microbiol. Biotechnol.* 103 (2019) 5231–5241. [https://doi.org/10.1007/s00253-019-](https://doi.org/10.1007/s00253-019-09803-1)
857 [09803-1](https://doi.org/10.1007/s00253-019-09803-1).
- 858 [77] P. Wu, S. Yang, Z. Zhan, G. Zhang, Origins and features of pectate lyases and their
859 applications in industry, *Appl. Microbiol. Biotechnol.* 104 (2020) 7247–7260.
860 <https://doi.org/10.1007/s00253-020-10769-8>.
- 861 [78] Z. Zhou, Y. Liu, Z. Chang, H. Wang, A. Leier, T.T. Marquez-Lago, Y. Ma, J. Li, J.
862 Song, Structure-based engineering of a pectate lyase with improved specific activity for
863 ramie degumming, *Appl. Microbiol. Biotechnol.* 101 (2017) 2919–2929.
864 <https://doi.org/10.1007/s00253-016-7994-6>.
- 865 [79] M.D. Joshi, G. Sidhu, I. Pot, G.D. Brayer, S.G. Withers, L.P. McIntosh, Hydrogen
866 bonding and catalysis: A novel explanation for how a single amino acid substitution
867 can change the pH optimum of a glycosidase, *J. Mol. Biol.* 299 (2000) 255–279.
868 <https://doi.org/10.1006/jmbi.2000.3722>.
- 869 [80] T. Yasuda, H. Takeshita, R. Iida, M. Ueki, T. Nakajima, Y. Kaneko, K. Mogi, Y.

- 870 Kominato, K. Kishi, A single amino acid substitution can shift the optimum pH of
871 DNase I for enzyme activity: Biochemical and molecular analysis of the piscine DNase
872 I family, *Biochim. Biophys. Acta - Gen. Subj.* 1672 (2004) 174–183.
873 <https://doi.org/10.1016/j.bbagen.2004.03.012>.
- 874 [81] H. Shibuya, S. Kaneko, K. Hayashi, A single amino acid substitution enhances the
875 catalytic activity of family 11 xylanase at alkaline pH, *Biosci. Biotechnol. Biochem.* 69
876 (2005) 1492–1497. <https://doi.org/10.1271/bbb.69.1492>.
- 877 [82] M. Goetz, T. Roitsch, The different pH optima and substrate specificities of
878 extracellular and vacuolar invertases from plants are determined by a single amino-acid
879 substitution, *Plant J.* 20 (1999) 707–711. [https://doi.org/10.1046/j.1365-](https://doi.org/10.1046/j.1365-313X.1999.00628.x)
880 [313X.1999.00628.x](https://doi.org/10.1046/j.1365-313X.1999.00628.x).
- 881

1 **The specificity of pectate lyase VdPelB from *Verticillium dahliae*: ~~its specificities is~~**
2 **highlighted by structural, dynamical and biochemical characterizations of *Verticillium***
3 ***dahliae* pectate lyase, VdPelB, highlight its specificities**

4
5 Josip Safran¹, Vanessa Ung², Julie Bouckaert³, Olivier Habrylo¹, Roland Molinié¹, Jean-Xavier
6 Fontaine¹, Adrien Lemaire¹, Aline Voxeur⁴, Serge Pilard⁵, Corinne Pau-Roblot¹, Davide
7 Mercadante², Jérôme Pelloux^{1*}, Fabien Sénéchal^{1*}

8

9

10 ¹ : UMRT INRAE 1158 BioEcoAgro – BIOPI Biologie des Plantes et Innovation, Université
11 de Picardie, 33 Rue St Leu, 80039 Amiens, France. ² : School of Chemical Sciences, The
12 University of Auckland, Private Bag 92019, Auckland 1142, New Zealand. ³ : UMR 8576
13 Unité de Glycobiologie Structurale et Fonctionnelle (UGSF) IRI50, Avenue de Halley, 59658
14 Villeneuve d'Ascq, France. ⁴ : Université Paris-Saclay, INRAE, AgroParisTech, Institut Jean-
15 Pierre Bourgin (IJPB), 78000, Versailles, France. ⁵ : Plateforme Analytique, Université de
16 Picardie, 33, Rue St Leu, 80039 Amiens, France.

17 *contributed equally as last authors

18 **Corresponding author:** Fabien Sénéchal (fabien.senechal@u-picardie.fr) and Jérôme Pelloux
19 (jerome.pelloux@u-picardie.fr)

20 UMR INRAE 1158 BioEcoAgro-Biologie des Plantes et Innovation, Université de Picardie
21 Jules Verne, UFR des Sciences, 33 Rue St Leu, 80039 Amiens, France

22

23 **Abstract**

24 Pectins, complex polysaccharides and major components of the plant primary cell wall, can be
25 degraded by pectate lyases (PLs). PLs cleave glycosidic bonds of homogalacturonans (HG), the
26 main pectic domain, by β -elimination, releasing unsaturated oligogalacturonides (OGs). To
27 understand the catalytic mechanism and structure/function of these enzymes, we characterized
28 VdPelB from *Verticillium dahliae*, ~~a plant pathogen~~. We first solved the crystal structure of
29 VdPelB at 1.2Å resolution showing that it is a right-handed parallel β -helix structure. Molecular
30 dynamics (MD) simulations further highlighted the dynamics of the enzyme in complex with
31 substrates that vary in their degree of methylesterification, identifying amino acids involved in
32 substrate binding and cleavage of non-methylesterified pectins. We then biochemically
33 characterized wild type and mutated forms of VdPelB. [Pectate lyase](#). VdPelB was most active
34 on non-methylesterified pectins, at pH ~~8.0–8~~ in presence of Ca^{2+} ions. [The](#) VdPelB-G125R
35 mutant was most active at pH ~~9.0–9~~ and showed higher relative activity compared to native
36 enzyme. The OGs released by VdPelB differed to that of previously characterized PLs, showing
37 its peculiar specificity in relation to its structure. OGs released from *Verticillium*-partially
38 tolerant and sensitive flax cultivars differed which could facilitate the identification VdPelB-
39 mediated elicitors of defence responses.

40

41

42

43 **Keywords:** Pectate lyase, pectins, homogalacturonan, oligogalacturonides, ~~Flax~~, *Verticillium*
44 *dahliae*.

45

46 1. Introduction

47 Primary cell wall, a complex structure of proteins and polysaccharides, cellulose and
48 hemicelluloses, is embedded in a pectin matrix. Pectins, are complex polysaccharides
49 composing up to 30% of cell wall dry mass in dicotyledonous species [1]. Pectin is mainly
50 constituted of homogalacturonan (HG), rhamnogalacturonan I (RG-I) and rhamnogalacturonan
51 II (RG-II) domains, but its composition can differ between plant organs and among species.
52 The most abundant pectic domain is HG, a linear homopolymer of α -1,4-linked galacturonic
53 acids (GalA), which represents up to 65% of pectins [2]. During synthesis, HG can be O-
54 acetylated at O-2 or O-3 and/or methylesterified at C-6 carboxyl, before being exported at the
55 cell wall with a degree of methylesterification (DM) of ~80% and a degree of acetylation (DA)
56 of ~5-10%, depending on species [3]. At the wall, HG chains can be modified by different
57 enzyme families, including pectin acetyltransferase (PAEs; EC 3.1.1.6), pectin methylesterases
58 (PMEs; CE8, EC 3.1.1.11), polygalacturonases (PGs; GH28, EC 3.2.1.15, EC 3.2.1.67, EC
59 3.2.1.82), and pectin lyases-like (PLLs), which comprise pectate lyases (PLs; EC 4.2.2.2) and
60 pectin lyase (PNLs, EC 4.2.2.10). All these enzymes are produced by plants to fine-tune pectin
61 during development [4–8], but they are also secreted by most phytopathogenic bacteria and
62 fungi during plant infection [9–13]. PMEs and PAE hydrolyse the O6-ester and O2-acetylated
63 linkages, respectively, leading to a higher susceptibility of HG to PG- and PLL-mediated
64 degradation [14]. PLL are pectolytic enzymes that cleave HG via a β -elimination mechanism
65 leading to the formation of an unsaturated C4-C5 bond [15], and can be divided into two
66 subfamilies depending on their biochemical specificities: i) PLs have a high affinity for non- or
67 low-methylesterified pectins and an optimal pH near 8.5. Their activity requires Ca^{2+} ions. ii)
68 PNLs are most active on high-DM pectins at acidic pH values [16]. Both type of enzymes can
69 degrade HG chains, and release oligogalacturonides (OGs), but their mode of action can differ.
70 For PLs both endo and exo modes of action have been described, while only endo-PNL have
71 been characterised so far [17]. For the latter, it was notably shown that endo-PNLs from *B.*
72 *fuckeliana*, *A. parasiticus* and *Aspergillus* sp., can first release OGs with degrees of
73 polymerisation (DP) 5–7, that are subsequently used as substrates, generating OGs of DP3 and
74 DP4 as end-products [9,18,19]. Despite having the same DP, the final products can differ in
75 their degrees and patterns of methylesterification and acetylation (DM/DA) depending on the
76 enzymes' specificities; implying potential differences in substrate binding, and therefore in
77 PLLs fine structures. Several crystallographic structures of bacterial and fungal PLL have been
78 reported [15,20–24]. Overall, the PLL fold resemble that of published PME, PGs and

79 rhamnogalacturonan lyases [25–27], and is composed of three parallel β -sheets forming a right-
80 handed parallel β -helix. The three β -sheets are called PB1, PB2 and PB3 and the turns
81 connecting them T1, T2 and T3 [28]. The active site features three Asp, localized on the PB1
82 β -sheet and, in the case of PLs, accommodates Ca^{2+} [29]. In PNLs, Ca^{2+} is, on the other hand,
83 replaced by Asp [15]. Additionally, the PL binding site is dominated by charged acidic and
84 basic residues (Gln, Lys, Arg) which can accommodate negatively charged pectate substrates.
85 In contrast, the PNL binding site is dominated by aromatic residues [15,29], which have less
86 affinity for lowly methylesterified pectins. These differences in structure could translate into
87 distinct enzyme dynamics when in complex with substrates of varying degrees of
88 methylesterification.

89 In fungi, PLLs are encoded by large multigenic families which are expressed during
90 infection. *Verticillium dahliae* Kleb., a soil-borne vascular fungus, targets a large number of
91 plant species, causing Verticillium wilt disease to become widespread among fiber flax, with
92 detrimental effects to fiber quality [30–32]. *V. dahliae* infects plants by piercing the root surface
93 using hyphae. When Verticillium reaches the vascular tissue, hyphae start to bud and form
94 conidia which are carried by progress in the xylem vessels and trapped at vessel end walls
95 before germinating and penetrating adjacent vessel elements to continue colonization and start
96 another infection cycle. [33,34]. During its colonization and proliferation Verticillium produces
97 and secretes a number of pectinolytic enzymes, including thirteen PLLs. Considering
98 the role of PLLs in determining pathogenicity, it is of paramount importance to determine their
99 biochemical and structural properties [30,35,36]. This could allow engineering novel strategies
100 to control or inhibit, the pathogen's pectinolytic arsenal. For this purpose, we characterized, via
101 combined experimental and computational approaches, one *V. dahliae* PLL (VdPelB,
102 VDAG_04718) after its heterologous expression in *P. pastoris*. The obtention of the 3D
103 structure of VdPelB after X-ray diffraction and the analysis of enzyme dynamics when in
104 complex with substrates of distinct DM, allowed the identification of the residues favouring
105 pectate lyase (PL) activity. Experiments confirmed the importance of these residues in
106 mediating PL activity showing that VdPelB is a *bona fide* PL, that releases peculiar OG as
107 compared to previously characterized PLs. More importantly, the OGs released from roots of
108 *Verticillium*-partially tolerant and sensitive flax cultivars differed, paving the way for the
109 identification of VdPelB-mediated OGs that can trigger plant defence mechanisms.

110

111 2. Material and methods

112 **2.1. Bioinformatical analysis**

113 *Verticillium dahliae* PLL sequences were retrieved using available genome database
114 (ftp.broadinstitute.org/). SignalP-5.0 Server (<http://www.cbs.dtu.dk/services/SignalP/>) was
115 used for identifying putative signal peptide and putative glycosylation sites were predicted
116 using ~~NetNGlyc 1.0 Server (<http://www.cbs.dtu.dk/services/NetNGlyc/>) and~~ NetOGlyc 4.0
117 Server (<http://www.cbs.dtu.dk/services/NetOGlyc/>). Sequences were aligned and phylogenetic
118 analysis was carried out using MEGA multiple sequence alignment program
119 (<https://www.megasoftware.net/>). Homology models used for molecular replacement were
120 created using I-TASSER structure prediction software
121 (<https://zhanglab.ccmb.med.umich.edu/I-TASSER/>) and UCSF Chimera
122 (<http://www.cgl.ucsf.edu/chimera/>) was used for creation of graphics.

123 **2.2. Fungal strain and growth**

124 *V. dahliae* was isolated from CALIRA company flax test fields (Martainneville, France) and
125 was kindly provided by Linéa-Semences company (Grandvilliers, France). Fungus was grown
126 as described in Safran et al. [37]. Briefly, fungus was grown in polygalacturonic acid sodium
127 salt (PGA, P3850, Sigma) at 10 g.L⁻¹ and in pectin methylesterified potassium salt from citrus
128 fruit (55–70% DM, P9436, Sigma) solutions to induce expression of PLLs-expression. After
129 15 days of growth in dark conditions at 25°C and 80 rpm shaking, mycelium was collected and
130 filtered under vacuum using Buchner flask. Collected mycelium was frozen in liquid nitrogen,
131 lyophilized and ground. Isolation of RNA and cDNA synthesis was realized as previously
132 described in Lemaire et al.[38].

133 **2.3. Cloning, heterologous expression and purification of VdPelB**

134 *V. dahliae* PelB ~~coding sequence~~gene (VdPelB, UNIPROT: G2X3Y1, GenBank:
135 EGY23280.1, *VDAG_04718*); consists of 1 single exon of 1002 bp length. The coding
136 sequence, minus the nucleotides encoding signal peptide, was PCR-amplified using cDNA and
137 gene-specific primers while -VdPelB mutants were generated by PCR mutagenesis, a method
138 for generating site-directed mutagenesis, following the same strategy and using cDNA and
139 specific primers carrying mutations (Table S1). Cloning of the PCR-amplified sequences in
140 pPICZαB, sequencing and expression in *P. pastoris* heterologous expression system as well as
141 purification steps were done Cloning, heterologous expression in *P. pastoris* and purification of
142 VdPelB was done as previously described in Safran et al. [37].

143 2.4. Crystallization of VdPelB

144 [Pectate lyase](#) VdPelB was concentrated at 10 mg.mL⁻¹ in Tris-HCl pH-7.5 buffer.
145 Crystallization conditions were screened using the sitting-drop vapor-diffusion method. [Pectate](#)
146 [lyase](#) VdPelB (100 nL) was mixed with an equal volume of precipitant (1:1) using Mosquito
147 robot (STP Labtech). The crystals that resulted in best diffraction data were obtained with 0.1
148 M MIB (Malonic acid, Imidazole, Boric acid system) at pH-8.0, with 25 % PEG 1500 as the
149 precipitant (condition B5 from the PACT premier kit, Molecular Dimensions, Sheffield, UK)
150 after 1 month. Optimization was realized using the hanging drop vapor-diffusion method
151 forming the drop by mixing 1 µL of precipitant solution with 1 µL of the enzyme. The ~~large~~
152 ~~beam-like~~ crystals (120 µm x 30 µm) – were cryo-protected by increasing PEG 1500
153 concentration to 35%, before mounting them in a loop and flash-cooling them in liquid nitrogen.

154 2.5. VdPelB X-ray data collection and processing

155 X-ray diffraction data were collected at the PROXIMA-2a beamline of the Soleil
156 synchrotron (Saint Aubin, France), at a temperature of -173°C using an EIGER 9M detector
157 (Dectris). Upon a first data collection to 1.3 Å resolution, three more data sets were collected
158 from the same crystal in order to obtain a complete data set. Thereby the kappa angle was tilted
159 once to 30°, once to 60° and finally a helical data set was collected at 1.2 Å resolution. The
160 reflections of each data set were indexed and integrated using XDS [39], scaled and merged
161 using XSCALE [40]. The VdPelB crystal has a primitive monoclinic lattice in the P 1 2₁ 1 space
162 group, with two molecules contained in asymmetric unit [41].

163 2.6. Structure solution and refinement

164 The structure of VdPelB was solved by molecular replacement using *Phaser* [42]. The data
165 were phased using pectate lyase BsPelA (PDB: 3VMV, Uniprot D0VP31), as a search model
166 [43]. Model was build using *Autobuild* and refined using *Refine* from PHENIX suite [44]. The
167 model was iteratively improved with *Coot* [45] and *Refine*. The final structure for VdPelB has
168 been deposited in the Protein Data Bank (PDB) as entry 7BBV.

169 2.7. VdPelB biochemical characterization

170 Pierce BCA Protein Assay Kit (Thermo Fisher Scientific, Waltham, Massachusetts, United
171 States) was used to determine the protein concentration, with Bovine Serum Albumin (A7906,
172 Sigma) as a standard. Deglycosylation was performed using Peptide-N-Glycosidase F (PNGase
173 F) at 37 °C for one hour according to the supplier's protocol (New England Biolabs, Hitchin,

174 UK). Enzyme purity and molecular weight were estimated using a 12% SDS-PAGE and mini-
175 PROTEAN 3 system (BioRad, Hercules, California, United States). Gels were stained using
176 PageBlue Protein Staining Solution (Thermo Fisher Scientific) according to the manufacturer's
177 protocol.

178 The substrate specificity of VdPelB was determined using PGA (81325, Sigma) and citrus
179 pectin of various DM: 20–34% (P9311, Sigma), 55–70% (P9436, Sigma) and >85% (P9561,
180 Sigma), with 0.5 μM CaCl_2 or 5 μM EDTA (Sigma) final concentrations. Enzyme activity was
181 measured by monitoring the increase in optical density at 235 nm due to formation of
182 unsaturated uronide product using UV/VIS Spectrophotometer (PowerWave Xs2, BioTek,
183 France) during 60 min. The optimum temperature was determined by incubating the enzymatic
184 reaction between ~~25–20~~ and ~~45–70~~^{20–30}°C for ~~8–12~~ min using PGA as a substrate (0.4%, w/v). The
185 optimum pH was determined between pH-~~5.0~~ and ~~10.0~~ using sodium phosphate (NaP, pH-~~5.0~~
186 to ~~7.0~~) and Tris-HCl buffer (pH-~~7.0~~ to ~~10.0~~) and 0.4% (w/v) PGA as a substrate. ~~All experiments~~
187 ~~were realized in triplicate. VdPelB and VdPelB-G125R kinetic parameters, K_m , V_{max} and k_{cat} ,~~
188 ~~were calculated using GraphPad Prism (8.4.2). The reactions were performed using 0.75 to 15~~
189 ~~mg.mL⁻¹ PGA concentrations at 50 mM Tris-HCl pH8.0 (native) and 9.0 (G125R) during 12~~
190 ~~min at 35°C.~~

191 All experiments were realized in triplicate. The statistical analysis was done using the
192 Welch's t-test.

193 ~~VdPelB and VdPelB-G125R kinetic parameters, K_m , V_{max} and k_{cat} , were calculated using~~
194 ~~GraphPad Prism (8.4.2). The reactions were performed using 0.75 to 15 mg.mL⁻¹ PGA~~
195 ~~concentrations at 50 mM Tris-HCl pH8.0 (native) and 9.0 (G125R) during 12 min at 35°C.~~

196 ~~All experiments were realized in triplicate.~~

197 **2.8. Digestion of commercial pectins and released OGs profiling**

198 OGs released after digestions by recombinant VdPelB or commercially available
199 Aspergillus PL (named AsPel) were identified as described in Voxeur et al., 2019 [9], using a
200 novel in-house OGs library. Briefly, DM 20–34% (P9311, Sigma) and sugar beet pectin with
201 DM 42% and degree of acetylation (DA) 31% (CP Kelco, Atlanta, United States) were prepared
202 at 0.4 % (w/v) final concentration diluted in 50 mM Tris-HCl buffer (pH-~~8.0~~) and incubated
203 with either VdPelB or AsPel (E-PCLYAN, Megazyme). For each substrate, enzyme
204 concentrations were adjusted to have enzymes at iso-activities (Table S2). For each substrate

205 two dilutions, were used for analysing OGs released in early, VdPelB-2 and AsPel-2, and late
206 phase, VdPelB-1 and AsPel-1, of digestions. Digestions were performed overnight. Non-
207 digested pectins were pelleted by centrifugation and the supernatant dried in a speed vacuum
208 concentrator (Concentrator plus, Eppendorf, Hamburg, Germany). Separation of OGs was done
209 as previously described using an ACQUITY UPLC Protein BEH SEC column (125Å, 1.7 µm,
210 4.6 mm x 300 mm) at a flow rate of 0.4 ml min⁻¹. MS detection ~~were-as~~ performed using an
211 ACQUITY UPLC H-Class system coupled to a SYNAPT G2-Si-Q-TOF hybrid quadrupole
212 time-of-flight instrument (Waters) equipped with an electrospray ionization (ESI) source (Z-
213 spray) and an additional sprayer for the reference compound (lock spray). Samples were
214 analysed by ESI-high-resolution MS (HRMS) and MS/MS in negative ionization mode. Data
215 acquisition and processing were performed with MASSLYNX software (v.4.1; Waters).
216 [9,37,46][44].

217 The intensities were defined as the area under the curve, for each OG. Peak areas were clustered
218 by hierarchical clustering with complete linkage on the euclidian distance matrix and visualized
219 in the heatmap-package using R version 3.6.0. The statistical analysis was done using the
220 Welch's t-test.

221 **2.9. Digestion of commercial pectins and released OGs profiling**

222 ~~OGs released after digestions by recombinant VdPelB or commercially available~~
223 ~~Aspergillus PL (named AsPel) were identified as described in Voxeur et al., 2019 [9], using a~~
224 ~~novel in-house OGs library. Briefly, DM 20-34% (P9311, Sigma) and sugar beet pectin with~~
225 ~~DM 42% and degree of acetylation (DA) 31% (CP Kelco, Atlanta, United States) were prepared~~
226 ~~at 0.4 % (w/v) final concentration diluted in 50 mM Tris HCl buffer (pH 8) and incubated with~~
227 ~~either VdPelB or AsPel (E-PCLYAN, Megazyme). For each substrate, enzyme concentrations~~
228 ~~were adjusted to have enzymes at iso-activities (Table S2). For each substrate two dilutions,~~
229 ~~were used for analysing OGs released in early, VdPelB-2 and AsPel-2 and late phase, VdPelB-~~
230 ~~1 and AsPel-1, of digestion. Digestions were performed overnight. Non-digested pectins were~~
231 ~~pelleted by centrifugation and the supernatant dried in a speed vacuum concentrator~~
232 ~~(Concentrator plus, Eppendorf, Hamburg, Germany). Separation of OGs was done as~~
233 ~~previously described using an ACQUITY UPLC Protein BEH SEC column (125Å, 1.7 µm, 4.6~~
234 ~~mm x 300 mm) [44]. The intensities were defined as the area under the curve, for each OG.~~
235 ~~Peak areas were clustered by hierarchical clustering with complete linkage on the euclidian~~
236 ~~distance matrix and visualized in the heatmap package using R version 3.6.0.~~

237 2.10.2.9. Molecular Dynamics simulations

238 Two sets of molecular dynamics (MD) simulations were conducted on the VdPelB protein:
239 one in complex with a fully non-methylesterified polygalacturonate decaaccharide, and the
240 other with a fully methylesterified polygalacturonate decaaccharide. Parameters specified by
241 the AMBER14SB_parmbsc1 forcefield [47] were used to create the molecular topologies of
242 the complexes. Each complex was set up in a cubic box with solute-box distances of 1.0 nm
243 and solvated with water molecules specific to the TIP3P water model [48]. Na⁺ and Cl⁻ ions
244 were added to neutralise the system's net charge and reach a salt concentration of 0.165 M.
245 Using a steep-descent algorithm with a step size of 0.01, energy minimisation was performed
246 to resolve clashes between particles, with convergence being established at a particle-particle
247 force of 1000 kJ mol⁻¹ nm⁻¹. Particle-particle forces were calculated by considering van der
248 Waals and electrostatic interactions occurring up to 1.0 nm, as well as long-range electrostatics
249 treated in the Fourier space using the Particle Mesh Ewald (PME) summation method. Solvent
250 equilibration was attained post minimisation in two stages: through the #VT-NVT and #PT-NPT
251 ensembles, to reach constant temperature and pressure, respectively. Equilibration of the
252 solvent under the #VT-NVT ensemble was conducted for 1 ns, integrating the equation of
253 motion at a time step of 2 fs. The target reference temperature was 310.15 K, coupled every 0.1
254 ps using the V-rescale thermostat³. Based on the Maxwell-Boltzmann distribution [49] at
255 310.15 K, random velocities were then assigned to each particle in the system. Finally, solvent
256 equilibration under the #PT-NPT ensemble was conducted for 1 ns, continuing from the last
257 step of the previous equilibration, in terms of particle coordinates and velocities, at a reference
258 temperature of 310.15 K, coupled every 0.1 ps using the V-rescale thermostat [50]. Here,
259 pressure coupling was isotropically coupled every 2.0 ps, at 1 bar, using the Parrinello-Rahman
260 barostat [51]. Particle-particle interactions were computed by constructing pair lists using the
261 Verlet scheme. Short-range van der Waals and electrostatic interactions sampled through a
262 Coulomb potential, were calculated at a cutoff of 1.0 nm. The PME algorithm [52] was used to
263 compute long-range electrostatic interactions beyond this cut-off in the Fourier space, utilising
264 a Fourier grid spacing of 0.16 and a cubic B-spline interpolation level at 4. The simulations
265 were then performed on in-house machines, using GROMACS (Groningen Machine for
266 Chemical Simulations) version 2021.37. Each set of simulations were run for 150 ns each, at a
267 time step of 2 fs, with molecular dynamics trajectories written out every 10 ps. Simulations
268 were replicated 7 times for a total production run time of 1.05 μs per complex. Replicates
269 differed with respect to the random particle velocity sets computed under the #VT-NVT

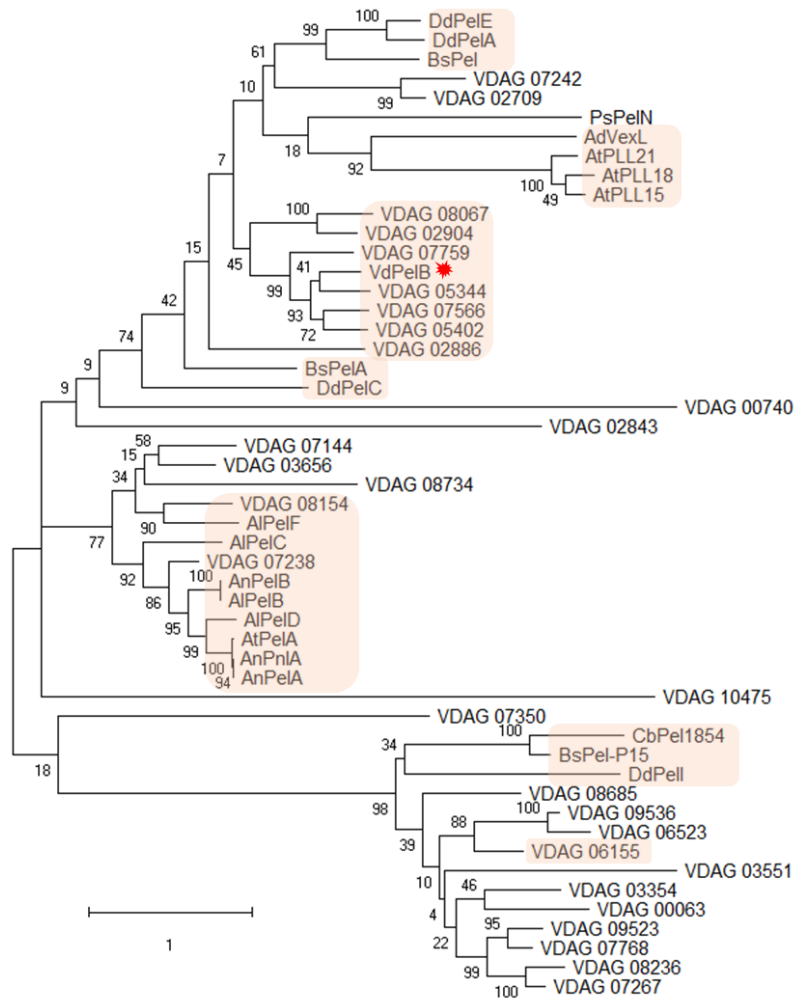
270 ensemble. For analysis, the first 50 ns of each production run were discarded as equilibration
271 time. In-house Python 3 scripts implemented using Jupyter notebooks [53] were used to carry
272 out analyses. Figures were created and rendered with Matplotlib [54] and VMD (Visual
273 Molecular Dynamics)[55].

274

275 3. Results and Discussion

276 3.1. Sequence and phylogeny analysis

277 In addition to 9 polygalacturonases (PGs) and 4 pectin methylesterases (PMEs), *V.*
278 *dahliae* encodes 30 putative endo-pectate lyases (EC 4.2.2.2), exo-pectate lyases (EC 4.2.2.9),
279 endo-pectin lyases (EC 4.2.2.10), belonging to PL1-PL3 and PL9 families, respectively [56].
280 For hierarchical clustering of *Verticilium*'s sequences with other PLLs, fifty-one amino acid
281 (~~aa~~) sequences encoding putative PLLs, belonging to bacteria, fungi and plants were aligned
282 and a phylogenetic tree was built. Different clades can be distinguished. (**Fig. 1**). *V. dahliae*
283 PelB (VdPelB, VDAG_04718) clustered with VDAG_05344 (59.68% sequence identity) with
284 close relations to VDAG_05402 (57.19% sequence identity) and VDAG_07566 (56.95%
285 sequence identity). VDAG_05402 and VDAG_05344, that are found in the protein secretome,
286 have orthologs in *V. alfa* (VDBG_07839 and VDBG_10041), which were shown to possess
287 putative lyase activity [36,57]. Plant PLLs from *A. thaliana* (AtPLL21, AtPLL15 and AtPLL18)
288 formed a separate clade with close connections to *A. denitrificans* (AdVexL), a PLL homologue
289 [58]. *D. dadanti* (DdPelI), *Bacillus Sp.* KSM-P15 (BsPel-P15) and *C. bescii* (CbPel1854)
290 formed separate clades similarly to *B. subtilis* and *D. dadantii* *PLs* (BsPel, DdPelA and
291 DdPelC). The clade corresponding to PNLs consisting of *A. tubingensis* PelA (AtPelA), *A.*
292 *niger* (AnPelA, AnPnIA and AnPelB), *A. luchuensis* AlPelB was closely related to
293 VDAG_07238 and VDAG_08154 which were indeed annotated as putative PNLs [18,56].
294 VDAG_06155 was previously named VdPelI and previously characterized as a pectate lyase
295 [35].



296

297 **Fig. 1. Phylogenetic analysis of *V. dahliae* *pectate lyase* VdPelB with selected PLLs**

298 Phylogenetic tree representing *V. dahliae* VdPelB (VDAG_04718, G2X3Y1, red star) amino acid sequence in
 299 comparison with PLLs from *Vorticillium* [VDAG_00740 (G2WQU8), VDAG_02904 (G2WXC5), VDAG_05344
 300 (G2X628), VDAG_07242 (G2XBA4), VDAG_07759 (G2XC77), VDAG_02709 (G2WWT0), VDAG_02843
 301 (G2WX64), VDAG_02886 (G2WXA7), VDAG_03656 (G2X1P5), VDAG_05402 (G2X597), VDAG_07144
 302 (G2X9U9), VDAG_07238 (G2XBA0), VDAG_07566 (G2XBY8), VDAG_08067 (G2XD35), VDAG_08154
 303 (G2XDC2), VDAG_08734 (G2XF02), VDAG_10475 (G2XJZ3), VDAG_03354 (G2WZB2), VDAG_03551
 304 (G2WZV9), VDAG_07267 (G2XBC9), VDAG_07768 (G2XC86), VDAG_08236 (G2XDK4), VDAG_06155
 305 (G2X8L4), VDAG_06523 (G2X7R5), VDAG_08685 (G2XEV0), VDAG_09523 (G2XH91), VDAG_09536
 306 (G2XHA4), VDAG_00063 (G2WR80), VDAG_07350 (G2XGG7)], *Arabidopsis thaliana* [AtPLL15
 307 (At5g63180), AtPLL18 (At3g27400), AtPLL21 (At5g48900)], *Dickeya dadanti* [DdPeLA (P0C1A2), DdPeLC

308 (P11073), DdPelE (P04960), DdPelI (O50325)], *Bacillus subtilis* [BsPel (P39116)], *Bacillus Sp.* KSM-P15
309 [BsPel-P15 (Q9RHW0)], *Bacillus sp.* N16-5 [BsPelA (D0VP31)], *Aspergillus niger* AnPelA [(Q01172), AnPelB
310 (Q00205), AnPnIA (A2R3I1)], *Achromobacter denitrificans* [AdVexL (A0A160EBC2)], *Aspergillus tubingensis*
311 [AtPelA (A0A100IK89)], *Aspergillus luchuensis* [AlPelB (G7Y0I4)], *Acidovorax citrulli* [AcPel343, (A1TSQ3)],
312 *Paenibacillus sp.* 0602 [PsPelN (W8CR80)], *Caldicellulosiruptor bescii* [CbPel1854 (B9MKT4)]. Maximum
313 likelihood tree was constructed with 1000 bootstrap replicates. Most important clades are indicated in orange
314 squares while VdPelB is marked by red star. Amino acids sequences were retrieved from Uniprot and TAIR.

315 **3.2. Cloning, eExpression and purification of VdPelB**

316 ~~The VdPelB (VDAG_04718) gene consists of 1 single exon of 1002 bp length. Since the~~
317 ~~expression was performed using the pPICZaB vector with the yeast alpha-factor directing, the~~
318 ~~VdPelB was secreted secretion in in the culture media. The coding sequence, minus the putative~~
319 ~~signal peptide was PCR amplified using gene specific primers, ligated in pPICZaB vector and~~
320 ~~expressed in P. pastoris heterologous expression system, allowing its secretion in the culture~~
321 ~~media. Thus, Secreted the secreted, the protein could be easily recovered and purified VdPelB~~
322 ~~was more easily purified. It consisted of~~ The protein is composed of 343 amino acids,
323 including the 6xHIS tag poly-histidine tag at the C-terminus used for affinity chromatography
324 purification. After purification, VdPelB purity was assessed using SDS-PAGE and had with an
325 apparent molecular mass of ~38 kDa (Fig. S1A), higher than what was predicted on the basis
326 of the amino acid sequence (33.8 kDa). However, this shift is likely to correspond to the two
327 tags that are fused to the protein (His and C-myc) and to the presence of 19 putative O-
328 glycosylation sites, as predicted by NetOGlyc 4.0 Server.

329 **3.3. VdPelB has a right-handed parallel β -helix fold**

330 Pectate lyase VdPelB was crystallized and its 3D structure was determined using X-ray
331 diffraction. VdPelB crystallized in monoclinic P 1 2₁ 1 asymmetric unit. Four data sets,
332 collected from the same crystal at 1.2 Å resolution, were integrated, scaled and merged. There
333 are two molecules in the asymmetric units: chains A and B are highly similar with a Ca root
334 mean square deviation (rmsd) value of 0.227 Å (Fig. S2A). The VdPelB structure consists of
335 298 amino acids (aa) with 18 aa at the N-terminus and 27 amino acids at the C-terminus that
336 were not resolved because of poor electron densities, while overall electron densities were well
337 defined. While no N-glycosylation sites could be revealed on the VdPelB structure, six O-
338 glycosylation sites carrying mannose are visible for each molecule: T22, T44, T45, T46, S48
339 and T54, in accordance with the shift in size previously observed (Fig. S2A). During data
340 acquisition no heating of the crystal was observed, as shown by low B factors and good
341 occupancies (Fig. S3A and B). The final models' geometry, processing and refinement
342 statistics are summarized (Table 1). The VdPelB's structure has been deposited in the Protein
343 Data Bank as entry 7BBV.

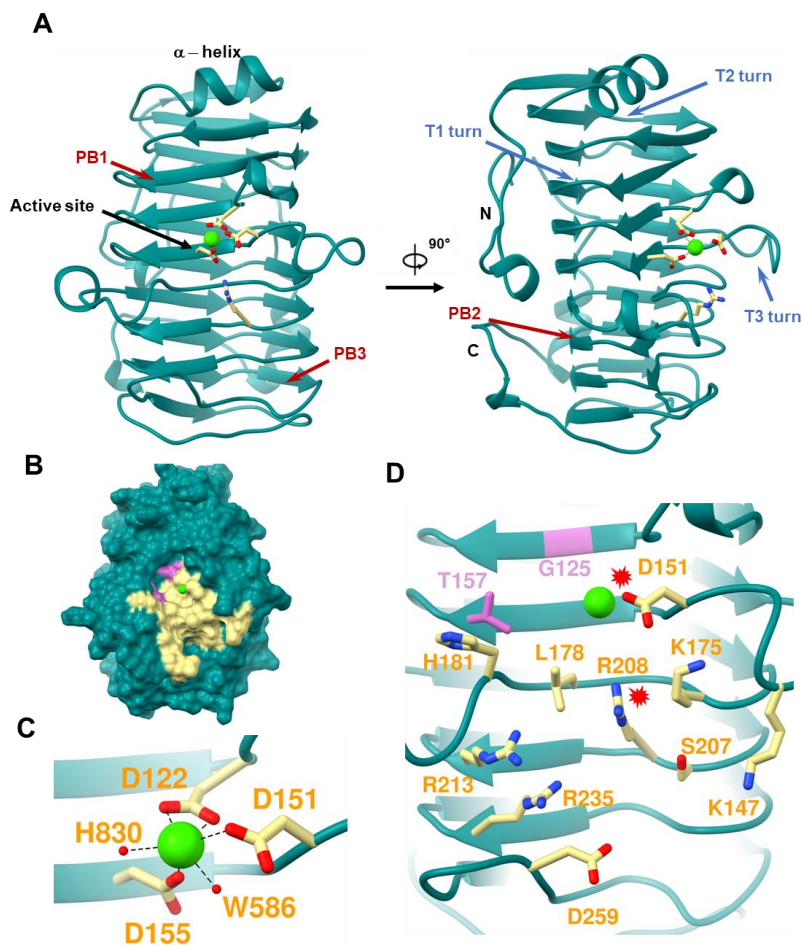
344 **Table 1. Data collection, processing and refinement for VdPelB**

Characteristics	VdPeIB
Data collection	
Diffraction source	PROXIMA2
Wavelength (Å)	0.980
Temperature (°C)	-100.15
Detector	DECTRIS EIGER X 9M
Crystal-to-detector distance (mm)	115.02
Rotation range per image (°)	0.1
Total rotation range (°)	360
Crystal data	
Space group	P1 21 1
a, b, c (Å)	60.89, 59.69, 93.87
α, β, γ, (°)	90.00, 96.35, 90.00
Subunits per asymmetric unit	2
Data statistics	
Resolution range (Å)	60.52-1.2 (1.243 - 1.2)
Total No. of reflection	8536161 (112943)
No. of unique reflection	207497 (19983)
No. of reflections, test set	10362 (1003)
R _{merge} (%)	0.1036 (4.709)
Completeness (%)	99.30 (96.11)
(I/σ(I))	18.03 (0.22)
Multiplicity	41.1 (5.6)
CC _{1/2} (%)	1 (0.116)
Refinement	
R _{crys} /R _{free} (%)	17.3 / 19.7
Average B – factor (Å ²)	33.18
No. of non-H atoms	
Protein	9097
Ion	2
Ligand	234
Water	1052
Total	10385
R.m.s. deviations	
Bonds (Å)	0.013
Angles (°)	1.39
Ramachandran plot	
Most favoured (%)	95.1
Allowed (%)	4.90
Outlier (%)	-

Commented [JS1]: Changed

346 [The](#) VdPelB has a right-handed parallel β -helix fold which is common in pectinases
347 [59]. The β -helix is formed by three parallel β -sheets - PB1, PB2 and PB3 which contain 7, 10
348 and 8 β -strands, respectively. Turns connecting the PB1-PB2, PB2-PB3 and PB3-PB1 β -sheets
349 are named T1-turns, T2-turns and T3-turns, respectively, according to Yoder and Jurnak (**Fig.**
350 **2A, S4A and B**) [60]. T1-turns consist of 2-14 [aaamino acids](#) and builds the loop around the
351 active site on the C-terminus. T2 turns mostly consist of 2 [aaamino acids](#) with Asn being one
352 of the predominant [amino acid](#), forming an N-ladder with the exception of an N245T mutation
353 in VdPelB [15,20]. [Pectate lyase](#). VdPelB has a α -helix on N-terminus end that shields the
354 hydrophobic core and is commonly conserved in PLs and PGs [15,61], while the C-terminus
355 end is also protected by tail-like structure carrying one α -helix. Interestingly N- and C- terminus
356 tails pack against PB2 (**Fig. 2A**). There are only two Cys (C25 and C137) that do not form a
357 disulphide bridge.

358 Sequence and structural alignments show that VdPelB belong to the PL1 family. [The](#)
359 VdPelB shares the highest structural similarity with BsPelA (PDB: 3VMV), with 30.06%
360 sequence identity and $C\alpha$ rmsd of 1.202 Å. The second-best structural alignment was with
361 DdPelC (PDB: 1AIR) with 24.20% identity and $C\alpha$ rmsd of 1.453 Å [43,62]. Both of these
362 structures lack the long T3 loop described in *A.niger* pectate lyase (AnPelA, PDB: 1IDJ, **Fig.**
363 **S2B and S5**) [15]. The putative active site is positioned between the T3 and T2 loops (**Fig. 2A**
364 **and B**).



365

366 **Fig. 2. Structure determination of VdPelB**

367 A) Ribbon diagram of VdPelB crystalized in P1 21 1 space group. VdPelB is a right-handed parallel β helical
 368 structure consisting of β strands (red arrows) and turns (blue arrows). VdPelB active site's aaamino acids are
 369 yellow-colored while Ca atom is green. B) Surface representation of VdPelB binding groove. C) Active site of
 370 VdPelB highlighting conserved aaamino acids and atoms interacting with Ca. D) Structure of VdPelB binding
 371 groove highlighting aaamino acids involved in the interaction (yellow) and aaamino acids not of previously
 372 characterized in-PLs (plum). Red stars indicates indicate aaamino acids from the active site.

373 **3.4. Active site harbours Ca^{2+} that is involved in catalysis**

374 The VdPelB active site is well conserved, harbouring strictly conserved acidic and basic
 375 aaamino acids that are required for Ca^{2+} binding. Previously reported structures showed that
 376 two Asp (D122 and D155) and one Arg (R208) in VdPelB, are conserved, while D151 can be

377 mutated to Glu, or Arg in PNLs (**Fig. 2C and D**, Mayans et al., 1997). Other conserved [aaamino](#)
378 [acids](#) in VdPelB include K175 and R213, with K175 being responsible for binding the carboxyl
379 oxygen while R213 hydrogen bonds to C-2 and C-3 of GalA (**Fig. 2D**) [29,63]. Mutating any
380 of these [aaamino acids](#) leads to decreased enzyme activity [64]. In VdPelB, Ca²⁺ ion is directly
381 coordinated by D122, two carboxyl oxygen, D151, D155 and two water molecules (W568 and
382 W830, **Fig. 2C**). In addition, mutation of D122T (VdPelB numbering) in BsPelA, is responsible
383 for reduced affinity for Ca²⁺ [43]. In the catalytic mechanism, Ca²⁺ is directly involved in
384 acidification of the proton absorption from C5 and elimination of group from C4, generating an
385 unsaturated product. R208 act as a base, similarly to the hydrolysis in the reaction mechanism
386 of the GH28 family [65,66].

387 **3.5. Structural analysis of VdPelB suggests a PL activity mediated by peculiar** 388 **specificities**

389 The VdPelB binding groove comprises a number of basic and acidic [aaamino acids](#)
390 including K147, D151, K175 L178, H181, S207, R208, R213 and R235 and D259 (**Fig. 2C**
391 **and D**), that have previously been shown to be characteristics of PLs. This would suggest an
392 enzyme activity on low DM pectins as [aaamino acids](#) positioned at the binding groove were
393 indeed shown to differ between PNL and PL [15,21,24,29]. These [aaamino acids](#) are indeed
394 mutated in Arg, Trp, Tyr, Gln and Gly in PNLs, which, by reducing their charge, would favour
395 higher affinity for highly methylesterified pectins [15,29]. In VdPelB, as the T3 loop is missing,
396 there are no equivalent to PNL specific W66, W81, W85, W151 [aaamino acids](#) (**Fig. S2B**,
397 AnPelA numbering) and, moreover, W212 and W215 are replaced by K175 and L178 in
398 VdPelB. In BsPelA and DdPelC, these [aaamino acids](#) are replaced by K177/K190 and
399 L180/L193, highlighting the high conservation of amino acids in VdPelB/BsPelA/DdPelC and
400 subsequently in PLs. When a DP4 ligand from DdPelC crystal structure is superimposed to
401 VdPelB, hydrogen bonds and van der Waals interactions are visible with the above-mentioned
402 [aaamino acids](#) (**Fig. S6**) [15,21,29,43].

403 Interestingly, despite this rather conserved PL-related binding groove, VdPelB harbors,
404 in the vicinity of the active site, G125 and T157 that are not present in the well characterized
405 DdPelC [62]. At these positions, DdPelC, which was shown to be a *bona fide* PL with a high
406 activity on polygalacturonic acid and alkaline pH with Ca²⁺-dependency, harbours Arg and Lys
407 [15,63,67]. In that respect, the presence of G125 and T157 in VdPelB is similar to that identified
408 in *Bacillus sp.* Pel-22, Pel-66, and Pel-90 and *Bacillus sp.* which showed activity on both PGA
409 and high methylesterified pectins (**Fig. 2B and D**) [22,68,69]. The DdPelC [aaamino acids](#) being

410 overall positively charged, could explain the binding preference towards non-methylesterified,
411 negatively charged substrates in the vicinity of the active site. In contrast, considering the size
412 of Gly and Thr, they would sterically accommodate the increased size of methylesterified
413 substrate. G125 and T157 could therefore account for a potential dual activity of VdPelB.
414 Moreover, in previously characterized PLs and PNLs there is the presence of a small aaamino
415 acids, Ser or Ala that replace H181. While H181 interacts directly with the substrate these
416 aaamino acids do not provide this interaction instead the primary Ca²⁺ in the active site induce
417 a substrate conformation that could be recognized by PLs [43]. Finally, L178 is positioned in-
418 between the catalytic Ca²⁺ and R208 and is involved in substrate binding making it a perfect
419 candidate to assess its importance (**Fig. 2D**).

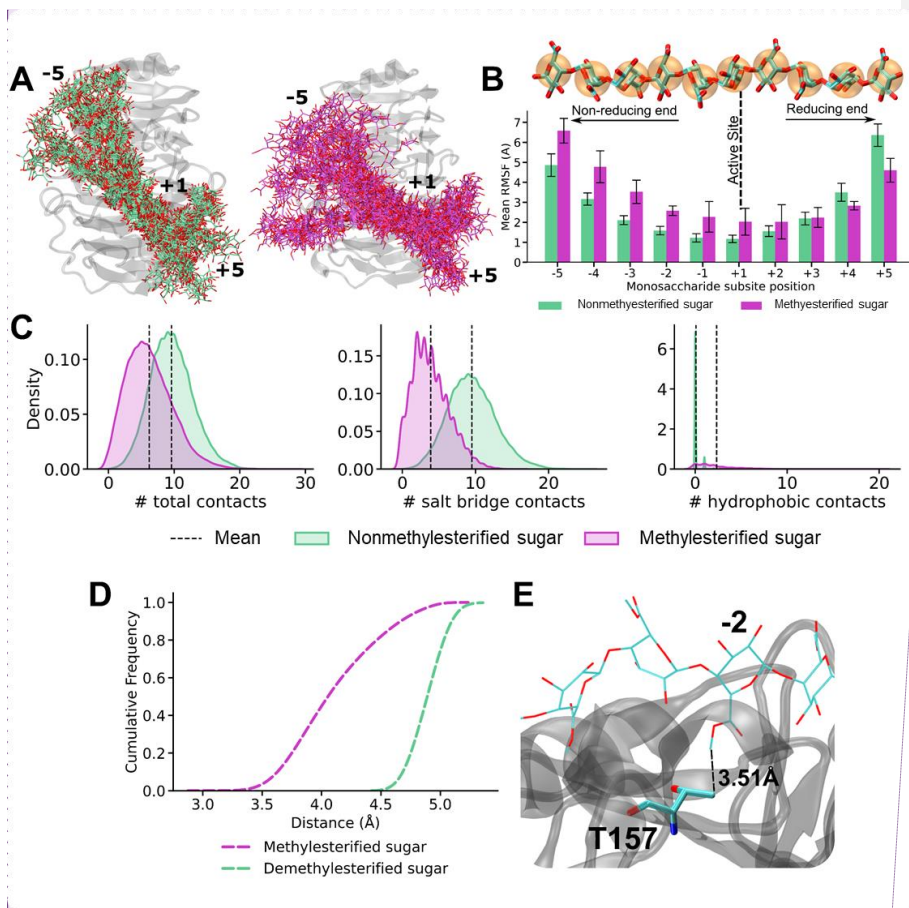
420 **3.6. Molecular dynamic simulations show higher dynamics of VdPelB in complex with** 421 **methylesterified substrates**

422 To determine how the structure of VdPelB and the observed differences in amino-acidic
423 composition might influence the affinity with differently methylated substrates, we performed
424 MD simulations on VdPelB in complex with either a non-methylesterified or fully
425 methylesterified deca-saccharides, which are able to occupy the entire binding groove (**Fig. 3**).
426 MD simulations show substantially differential dynamic profiles for oligosaccharides with and
427 without methylesterification. Expectedly, the dynamics is lowest in proximity of the catalytic
428 subsite (+1) and increases consistently towards both the reducing and non-reducing ends of the
429 substrate: with the highest dynamics found at the non-reducing end (**Fig. 3A**).

430 A quantitative estimation of the substrate dynamics was obtained by monitoring the root
431 square mean fluctuations (RMSF) of each sugar residue and shows that a polygalacturonate
432 substrate associates more stably in the subsites of the binding groove placed towards the sugar's
433 reducing end (subsites -1 to -5), with differences between methylesterified and non-
434 methylesterified substrates approaching the obtained standard deviation. In some cases, the
435 dynamics reversed for non-methylesterified sugars, with a higher RMSF for de-methylesterified
436 sugars towards the saccharide's reducing end (**Fig. 3B**). Moreover, and in line with an observed
437 positively charged binding groove, non-methylesterified substrates retain a higher number of
438 contacts than methylesterified sugars, with salt-bridges contributing the most to the observed
439 differences (**Fig. 3C**).

440 We then additionally and specifically focused on the analysis of the interactions made by
441 T157, which is nested with the -2 subsite of the binding groove. Simulations sample consistently

442 higher contacts formation between a methylesterified sugar docked in subsite -2 and T157, with
 443 distances shifted to lower values when compared to a non-methylesterified sugar (**Fig. 3D**),
 444 even the RMSF of non-methylesterified monosaccharides docked in subsite -2 experience on
 445 average, significantly lower dynamics. Altogether, the formation of a larger number of contacts
 446 between methylesterified saccharides docked in the -2 subsite suggests an active role of T157
 447 in the binding of methylesterified chains: with the butanoic moiety of T157 engaging in
 448 hydrophobic interactions with the methyl-ester presented by methylesterified sugar units (**Fig.**
 449 **3E**). While T157 is seen to have an active role in engaging with the substrate's hydrophobic
 450 moieties, an active role of G125, also in the same subsite, was not observed but it is plausible
 451 that the minimal size of G125 would increase the accommodability of methylesterified sugars
 452 in that position.



Commented [JS2]: Changed

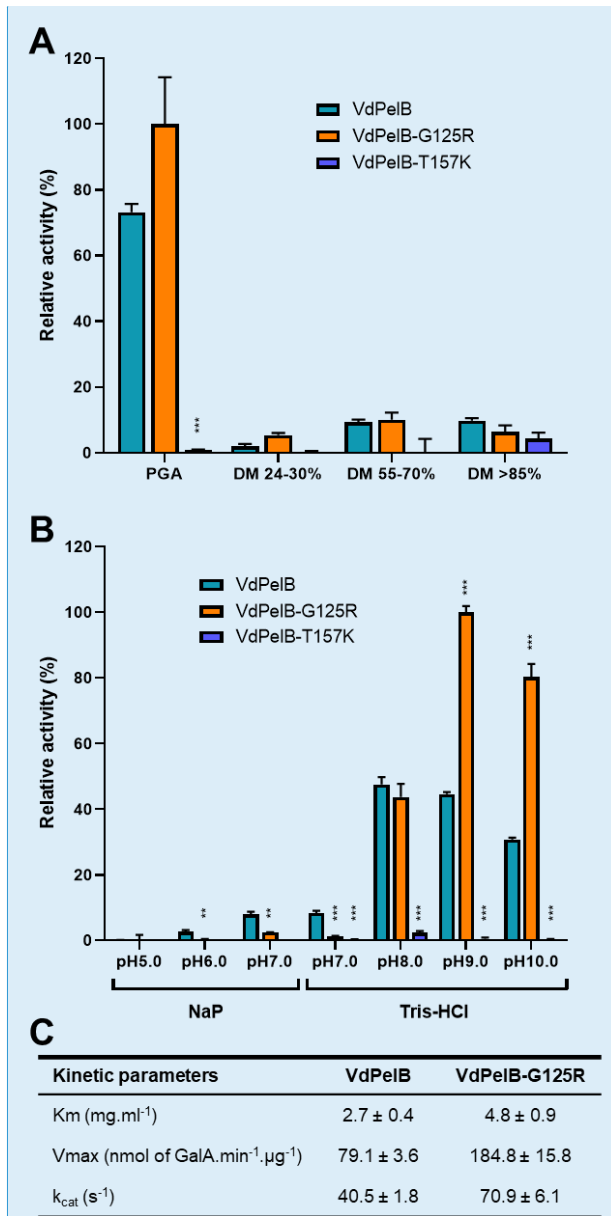
454 **Fig. 3. VdPelB substrate dynamics in complex with fully de-methylesterified and methylesterified complex**

455 A) Ensembles of non-methylesterified (green, left panel) and methylesterified (pink, right panel) HG
456 deca-saccharide at every 100 frames for the simulated VdPelB complexes. Substrate within the enzymes' binding
457 grooves are labelled from -5 (HG-non-reducing end) to +5 (HG-reducing end) B) RMSF of non-methylesterified
458 (green) and methylesterified (pink) HG bound across the binding groove of VdPelB. Numbers indicate the beta
459 sheet position from the active site. C) Analysis of the contacts between VdPelB and non-methylesterified (green)
460 and methylesterified substrate (pink). D) Distance between T157K residue and the substrate residues plotted as
461 cumulative frequency. E) T157 hydrophobic interaction with methyl-ester of methylesterified substrate.

462 **3.7. Biochemical characterization of VdPelB**

463 We first determined the activity of VdPelB by following the release of 4,5-unsaturated
464 bonds which can be detected at 235 nm using UV spectrophotometer. [The](#) VdPelB activity was
465 first tested for its dependency towards Ca^{2+} . Using a standard PL assay, with PGA as a substrate,
466 an increase in the VdPelB activity was measured in presence of calcium. In contrast in presence
467 of EDTA, used as a chelating agent, no activity was detected, confirming the calcium-dependent
468 activity of the enzyme (**Fig. S7A**) [15]. Activity measured in absence of added CaCl_2 reflects
469 the presence of calcium from the culture media that is bound to VdPelB during production, and
470 previously identified in the 3D structure. We tested the effects of increasing CaCl_2
471 concentrations and showed that the maximum activity was already reached when using as low
472 as 0.125 μM (**Fig. S7B**). To test the substrate-dependence of VdPelB, four substrates of
473 increasing degrees of methyl-esterification were used. [The](#) VdPelB showed the highest activity
474 on PGA, with less than 10% of the maximum activity measured on the three others substrates
475 (**Fig. 4A**). This shows that, as inferred from above-mentioned structural and dynamical data,
476 [The](#) VdPelB act mainly as a PL although it can still show residual activity on high DM pectins.
477 Considering this, PGA was used as substrate to test the pH-dependence of the enzyme's activity
478 in sodium acetate and Tris-HCl buffers (**Fig. 4A**). [Pectate lyase](#) VdPelB was most active at pH
479 8, with only a slight decrease in activity at pH 9 (93%). In contrast, the relative activity at pH
480 5-7 was close to null. The pH optimum for VdPelB was the same as *B. fuckeliana* Pel (pH 8)
481 [70], close to that reported for *D. dadantii* PelN (pH 7.4) [71], but was lower to that measured
482 for *B. clausii* Pel (pH 10.5) [72]. In contrast, the pH optimum was higher compared to five PNLs
483 from *Aspergillus* sp. AaPelA (pH 6.1), AtPelA (pH 4.5), AtPelA (pH 6.4), AtPelD (pH 4.3)
484 [18] and *A. parasiticus* Pel (pH 4) [19]. The optimum temperature assay showed that VdPelB
485 was most active at 35°C (**Fig. S8**). [The](#) VdPelB appeared less heat-tolerant as compared to
486 thermophilic PLLs reported from *Bacillus* sp. RN1 90°C [73], *B. clausii* Pel, 70°C [72], *B.*
487 *subtilis* Pel168, 50°C [74]. However, its optimum temperature is in the range of that measured

488 for *X. campestris* Pel [75] and cold-active Pel1 from *M. eurypsychrophila* [76]. The lack of
 489 disulphide bridges previously shown in the structure could be responsible for the lower stability
 490 of the enzyme at high temperatures, in comparison with previously characterized PLs [77].



Commented [FS3]: changed

492 **Fig. 4. Biochemical characterization of VdPelB**

493 A) Substrate-dependence of VdPelB-N, G125R and T157K. The activities were measured after 12 min of
494 incubation with PGA, pectins DM 24-30%, DM 55-70%, DM>85% with addition of Ca²⁺ at 35°C. B) pH-
495 dependence of VdPelB-N, G125R and T157K activity. The activities were measured after 12 min of incubation
496 with PGA in sodium phosphate (NaP) and Tris-HCl buffer at 35°C. Values correspond to means ± SD of three
497 replicates. Welch t-test comparing native with mutant VdPelB forms was used for statistical analysis. P value
498 ***<0.001 and **<0.01. C) Determination of Km, Vmax and kcat for ADPG2 and PGLR. Activity was assessed
499 using various concentrations of PGA at 35°C and pH8.0 (VdPelB) and pH9.0 (VdPelB-G125R). Values
500 correspond to means ± SE of three replicates.

501 **3.8. Mutation of specific amino-acids affects VdPelB activity**

502 Considering the ~~fine~~ structure of VdPelB ~~and our hypothesis about~~ related to the role of
503 some amino acids relevant in determining for the mode of action of VdPelB, ~~structural~~ we
504 generated mutated forms of the enzymes for five amino acids that likely to be involved in the
505 catalytic mechanism and/or substrate binding: G125R, D151R, T157K, L178K and H181A.
506 Enzymes were produced in *P. pastoris* and purified (**Fig. S1B**). If the importance of some of
507 these ~~amino acids~~ (i.e. D151 and H181) in the catalytic mechanism was previously shown for
508 others PL [43,78], our study highlights the key role of some novel ~~amino acids~~ in the catalytic
509 mechanism. The activities of mutants were tested at iso-quantities of wild-type enzyme.
510 Surprisingly, the G125R mutant was 25% more active on PGA compared to the native enzyme
511 and a shift in the optimum pH was observed (**Fig. 4A**). While native enzyme was most active
512 at pH8.0 with slight decrease in activity at pH9.0, the activity of G125R mutant was
513 approximately doubled ~~increased by circa 50%~~ at pH9.0 and pH10.0 (**Fig. 4B**). Both enzymes
514 kept the same activity at pH8.0. ~~The~~ Moreover, using PGA as a substrate, at 35°C, VdPelB and
515 VdPelB-G125R differ slightly in their Km (2.7 versus 4.8 mg.ml⁻¹), Vmax (79.1 versus 184.8
516 nmol of GalA.min⁻¹.µg⁻¹) and kcat (40.5 versus 70.9 s⁻¹, Fig. 4C). The substitution of Gly with
517 Arg, present in a number of previously characterized PL could facilitate the interaction with the
518 substrate and ~~basification~~ alkalinization of the active site thanks to its physio-chemical
519 properties [62]. ~~Despite not knowing the exact rotamer orientation,~~ the presence of Arg with
520 highly elevated pKa which can allowing interact in strong hydrogen bonding and complex
521 electrostatic interactions ~~inside~~ within the active site, could change the optimal pH by acting on
522 the protonation state of amino acids involved in catalysis, as previously reported for a number
523 of different enzymes [65,79–82]. The activity of T157K was closed to null when tested on PGA
524 and different pHs. The introduction of a Lys, a chemically different and larger ~~amino acids~~
525 is likely to introduce steric clashes notably with H181 and L178 that are important for the

Formatted: Subscript

526 activity. The H181A mutant lost much of its activity as there are less interaction/recognition
527 with the substrate. No activity for D151R and L178K mutants were observed in line with the
528 fact that D151 is an active site [aaamino acids](#) that binds the Ca^{2+} . Mutation of this amino-acid
529 is negatively impairing the functioning of the enzyme (**Fig. S7A and B**) [43,78]. We can
530 hypothesize that L178K mutation positioned in between Ca^{2+} , R208 and the substrate, induces
531 specific substrate conformation that diminishes the direct interaction between the enzyme
532 catalytic centre and the substrate, which translates to loss of activity (**Fig. S9**).

533 **3.9. Identification of the OGs released by VdPelB from commercial and cell wall** 534 **pectins**

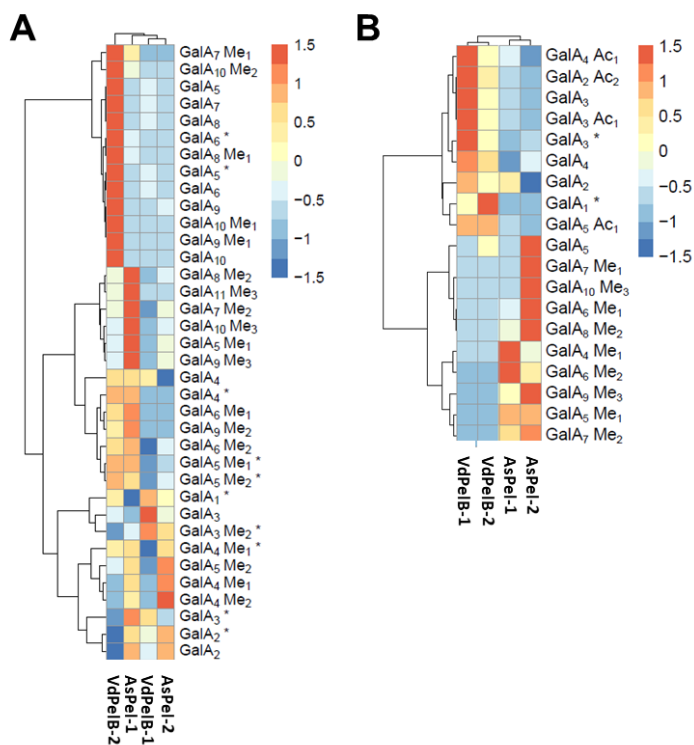
535 To further understand the specificity of VdPelB on different substrates, we performed
536 LC-ESI-MS/MS to determine the profiles of digestion products (OGs) and to compare with that
537 of commercially available *Aspergillus sp.* Pel (AsPel, **Fig. S10**). To be fully comparable,
538 digestions were realized, for each substrate, at iso-activities for the two enzymes. On the basis
539 of digestion profiles, we identified 48 OGs and created a dedicated library that was used for
540 identification and integration of peaks (**Table 2S3**). MS² fragmentation allowed determining
541 the structure of some of the OGs (**Fig. S11 and S12**). The OGs released by either of the enzymes
542 [were](#) mainly corresponded to 4,5-unsaturated OGs, which is in accordance with β -eliminating
543 action of PLLs. When using pectins DM 20-34% and at low enzyme's concentration (VdPelB-
544 2), VdPelB mainly released non-methylesterified OGs of high DP (GalA₅, GalA₆, GalA₇,
545 GalA₈, GalA₉, GalA₁₀) that were subsequently hydrolysed when using more concentrated
546 VdPelB (VdPelB-1, **Fig. 5A**). These digestion products strikingly differed to that generated by
547 AsPel, that are methylesterified OGs of higher DP (GalA₄Me₁, GalA₄Me₂, GalA₅Me₁,
548 GalA₆Me₂, GalA₁₁Me₃...), thus showing distinct enzymatic specificities. Altogether, these first
549 results unequivocally shows [both VdPelB and AsPel act as \$\alpha\$ -endo-PLs, but they differ in their](#)
550 [processivity and that its processivity differ to that of AsPel, which act as well as an endo-PL](#)
551 [9]. When using sugar beet pectins, that are known to be highly acetylated (DM 42%, DA 31%),
552 VdPelB released acetylated OGs (GalA₂Ac₂, GalA₃Ac₁, GalA₄Ac₁, GalA₅Ac₁), while AsPel
553 showed much lower activity and relative abundance of these OGs (**Fig. 5B**). Previous reports
554 have shown that differences exist between PNL, in particular with regards to acetyl substitutions
555 [18]. In contrast, AsPel released mainly methylesterified OGs (GalA₆Me₁, GalA₈Me₁,
556 GalA₁₀Me₃...).

557 [Table 2. List of oligogalacturonides identified by LC-MS/MS analysis.](#)

558 For each OG, elemental composition, retention time (RT) and ion mass used for the analysis are highlighted. In
559 the case of detection of mono and di-charged OGs, the *italicized* and **BOLD** mass, corresponding to the more
560 intense ion, were used for the quantification. * indicates non-unsaturated OGs.

Name	Elemental composition	RT (min)	[M-H]-	[M-2H]2-
GalA1*	C6H10O7	9.3	193.0353763	
GalA1Ac2	C10H12O8	9.1	259.045941	
GalA2*	C12H18O13	8.88	369.0674644	
GalA2	C12H16O12	8.95	351.0568997	
GalA2Ac2	C16H20O14	8.67	435.0780291	
GalA2Me1*	C13H20O13	8.85	383.0831145	
GalA2Me1	C13H18O12	8.92	365.0725498	
GalA3*	C18H26O19	8.56	545.0995525	
GalA3	C18H24O18	8.61	527.0889878	
GalA3Ac1	C20H26O19	8.59	569.0995525	
GalA3Me1	C19H26O18	8.56	541.1046379	
GalA3Me2*	C20H30O19	8.62	573.1308527	
GalA4*	C24H34O25	8.27	721.1316406	
GalA4	C24H32O24	8.33	703.1210759	351.0568997
GalA4Ac1	C26H34O25	8.31	745.1316406	
GalA4Me1*	C25H36O25	8.37	735.1472907	
GalA4Me1	C25H34O24	8.32	717.136726	358.0647248
GalA4Me2	C26H36O24	8.3	731.1523761	
GalA5*	C30H42O31	8.04	897.1637287	
GalA5	C30H40O30	8.09	879.153164	439.0729438
GalA5Ac1	C32H42O31	8.09	921.1637287	
GalA5Me1*	C31H44O31	8.11	911.1793788	455.0860512
GalA5Me1	C31H42O30	8.13	893.1688141	446.0807688
GalA5Me2*	C32H46O31	8.13	925.1950289	
GalA5Me2	C32H44O30	8.03	907.1844642	453.0885939
GalA6*	C36H50O37	7.84		536.0942702
GalA6	C36H48O36	7.82	1055.185252	527.0889878
GalA6Me1	C37H50O36	7.92	1069.200902	534.0968129
GalA6Me2	C38H52O36	7.83	1083.216552	541.1046379
GalA7*	C42H58O43	7.65		624.1103142
GalA7	C42H56O42	7.62	1231.21734	615.1050318
GalA7Me1	C43H58O42	7.72	1245.23299	622.1128569
GalA7Me2*	C44H62O43	7.75		638.1259643
GalA7Me2	C44H60O42	7.72	1259.24864	629.1206819
GalA8	C48H64O48	7.45		703.1210759
GalA8Me1*	C49H68O49	7.53		719.1341833
GalA8Me1	C49H66O48	7.52	1421.265078	710.1289009
GalA8Me2*	C50H70O49	7.55		726.1420083
GalA8Me2	C50H68O48	7.58	1435.280728	717.136726

Name	Elemental composition	RT (min)	[M-H]-	[M-2H]2-
GalA9*	C54H74O55	7.29		800.1424023
GalA9	C54H72O54	7.3		791.1371199
GalA9Me1	C55H74O54	7.34		798.144945
GalA9Me2	C56H76O54	7.37		805.15277
GalA9Me2	C56H76O54	7.41		805.15277
GalA9Me3	C57H78O54	7.45		812.1605951
GalA10	C60H80O60	7.15		879.153164
GalA10Ac1	C62H82O61	7.29		900.1584463
GalA10Me1	C61H82O60	7.19		886.160989
GalA10Me2*	C62H86O61	7.24		902.1740964
GalA10Me2	C62H84O60	7.24		893.1688141
GalA10Me3	C63H86O60	7.3		900.1766391
GalA11	C66H88O66	7.03		967.169208
GalA11Ac1	C68H90O67	7.14		988.1744904
GalA11Me1	C67H90O66	7.06		974.1770331
GalA11Me2	C68H92O66	7.09		981.1848581
GalA11Me3	C69H94O66	7.14		988.1926832
GalA12Me2	C74H100O72	6.96		1069.200902
GalA12Me3	C75H102O72	6.99		1076.208727
GalA12Me4	C76H104O72	7.0419		1083.216552
GalA13Me2	C80H108O78	6.82		1157.216946
GalA13Me3	C81H110O78	6.86		1164.224771
GalA13Me4	C82H112O78	6.9		1171.232596
GalA14Me3	C87H118O84	6.73		1252.240815
GalA14Me4	C88H120O84	6.77		1259.24864
GalA15Me5	C95H130O90	6.69		1354.272509



563

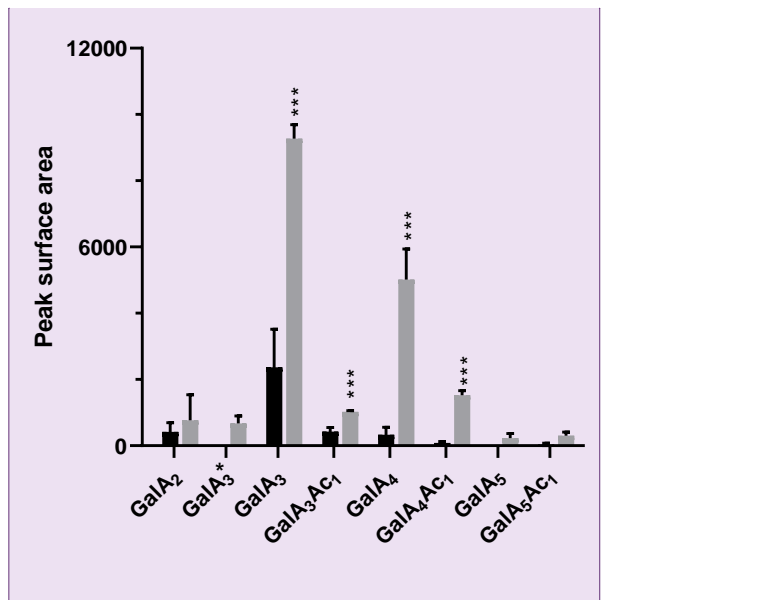
564 **Fig. 5. Analysis of OGs produced by the action of VdPelB and AsPel on pectins of various degrees of**
 565 **methylesterification and acetylation.**

566 OGs were separated by SEC and analysed by MS/MS. A) Pectins DM 24-30%. B) Sugar beet pectins (DM 42%
 567 DA 31%). Substrates were digested overnight at 40°C and pH-8.0 –using isoactivities of VdPelB and AsPel.
 568 Enzyme concentrations are stated in Table S2. Subscript numbers indicate the DP, DM and DA. * indicate non-
 569 unsaturated OGs. Values correspond to means of three replicates.

570 *V. dahliae* and closely related fungus from the same genus are known flax pathogens,
 571 where they use their enzymatic arsenal, that includes pectin degrading enzymes, for penetrating
 572 the host cell leading to infection [30]. To assess the potential role of VdPelB in flax
 573 pathogenicity we digested root cell walls from two flax cultivars, Evea (Verticillium-partially
 574 resistant), and Violin (Verticillium-susceptible), and we compared the OGs released. On root
 575 cell walls, VdPelB released mainly unsaturated OGs up to DP5 (**Fig. 6**). From similar starting
 576 root material, the OG total peak area detected was five times lower for Evea compared to Violin,
 577 suggesting that it is less susceptible to digestion by VdPelB. OGs released by VdPelB were
 578 mainly non-methylesterified but could be acetylated (GalA₂, GalA₃, GalA₃Ac₁, GalA₄,

Formatted: English (United Kingdom)

579 GalA₄Ac₁ GalA₅, GalA₅Ac₁), and the abundance of GalA₃ and GalA₄ was five and fifteen times
 580 higher in Violin, respectively. These data together with that obtained from sugar beet pectins
 581 strongly suggests that VdPelB preference is for non-methylesterified and acetylated substrates.
 582 Our data suggest that cell wall structure differ between the two cultivars and that VdPelB could
 583 determine Verticillium pathogenicity thanks to a better degradation of the cell wall pectins of
 584 sensitive cultivars [37]. Similarly, VdPel1 was previously identified as virulence factor, where
 585 the deletion of this gene decreased virulence in tobacco, as compared with the wild-type
 586 Verticillium [35].



587

588 **Fig. 6. Analysis of OGs released by VdPelB from flax roots.**

589 The Ψ VdPelB was incubated overnight with roots from Évéa (spring flax, partially resistant to Verticillium wilt,
 590 black) and Violin (winter flax, more susceptible to Verticillium wilt, grey). Values correspond to means \pm SD of
 591 three replicates. Welch t-test comparing Eevea with Violin was used for statistical analysis. P value ***<0.001.
 592 Subscript numbers indicate the DP, DM and DA. dPelB was incubated overnight with roots from Évéa (spring flax,
 593 partially resistant to Verticillium wilt, black) and Violin (winter flax, more susceptible to Verticillium wilt, grey)-
 594 Data are means \pm SD; n = 3. Subscript numbers indicate the DP, DM and DA. Values correspond to means of three
 595 replicates.

596

597 **4. Conclusion**

Commented [JS4]: changed

598 We have ~~fully~~-characterized, by multidisciplinary approaches, a novel pectinolytic
599 enzyme from *V.dahliae*, VdPelB, that belongs to the PLL family. The protein was crystallised
600 and its 3D structure determined at a high resolution. [Pectate lyase](#) VdPelB showed a conserved
601 structure, with ~~typical-parallel β -topology~~[sheet topology](#) for PLs and the active site harboured
602 three conserved Asp coordinating Ca^{2+} and Arg involved in the β -elimination mechanism. The
603 binding groove of VdPelB ~~showed-reveals~~ conserved ~~aa~~[amino acids](#) that are characteristic of
604 PLs, with MD simulations confirming the lower dynamics/higher affinity of the enzyme
605 towards non-methylesterified pectins. As inferred from structural and dynamical analyses,
606 VdPelB showed high activity on non-methylesterified substrates, with a maximum activity at
607 pH-[8.0](#) and 35°C. The analysis of the structure led the identification, in the VdPelB, of peculiar
608 ~~aa~~[amino acids](#) that are normally present in PNL. In particular, G125R mutant ~~showed~~-increased
609 activity on PGA and switch in pH optimum from [8.0](#) to [9.0](#) ~~related to amino acids protonation.~~
610 The analysis of the digestion products ~~of~~ showed that VdPelB act as an endo enzyme and that
611 it can release a large diversity of OGs with a preference for non-methylesterified and acetylated
612 products. The OGs generated by VdPelB from [pectins extracted from](#) Verticillium-partially
613 tolerant and Verticillium-sensitive flax cultivars showed that the enzyme could be a determinant
614 of pathogenicity, [since these OGs differ](#) as a function of pectins' structure. [Thus, our study now](#)
615 [paves the way for generating, using dedicated enzymes, OG pools that could be used for](#)
616 [protecting plants against phytopathogens.](#)

617

618 **Funding sources**

619 This work was supported by the Conseil Regional Hauts-de-France and the FEDER
620 (Fonds ~~E~~uropéen de ~~D~~éveloppement ~~régional~~~~Régional~~) through a PhD grant awarded to J.S.
621

622 **Acknowledgements**

623 We wish to thank Sylvain Lecomte and Mehdi Cherkaoui for providing the *Verticillium*
624 *dahliae* DNA, Martin Savko and the staff at Proxima 2a beamline (Synchrotron SOLEIL, Gif
625 sur Yvette, France) for X-ray diffraction and data collection.

626 **Author's contribution**

627 **Josip Safran**: Conceptualization, Data curation, Formal analysis, Investigation, Methodology,
628 Writing - original draft. **Vanessa Ung**: Data curation, Investigation, Methodology. **Julie**
629 **Bouckaert**: Data curation, Investigation, Methodology. **Olivier Habrylo**: Formal analysis,
630 Investigation, Methodology. **Roland Molinié**: Data curation, Formal analysis, Investigation,
631 Methodology. **Jean-Xavier Fontaine**: Data curation, Formal analysis, Investigation,
632 Methodology. **Adrien Lemaire**: Investigation, Methodology. **Aline Voxeur**: Investigation,
633 Methodology. **Serge Pilard**: Investigation, Methodology. **Corinne Pau-Roblot**
634 Conceptualization, Methodology. **Davide Mercadante**: Data curation, Methodology, Writing
635 - review & editing. **Jérôme Pelloux**: Funding acquisition, Conceptualization, Writing - review
636 & editing. **Fabien Sénéchal**: Conceptualization, Writing - review & editing.

637 **Conflicts of interest**

638 There are no conflicts of interest.

639

640 **References**

- 641 [1] B.L. Ridley, M.A. O'Neill, D. Mohnen, Pectins: structure, biosynthesis, and
642 oligogalacturonide-related signaling, *Phytochemistry*. 57 (2001) 929–967.
643 [https://doi.org/10.1016/S0031-9422\(01\)00113-3](https://doi.org/10.1016/S0031-9422(01)00113-3).
- 644 [2] D. Mohnen, Pectin structure and biosynthesis, *Curr. Opin. Plant Biol.* 11 (2008) 266–
645 277. <https://doi.org/10.1016/j.pbi.2008.03.006>.
- 646 [3] M.A. Atmodjo, Z. Hao, D. Mohnen, Evolving views of pectin biosynthesis, *Annu. Rev.*
647 *Plant Biol.* 64 (2013) 747–779. [https://doi.org/10.1146/annurev-arplant-042811-](https://doi.org/10.1146/annurev-arplant-042811-105534)
648 105534.
- 649 [4] Y. Rui, C. Xiao, H. Yi, B. Kandemir, J.Z. Wang, V.M. Puri, C.T. Anderson,
650 POLYGALACTURONASE INVOLVED IN EXPANSION3 functions in seedling
651 development, rosette growth, and stomatal dynamics in *Arabidopsis thaliana*, *Plant*
652 *Cell*. 29 (2017) 2413–2432. <https://doi.org/10.1105/tpc.17.00568>.
- 653 [5] C. Xiao, C. Somerville, C.T. Anderson, POLYGALACTURONASE INVOLVED IN
654 EXPANSION1 functions in cell elongation and flower development in *Arabidopsis*,
655 *Plant Cell*. 26 (2014) 1018–1035. <https://doi.org/10.1105/tpc.114.123968>.
- 656 [6] J. Pelloux, C. Rustérucci, E.J. Mellerowicz, New insights into pectin methylesterase
657 structure and function, *Trends Plant Sci.* 12 (2007) 267–277.
658 <https://doi.org/10.1016/j.tplants.2007.04.001>.
- 659 [7] F. Sénéchal, A. Mareck, P. Marcelo, P. Lerouge, J. Pelloux, *Arabidopsis* PME17
660 Activity can be Controlled by Pectin Methylesterase Inhibitor4, *Plant Signal. Behav.* 10
661 (2015) e983351. <https://doi.org/10.4161/15592324.2014.983351>.
- 662 [8] V.S. Nocker, L. Sun, Analysis of promoter activity of members of the Pectate lyase-
663 like(PLL) gene family in cell separation in *Arabidopsis*, *BMC Plant Biol.* 10 (2010)
664 152. <https://doi.org/10.1186/1471-2229-10-152>.
- 665 [9] A. Voxeur, O. Habrylo, S. Guénin, F. Miart, M.C. Soulié, C. Rihouey, C. Pau-Roblot,
666 J.M. Domon, L. Gutierrez, J. Pelloux, G. Mouille, M. Fagard, H. Höfte, S. Vernhettes,
667 Oligogalacturonide production upon *Arabidopsis thaliana*-*Botrytis cinerea* interaction,
668 *Proc. Natl. Acad. Sci. U. S. A.* 116 (2019) 19743–19752.
669 <https://doi.org/10.1073/pnas.1900317116>.

- 670 [10] I. Kars, G.H. Krooshof, L. Wagemakers, R. Joosten, J.A.E. Benen, J.A.L. Van Kan,
671 Necrotizing activity of five *Botrytis cinerea* endopolygalacturonases produced in *Pichia*
672 *pastoris*, *Plant J.* 43 (2005) 213–225. [https://doi.org/10.1111/j.1365-](https://doi.org/10.1111/j.1365-313X.2005.02436.x)
673 [313X.2005.02436.x](https://doi.org/10.1111/j.1365-313X.2005.02436.x).
- 674 [11] R.P. Jolie, T. Duvetter, A.M. Van Loey, M.E. Hendrickx, Pectin methylesterase and its
675 proteinaceous inhibitor: A review, *Carbohydr. Res.* 345 (2010) 2583–2595.
676 <https://doi.org/10.1016/j.carres.2010.10.002>.
- 677 [12] R.S. Jayani, S. Saxena, R. Gupta, Microbial pectinolytic enzymes: A review, *Process*
678 *Biochem.* 40 (2005) 2931–2944. <https://doi.org/10.1016/j.procbio.2005.03.026>.
- 679 [13] H. Suzuki, T. Morishima, A. Handa, H. Tsukagoshi, M. Kato, M. Shimizu,
680 Biochemical Characterization of a Pectate Lyase AnPL9 from *Aspergillus nidulans*,
681 *Appl. Biochem. Biotechnol.* (2022). <https://doi.org/10.1007/s12010-022-04036-x>.
- 682 [14] G. Limberg, R. Körner, H.C. Buchholt, T.M.I.E. Christensen, P. Roepstorff, J.D.
683 Mikkelsen, Analysis of different de-esterification mechanisms for pectin by enzymatic
684 fingerprinting using endopectin lyase and endopolygalacturonase II from *A. Niger*,
685 *Carbohydr. Res.* 327 (2000) 293–307. [https://doi.org/10.1016/S0008-6215\(00\)00067-7](https://doi.org/10.1016/S0008-6215(00)00067-7).
- 686 [15] O. Mayans, M. Scott, I. Connerton, T. Gravesen, J. Benen, J. Visser, R. Pickersgill, J.
687 Jenkins, Two crystal structures of pectin lyase A from *Aspergillus* reveal a pH driven
688 conformational change and striking divergence in the substrate-binding clefts of pectin
689 and pectate lyases, *Structure.* 5 (1997) 677–689. [https://doi.org/10.1016/S0969-](https://doi.org/10.1016/S0969-2126(97)00222-0)
690 [2126\(97\)00222-0](https://doi.org/10.1016/S0969-2126(97)00222-0).
- 691 [16] S. Yadav, P.K. Yadav, D. Yadav, K.D.S. Yadav, Pectin lyase: A review, *Process*
692 *Biochem.* 44 (2009) 1–10. <https://doi.org/10.1016/j.procbio.2008.09.012>.
- 693 [17] F. Sénéchal, C. Wattier, C. Rustérucci, J. Pelloux, Homogalacturonan-modifying
694 enzymes: Structure, expression, and roles in plants, *J. Exp. Bot.* 65 (2014) 5125–5160.
695 <https://doi.org/10.1093/jxb/eru272>.
- 696 [18] B. Zeuner, T.B. Thomsen, M.A. Stringer, K.B.R.M. Krogh, A.S. Meyer, J. Holck,
697 Comparative Characterization of *Aspergillus* Pectin Lyases by Discriminative
698 Substrate Degradation Profiling, *Front. Bioeng. Biotechnol.* 8 (2020).
699 <https://doi.org/10.3389/fbioe.2020.00873>.

- 700 [19] G. Yang, W. Chen, H. Tan, K. Li, J. Li, H. Yin, Biochemical characterization and
701 evolutionary analysis of a novel pectate lyase from *Aspergillus parasiticus*, *Int. J. Biol.*
702 *Macromol.* 152 (2020) 180–188. <https://doi.org/10.1016/j.ijbiomac.2020.02.279>.
- 703 [20] M.D. Yoder, S.E. Lietzke, F. Jurnak, Unusual structural features in the parallel β -helix
704 in pectate lyases, *Structure*. 1 (1993) 241–251. [https://doi.org/10.1016/0969-](https://doi.org/10.1016/0969-2126(93)90013-7)
705 2126(93)90013-7.
- 706 [21] J. Vitali, B. Schick, H.C.M. Kester, J. Visser, F. Jurnak, The Three-Dimensional
707 Structure of *Aspergillus niger* Pectin Lyase B at 1.7-Å Resolution, *Plant Physiol.* 116
708 (1998) 69–80. <https://doi.org/10.1104/pp.116.1.69>.
- 709 [22] S.E. Lietzke, R.D. Scavetta, M.D. Yoder, F. Jurnak, The Refined Three-Dimensional
710 Structure of Pectate Lyase E from *Erwinia chrysanthemi* at 2.2 Å Resolution, *Plant*
711 *Physiol.* 111 (1996) 73–92. <https://doi.org/10.1104/pp.111.1.73>.
- 712 [23] M. Akita, A. Suzuki, T. Kobayashi, S. Ito, T. Yamane, The first structure of pectate
713 lyase belonging to polysaccharide lyase family 3, *Acta Crystallogr. Sect. D Biol.*
714 *Crystallogr.* 57 (2001) 1786–1792. <https://doi.org/10.1107/S0907444901014482>.
- 715 [24] R. Pickersgill, J. Jenkins, G. Harris, W. Nasser, J. Robert Baudouy, The structure of
716 *Bacillus subtilis* pectate lyase in complex with calcium, *Nat. Struct. Biol.* 1 (1994)
717 717–723. <https://doi.org/10.1038/nsb1094-717>.
- 718 [25] A.S. Luis, J. Briggs, X. Zhang, B. Farnell, D. Ndeh, A. Labourel, A. Baslé, A.
719 Cartmell, N. Terrapon, K. Stott, E.C. Lowe, R. McLean, K. Shearer, J. Schückel, I.
720 Venditto, M.C. Ralet, B. Henrissat, E.C. Martens, S.C. Mosimann, D.W. Abbott, H.J.
721 Gilbert, Dietary pectic glycans are degraded by coordinated enzyme pathways in
722 human colonic *Bacteroides*, *Nat. Microbiol.* 3 (2018) 210–219.
723 <https://doi.org/10.1038/s41564-017-0079-1>.
- 724 [26] K. Johansson, M. El-Ahmad, R. Friemann, H. Jörnvall, O. Markovič, H. Eklund,
725 Crystal structure of plant pectin methylesterase, *FEBS Lett.* 514 (2002) 243–249.
726 [https://doi.org/10.1016/S0014-5793\(02\)02372-4](https://doi.org/10.1016/S0014-5793(02)02372-4).
- 727 [27] S.W. Cho, S. Lee, W. Shin, The X-ray structure of *Aspergillus aculeatus*
728 Polygalacturonase and a Modeled structure of the Polygalacturonase-Octagalacturonate
729 Complex, *J. Mol. Biol.* 311 (2001) 863–878. <https://doi.org/10.1006/jmbi.2001.4919>.

- 730 [28] T.N. Petersen, S. Kauppinen, S. Larsen, The crystal structure of rhamnogalacturonase a
731 from *Aspergillus aculeatus*: A right-handed parallel β helix, *Structure*. 5 (1997) 533–
732 544. [https://doi.org/10.1016/S0969-2126\(97\)00209-8](https://doi.org/10.1016/S0969-2126(97)00209-8).
- 733 [29] R.D. Scavetta, S.R. Herron, A.T. Hotchkiss, N. Kita, N.T. Keen, J.A.E. Benen, H.C.M.
734 Kester, J. Visser, F. Jurnak, Structure of a plant cell wall fragment complexed to
735 pectate lyase C, *Plant Cell*. 11 (1999) 1081–1092.
736 <https://doi.org/10.1105/tpc.11.6.1081>.
- 737 [30] A. Blum, M. Bressan, A. Zahid, I. Trinsoutrot-Gattin, A. Driouich, K. Laval,
738 *Verticillium Wilt on Fiber Flax: Symptoms and Pathogen Development In Planta*, *Plant*
739 *Dis.* 102 (2018) 2421–2429. <https://doi.org/10.1094/PDIS-01-18-0139-RE>.
- 740 [31] K. Zeise, A. Von Tiedemann, Host specialization among vegetative compatibility
741 groups of *Verticillium dahliae* in relation to *Verticillium longisporum*, *J. Phytopathol.*
742 150 (2002) 112–119. <https://doi.org/10.1046/j.1439-0434.2002.00730.x>.
- 743 [32] J. Zhang, X. Yu, C. Zhang, Q. Zhang, Y. Sun, H. Zhu, C. Tang, Pectin lyase enhances
744 cotton resistance to *Verticillium wilt* by inducing cell apoptosis of *Verticillium dahliae*,
745 *J. Hazard. Mater.* 404 (2021) 124029. <https://doi.org/10.1016/j.jhazmat.2020.124029>.
- 746 [33] J.Y. Chen, H.L. Xiao, Y.J. Gui, D.D. Zhang, L. Li, Y.M. Bao, X.F. Dai,
747 Characterization of the *Verticillium dahliae* exoproteome involves in pathogenicity
748 from cotton-containing medium, *Front. Microbiol.* 7 (2016) 1–15.
749 <https://doi.org/10.3389/fmicb.2016.01709>.
- 750 [34] S.J. Klosterman, Z.K. Atallah, G.E. Vallad, K. V. Subbarao, Diversity, Pathogenicity,
751 and Management of *Verticillium* Species, *Annu. Rev. Phytopathol.* 47 (2009) 39–62.
752 <https://doi.org/10.1146/annurev-phyto-080508-081748>.
- 753 [35] Y. Yang, Y. Zhang, B. Li, X. Yang, Y. Dong, D. Qiu, A *Verticillium dahliae* Pectate
754 Lyase Induces Plant Immune Responses and Contributes to Virulence, *Front. Plant Sci.*
755 9 (2018) 1–15. <https://doi.org/10.3389/fpls.2018.01271>.
- 756 [36] D. Duressa, A. Anchieta, D. Chen, A. Klimes, M.D. Garcia-Pedrajas, K.F. Dobinson,
757 S.J. Klosterman, RNA-seq analyses of gene expression in the microsclerotia of
758 *Verticillium dahliae*, *BMC Genomics*. 14 (2013) 5–18. <https://doi.org/10.1186/1471-2164-14-607>.

- 760 [37] J. Safran, O. Habrylo, M. Cherkaoui, S. Lecomte, A. Voxeur, S. Pilard, S. Bassard, C.
761 Pau-Roblot, D. Mercadante, J. Pelloux, F. Sénéchal, New insights into the specificity
762 and processivity of two novel pectinases from *Verticillium dahliae*, *Int. J. Biol.*
763 *Macromol.* 176 (2021) 165–176. <https://doi.org/10.1016/j.ijbiomac.2021.02.035>.
- 764 [38] A. Lemaire, C. Duran Garzon, A. Perrin, O. Habrylo, P. Trezel, S. Bassard, V.
765 Lefebvre, O. Van Wuytswinkel, A. Guillaume, C. Pau-Roblot, J. Pelloux, Three novel
766 rhamnogalacturonan I-pectins degrading enzymes from *Aspergillus aculeatinus*:
767 Biochemical characterization and application potential, *Carbohydr. Polym.* 248 (2020)
768 116752. <https://doi.org/10.1016/j.carbpol.2020.116752>.
- 769 [39] W. Kabsch, Xds., *Acta Crystallogr. D. Biol. Crystallogr.* 66 (2010) 125–32.
770 <https://doi.org/10.1107/S0907444909047337>.
- 771 [40] W. Kabsch, Integration, scaling, space-group assignment and post-refinement, *Acta*
772 *Crystallogr. Sect. D Biol. Crystallogr.* 66 (2010) 133–144.
773 <https://doi.org/10.1107/S0907444909047374>.
- 774 [41] B.W. Matthews, Solvent content of protein crystals., *J. Mol. Biol.* 33 (1968) 491–497.
775 [https://doi.org/10.1016/0022-2836\(68\)90205-2](https://doi.org/10.1016/0022-2836(68)90205-2).
- 776 [42] A.J. McCoy, R.W. Grosse-Kunstleve, P.D. Adams, M.D. Winn, L.C. Storoni, R.J.
777 Read, Phaser crystallographic software, *J. Appl. Crystallogr.* 40 (2007) 658–674.
778 <https://doi.org/10.1107/S0021889807021206>.
- 779 [43] Y. Zheng, C.H. Huang, W. Liu, T.P. Ko, Y. Xue, C. Zhou, R.T. Guo, Y. Ma, Crystal
780 structure and substrate-binding mode of a novel pectate lyase from alkaliphilic *Bacillus*
781 sp. N16-5, *Biochem. Biophys. Res. Commun.* 420 (2012) 269–274.
782 <https://doi.org/10.1016/j.bbrc.2012.02.148>.
- 783 [44] D. Liebschner, P. V. Afonine, M.L. Baker, G. Bunkoczi, V.B. Chen, T.I. Croll, B.
784 Hintze, L.W. Hung, S. Jain, A.J. McCoy, N.W. Moriarty, R.D. Oeffner, B.K. Poon,
785 M.G. Prisant, R.J. Read, J.S. Richardson, D.C. Richardson, M.D. Sammito, O. V.
786 Sobolev, D.H. Stockwell, T.C. Terwilliger, A.G. Urzhumtsev, L.L. Videau, C.J.
787 Williams, P.D. Adams, Macromolecular structure determination using X-rays, neutrons
788 and electrons: Recent developments in Phenix, *Acta Crystallogr. Sect. D Struct. Biol.*
789 75 (2019) 861–877. <https://doi.org/10.1107/S2059798319011471>.
- 790 [45] P. Emsley, B. Lohkamp, W.G. Scott, K. Cowtan, Features and development of Coot,

- 791 Acta Crystallogr. Sect. D Biol. Crystallogr. 66 (2010) 486–501.
792 <https://doi.org/10.1107/S0907444910007493>.
- 793 [46] L. Hocq, S. Guinand, O. Habrylo, A. Voxeur, W. Tabi, J. Safran, F. Fournet, J.-M.
794 Domon, J.-C. Mollet, S. Pilard, C. Pau- Roblot, A. Lehner, J. Pelloux, V. Lefebvre,
795 The exogenous application of AtPGLR, an endo - polygalacturonase, triggers pollen
796 tube burst and repair, *Plant J.* 103 (2020) 617–633. <https://doi.org/10.1111/tpj.14753>.
- 797 [47] K. Lindorff-Larsen, S. Piana, K. Palmo, P. Maragakis, J.L. Klepeis, R.O. Dror, D.E.
798 Shaw, Improved side-chain torsion potentials for the Amber ff99SB protein force field,
799 *Proteins Struct. Funct. Bioinforma.* 78 (2010) 1950–1958.
800 <https://doi.org/10.1002/prot.22711>.
- 801 [48] W.L. Jorgensen, J. Chandrasekhar, J.D. Madura, R.W. Impey, M.L. Klein, Comparison
802 of simple potential functions for simulating liquid water, *J. Chem. Phys.* 79 (1983)
803 926–935. <https://doi.org/10.1063/1.445869>.
- 804 [49] J.S. Rowlinson, The Maxwell-boltzmann distribution, *Mol. Phys.* 103 (2005) 2821–
805 2828. <https://doi.org/10.1080/002068970500044749>.
- 806 [50] H.J.C. Berendsen, J.P.M. Postma, W.F. Van Gunsteren, A. Dinola, J.R. Haak,
807 Molecular dynamics with coupling to an external bath, *J. Chem. Phys.* 81 (1984) 3684–
808 3690. <https://doi.org/10.1063/1.448118>.
- 809 [51] M. Parrinello, A. Rahman, Polymorphic transitions in single crystals: A new molecular
810 dynamics method, *J. Appl. Phys.* 52 (1981) 7182–7190.
811 <https://doi.org/10.1063/1.328693>.
- 812 [52] T. Darden, D. York, L. Pedersen, Particle mesh Ewald: An $N \cdot \log(N)$ method for Ewald
813 sums in large systems, *J. Chem. Phys.* 98 (1993) 10089–10092.
814 <https://doi.org/10.1063/1.464397>.
- 815 [53] T. Kluyver, B. Ragan-Kelley, F. Pérez, B. Granger, M. Bussonnier, J. Frederic, K.
816 Kelley, J. Hamrick, J. Grout, S. Corlay, P. Ivanov, D. Avila, S. Abdalla, C. Willing,
817 Jupyter Notebooks—a publishing format for reproducible computational workflows,
818 *Position. Power Acad. Publ. Play. Agents Agendas - Proc. 20th Int. Conf. Electron.*
819 *Publ. ELPUB 2016.* (2016) 87–90. <https://doi.org/10.3233/978-1-61499-649-1-87>.
- 820 [54] J.D. Hunter, Matplotlib: A 2D graphics environment, *Comput. Sci. Eng.* 9 (2007) 90–

- 821 95. <https://doi.org/10.1109/MCSE.2007.55>.
- 822 [55] W. Humphrey, A. Dalke, K. Schulten, VMD: Visual Molecular Dynamics, *J. Mol.*
823 *Graph.* 14 (1996) 33–38.
- 824 [56] S.J. Klosterman, K. V. Subbarao, S. Kang, P. Veronese, S.E. Gold, B.P.H.J. Thomma,
825 Z. Chen, B. Henrissat, Y.-H. Lee, J. Park, M.D. Garcia-Pedrajas, D.J. Barbara, A.
826 Anchieta, R. de Jonge, P. Santhanam, K. Maruthachalam, Z. Atallah, S.G. Amyotte, Z.
827 Paz, P. Inderbitzin, R.J. Hayes, D.I. Heiman, S. Young, Q. Zeng, R. Engels, J. Galagan,
828 C.A. Cuomo, K.F. Dobinson, L.-J. Ma, Comparative Genomics Yields Insights into
829 Niche Adaptation of Plant Vascular Wilt Pathogens, *PLoS Pathog.* 7 (2011) e1002137.
830 <https://doi.org/10.1371/journal.ppat.1002137>.
- 831 [57] S. Mandelc, B. Javornik, The secretome of vascular wilt pathogen *Verticillium albo-*
832 *atrum* in simulated xylem fluid, *Proteomics.* 15 (2015) 787–797.
833 <https://doi.org/10.1002/pmic.201400181>.
- 834 [58] S.D. Liston, S.A. McMahon, A. Le Bas, M.D.L. Suits, J.H. Naismith, C. Whitfield,
835 Periplasmic depolymerase provides insight into ABC transporter-dependent secretion
836 of bacterial capsular polysaccharides, *Proc. Natl. Acad. Sci. U. S. A.* 115 (2018)
837 E4870–E4879. <https://doi.org/10.1073/pnas.1801336115>.
- 838 [59] J. Jenkins, R. Pickersgill, The architecture of parallel β -helices and related folds, *Prog.*
839 *Biophys. Mol. Biol.* 77 (2001) 111–175. [https://doi.org/10.1016/S0079-](https://doi.org/10.1016/S0079-6107(01)00013-X)
840 [6107\(01\)00013-X](https://doi.org/10.1016/S0079-6107(01)00013-X).
- 841 [60] M.D. Yoder, F. Journak, The Refined Three-Dimensional Structure of Pectate Lyase C
842 Implications for an Enzymatic Mechanism, *Plant Physiol.* 107 (1995) 349–364.
- 843 [61] Y. van Santen, J.A.E. Benen, K.H. Schroter, K.H. Kalk, S. Armand, J. Visser, B.W.
844 Dijkstra, 1.68-angstrom crystal structure of endopolygalacturonase II from *Aspergillus*
845 *niger* and identification of active site residues by site-directed mutagenesis, *J. Biol.*
846 *Chem.* 274 (1999) 30474–30480. <https://doi.org/10.1074/JBC.274.43.30474>.
- 847 [62] S.E. Lietzke, R.D. Scavetta, M.D. Yoder, The Refined Three-Dimensional Structure of
848 Pectate Lyase E from, *Plant Physiol.* 111 (1996) 73–92.
- 849 [63] B. Henrissat, S.E. Heffron, M.D. Yoder, S.E. Lietzke, F. Journak, Functional
850 implications of structure-based sequence alignment of proteins in the extracellular

- 851 pectate lyase superfamily., *Plant Physiol.* 107 (1995) 963–76.
852 <https://doi.org/10.1104/pp.107.3.963>.
- 853 [64] N. Kita, C.M. Boyd, M.R. Garrett, F. Jurnak, N.T. Keen, Differential Effect of Site-
854 directed Mutations in pelC on Pectate Lyase Activity, Plant Tissue Maceration, and
855 Elicitor Activity, *J. Biol. Chem.* 271 (1996) 26529–26535.
856 <https://doi.org/10.1074/jbc.271.43.26529>.
- 857 [65] S. Ali, C.R. Søndergaard, S. Teixeira, R.W. Pickersgill, Structural insights into the loss
858 of catalytic competence in pectate lyase activity at low pH, *FEBS Lett.* 589 (2015)
859 3242–3246. <https://doi.org/10.1016/j.febslet.2015.09.014>.
- 860 [66] C. Creze, S. Castang, E. Derivery, R. Haser, N. Hugouvieux-Cotte-Pattat, V.E.
861 Shevchik, P. Gouet, The Crystal Structure of Pectate Lyase PelI from Soft Rot
862 Pathogen *Erwinia chrysanthemi* in Complex with Its Substrate, *J. Biol. Chem.* 283
863 (2008) 18260–18268. <https://doi.org/10.1074/jbc.M709931200>.
- 864 [67] A. Dubey, S. Yadav, M. Kumar, G. Anand, D. Yadav, Molecular Biology of Microbial
865 Pectate Lyase: A Review, *Br. Biotechnol. J.* 13 (2016) 1–26.
866 <https://doi.org/10.9734/bbj/2016/24893>.
- 867 [68] H.G. Ouattara, S. Reverchon, S.L. Niamke, W. Nasser, Biochemical Properties of
868 Pectate Lyases Produced by Three Different Bacillus Strains Isolated from Fermenting
869 Cocoa Beans and Characterization of Their Cloned Genes, *Appl. Environ. Microbiol.*
870 76 (2010) 5214–5220. <https://doi.org/10.1128/AEM.00705-10>.
- 871 [69] M. Soriano, A. Blanco, P. Díaz, F.I.J. Pastor, An unusual pectate lyase from a Bacillus
872 sp. with high activity on pectin: Cloning and characterization, *Microbiology.* 146
873 (2000) 89–95. <https://doi.org/10.1099/00221287-146-1-89>.
- 874 [70] G. Chilosi, P. Magro, Pectin lyase and polygalacturonase isoenzyme production by
875 Botrytis cinerea during the early stages of infection on different host plants, *J. Plant*
876 *Pathol.* 79 (1997) 61–69. <https://doi.org/10.1080/01904167.2015.1112950>.
- 877 [71] S. Hassan, V.E. Shevchik, X. Robert, N. Hugouvieux-Cotte-Pattat, PelN is a new
878 pectate lyase of *dickeya dadantii* with unusual characteristics, *J. Bacteriol.* 195 (2013)
879 2197–2206. <https://doi.org/10.1128/JB.02118-12>.
- 880 [72] C. Zhou, Y. Xue, Y. Ma, Cloning, evaluation, and high-level expression of a thermo-

- 881 alkaline pectate lyase from alkaliphilic *Bacillus clausii* with potential in ramie
882 degumming, *Appl. Microbiol. Biotechnol.* 101 (2017) 3663–3676.
883 <https://doi.org/10.1007/s00253-017-8110-2>.
- 884 [73] W. Sukhumsirchart, S. Kawanishi, W. Deesukon, K. Chansiri, H. Kawasaki, T.
885 Sakamoto, Purification, Characterization, and Overexpression of Thermophilic Pectate
886 Lyase of *Bacillus* sp. RN1 Isolated from a Hot Spring in Thailand, *Biosci. Biotechnol.*
887 *Biochem.* 73 (2009) 268–273. <https://doi.org/10.1271/bbb.80287>.
- 888 [74] C. Zhang, J. Yao, C. Zhou, L. Mao, G. Zhang, Y. Ma, The alkaline pectate lyase
889 PEL168 of *Bacillus subtilis* heterologously expressed in *Pichia pastoris* more stable
890 and efficient for degumming ramie fiber, *BMC Biotechnol.* 13 (2013) 26.
891 <https://doi.org/10.1186/1472-6750-13-26>.
- 892 [75] P. Yuan, K. Meng, Y. Wang, H. Luo, P. Shi, H. Huang, T. Tu, P. Yang, B. Yao, A
893 Low-Temperature-Active Alkaline Pectate Lyase from *Xanthomonas campestris*
894 ACCC 10048 with High Activity over a Wide pH Range, *Appl. Biochem. Biotechnol.*
895 168 (2012) 1489–1500. <https://doi.org/10.1007/s12010-012-9872-8>.
- 896 [76] Y. Tang, P. Wu, S. Jiang, J.N. Selvaraj, S. Yang, G. Zhang, A new cold-active and
897 alkaline pectate lyase from Antarctic bacterium with high catalytic efficiency, *Appl.*
898 *Microbiol. Biotechnol.* 103 (2019) 5231–5241. <https://doi.org/10.1007/s00253-019-09803-1>.
- 900 [77] P. Wu, S. Yang, Z. Zhan, G. Zhang, Origins and features of pectate lyases and their
901 applications in industry, *Appl. Microbiol. Biotechnol.* 104 (2020) 7247–7260.
902 <https://doi.org/10.1007/s00253-020-10769-8>.
- 903 [78] Z. Zhou, Y. Liu, Z. Chang, H. Wang, A. Leier, T.T. Marquez-Lago, Y. Ma, J. Li, J.
904 Song, Structure-based engineering of a pectate lyase with improved specific activity for
905 ramie degumming, *Appl. Microbiol. Biotechnol.* 101 (2017) 2919–2929.
906 <https://doi.org/10.1007/s00253-016-7994-6>.
- 907 [79] M.D. Joshi, G. Sidhu, I. Pot, G.D. Brayer, S.G. Withers, L.P. McIntosh, Hydrogen
908 bonding and catalysis: A novel explanation for how a single amino acid substitution
909 can change the pH optimum of a glycosidase, *J. Mol. Biol.* 299 (2000) 255–279.
910 <https://doi.org/10.1006/jmbi.2000.3722>.
- 911 [80] T. Yasuda, H. Takeshita, R. Iida, M. Ueki, T. Nakajima, Y. Kaneko, K. Mogi, Y.

- 912 Kominato, K. Kishi, A single amino acid substitution can shift the optimum pH of
913 DNase I for enzyme activity: Biochemical and molecular analysis of the piscine DNase
914 I family, *Biochim. Biophys. Acta - Gen. Subj.* 1672 (2004) 174–183.
915 <https://doi.org/10.1016/j.bbagen.2004.03.012>.
- 916 [81] H. Shibuya, S. Kaneko, K. Hayashi, A single amino acid substitution enhances the
917 catalytic activity of family 11 xylanase at alkaline pH, *Biosci. Biotechnol. Biochem.* 69
918 (2005) 1492–1497. <https://doi.org/10.1271/bbb.69.1492>.
- 919 [82] M. Goetz, T. Roitsch, The different pH optima and substrate specificities of
920 extracellular and vacuolar invertases from plants are determined by a single amino-acid
921 substitution, *Plant J.* 20 (1999) 707–711. [https://doi.org/10.1046/j.1365-](https://doi.org/10.1046/j.1365-313X.1999.00628.x)
922 [313X.1999.00628.x](https://doi.org/10.1046/j.1365-313X.1999.00628.x).
- 923



Jérôme Pelloux/Fabien Sénéchal

UMR INRAE 1158 BioEcoAgro

BIOPI Biologie des Plantes et Innovation

UFR des Sciences

Université de Picardie Jules Verne

33 Rue St Leu

80039 Amiens, France

Tel : 03 22 82 75 40

jerome.pelloux@u-picardie.fr

fabien.senechal@u-picardie.fr

Prof. Aichun Dong

Editor in Chief

International Journal of Biological Macromolecules

University of Northern Colorado

Dear Prof. Dong,

Please find enclosed a revised version of the manuscript now entitled “The specificity of pectate lyase VdPelB from *Verticillium dahliae* is highlighted by structural, dynamical and biochemical characterizations”, by Safran *et al.* I would like to thank you and the International Journal of Biological Macromolecules for your interest in publishing our research.

We have carefully considered the reviewers’ comments and questions. You will find our comments to each specific point in the response to reviewers. Regarding suggested additional experiments made by reviewer#1 for having a full biochemical characterization, we indeed added some novel elements regarding to the temperature optimum, as well as K_m , V_{max} and k_{cat} of wild-type and mutant isoforms. We agree that more experiments could be done (ion-dependency...) but we initially aimed at a characterization of VdPelB in relation with its

structure and dynamics in complex with its substrate. We believe that it's highly original and highlight the specificities of the enzyme. We justified this in our responses to reviewers' comments.

In the same way, we notably changed title, modified figure colours, corrected misspellings, simplified some sections, added statistics and improved conclusion in the Ms.

We hope that this revised version of the manuscript and our responses to the reviewers' comments will now meet the standards for publishing in International Journal of Biological Macromolecules.

Looking forward to hearing from you soon

Kind regards



Fabien Sénéchal



Jérôme Pelloux

Response to reviewers

1. Are the objectives and the rationale of the study clearly stated?

Reviewer #1: Yes.

Reviewer #2: Yes

Reviewer #3: The objectives and the rationale of the study have been clearly stated.

Reviewer #4: The authors report first crystallographic structure of Verticillium pectate lyase (VdPelB) at 1.2Å resolution in the presence of Ca²⁺ ions and revealed that it is a right-handed parallel β-helix structure, Molecular dynamics (MD) simulations and biochemical characterization of wild type and mutated forms of VdPelB were also carried out by authors to identify key amino-acids for the activity and further highlight the dynamics of the enzyme in complex with substrates that vary in their degree of methylesterification and finally showed that VdPelB was most active on non-methylesterified pectins, at pH 8 in presence of Ca²⁺ ions.

Overall, the findings are remarkable and will be important to better understand the mechanism of the OGs generated by VdPelB from Verticillium-partially tolerant and Verticillium-sensitive flax cultivars showed that the enzyme could be a determinant of pathogenicity, as a function of pectin's structure.

2. If applicable, is the method/study reported in sufficient detail to allow for its replicability and/or reproducibility?

Reviewer #1: Mark as appropriate with an X:

Yes No N/A

Provide further comments here:

Reviewer #2: Mark as appropriate with an X:

Yes No N/A

Provide further comments here:

Reviewer #3: Mark as appropriate with an X:

Yes No N/A

Provide further comments here:

Reviewer #4: Mark as appropriate with an X:

Yes No N/A

Provide further comments here: yes the authors have reported it

3. If applicable, are statistical analyses, controls, sampling mechanism, and statistical reporting (e.g., P-values, CIs, effect sizes) appropriate and well described?

Reviewer #1: Mark as appropriate with an X:

Yes No N/A

Provide further comments here: See report.

Reviewer #2: Mark as appropriate with an X:

Yes No N/A

Provide further comments here:

1. Please provide P values where relative activities of the enzymes under different concentrations are compared. For example. when the authors state that the G125R has higher activity as compared to WT. Support of their data with P values would make their arguments stronger.

The statistics were done and symbols showing significant differences were added on the bar plots for relative activities, as well as for other graphs as suggested by the reviewer#2.

Reviewer #3: Mark as appropriate with an X:

Yes No N/A

Provide further comments here:

Reviewer #4: Mark as appropriate with an X:

Yes No N/A

Provide further comments here: The manuscript does not require additional peer review

4. Could the manuscript benefit from additional tables or figures, or from improving or removing (some of the) existing ones?

Reviewer #1: Yes.

Reviewer #2: Not required

Reviewer #3: No.

Reviewer #4: Tables and figures are well addressed

5. If applicable, are the interpretation of results and study conclusions supported by the data?

Reviewer #1: Mark as appropriate with an X:

Yes No N/A

Provide further comments here:

See report.

Reviewer #2: Mark as appropriate with an X:

Yes No N/A

Provide further comments here:

Reviewer #3: Mark as appropriate with an X:

Yes No N/A

Provide further comments here:

Reviewer #4: Mark as appropriate with an X:

Yes No N/A

Provide further comments here:

6. Have the authors clearly emphasized the strengths of their study/methods?

Reviewer #1: Yes.

Reviewer #2: The authors have used very standard methods.

Reviewer #3: Yes, the strengths of their study have been clearly emphasized.

Reviewer #4: The authors report first crystallographic structure of Verticillium pectate lyase (VdPelB) at 1.2Å resolution in the presence of Ca²⁺ ions and revealed that it is a right-handed parallel β-helix structure, Molecular dynamics (MD) simulations and biochemical characterization of wild type and mutated forms of VdPelB were also carried out by authors to identify key amino-acids for the activity and further highlight the dynamics of the enzyme in complex with substrates that vary in their degree of methylesterification and finally showed that VdPelB was most active on non-methylesterified pectins, at pH 8 in presence of Ca²⁺ ions.

Overall, the findings are remarkable and will be important to better understand the mechanism of the OGs generated by VdPelB from Verticillium-partially tolerant and Verticillium-sensitive flax cultivars showed that the enzyme could be a determinant of pathogenicity, as a function of pectin's structure.

Concerns:

1. The data collection for the crystals were carried out at a temperature of 100.15 °C (Table 1). Could you please elaborate this data collection at that temperature because there would be lot of radiation damage during the data collection at the reported temperature.

We thank the reviewer#4 for pointing out this mistake on the temperature used for X-Ray diffraction data collection of the crystal. Indeed, we apologize for omitting the minus symbol, the acquisition being realized at -100.15°C and not 100.15°C.

2. Authors can report the role of 18 aa at the N-terminus and 27 aa at the C-terminus that were not resolved because of poor electron densities by making the constructs without these residues and can characterize these mutants with respect to wildtype VdPelB.

We thank the reviewer #4 for this suggestion. While we do not see the N and C terminus of the protein in the X-ray diffracted structure we know that they are present in the purified enzyme as i) the right mass of the VdPelB is observed on SDS-PAGE, ii) the His-tag on C-terminus was used for IMAC purification. We think that these amino acids are not visible in the crystal structure as they are disordered and they do not form any alpha helixes or beta sheets. Considering that, we do not think that making constructs without these residues would be scientifically justified as it is known from previously published pectate lyase structures that these disordered parts do not play a role in the pectate lyase activity [1,2].

3. Did authors try to crystallize the VdPelB without Ca²⁺ ions because this can provide the crystal structure of VdPelB in inactive conformation.

We did not resolve the structure without Ca²⁺, since the Ca²⁺ comes from the yeast extract used in buffered complex methanol medium (Invitrogen) and it is incorporated in the protein structure during the expression process. Consequently, it is impossible to obtain crystal structure without Ca²⁺ because we cannot remove this ion from the media.

4. The text needs to be cross checked because there are misspellings of words like in the supplementary materials caption using 1 mL Ni NTA column but it is 1 mL Ni NTA column.

We thank reviewer #4 for highlighting some misspellings of words in the text. We have checked and corrected them.

7. Have the authors clearly stated the limitations of their study/methods?

Reviewer #1: See report.

Reviewer #2: The authors have used very standard methods.

Reviewer #3: See the comments to authors.

Reviewer #4: yes

8. Does the manuscript structure, flow or writing need improving (e.g., the addition of subheadings, shortening of text, reorganization of sections, or moving details from one section to another)?

Reviewer #1: Yes.

Reviewer #2: No. The manuscript is well organized into subheadings

Reviewer #3: See the comments to authors.

Reviewer #4: The authors need to check the spelling of words

9. Could the manuscript benefit from language editing?

Reviewer #1: Yes

Reviewer #2: Yes

Reviewer #3: Yes

Reviewer #4: Yes

Reviewer #1: Major issues:

- The title should be improved, and it should be pectate lyase VdPelB from *Verticillium dahlia*.
The title has been changed as suggested by reviewer #1

- Does it show additional salt bridges by the mutant V461K from MD analysis?

We have not done the V461K mutant.

- In the abstract, it shows "a plant pathogen", and these words are not necessary to highlight this work.

We removed these words in the abstract as mentioned by reviewer #1

- The descriptions of "pH 8", and "pH 9", e.g. are not an exact science. Should it show as pH7.0? pH 9.0? Please check them carefully throughout this paper.

We thank the reviewer #1 for this comment. It is true that pH7.0 is more exact science than pH 7. We carefully checked throughout the Ms for misspelled pH values.

- For a clear description of this work, some text which is shortened as VdPelB may be not easy to review, and it may be pectate lyase VdPelB.

VdPelB is the abbreviation for *Verticillium dahliae* pectate lyase B, but to further highlight the function of the enzyme for readers, we included pectate lyase before VdPelB, notably at the beginning of sentences.

- In keywords, Flax?

We initially added Flax as keyword since *Verticillium* is a pathogen of this plant. Moreover, we digested cell wall pectins from two Flax cultivars (Evea and Violin) to investigate the released OGs that are produced by VdPelB. Results show that there is a difference between the two cultivars. This is why we initially put this plant species as a keyword but, as mentioned by reviewer #1 flax being not the main interest in this publication, we agree to remove it.

- Line 108, *Verticillium dahliae* PLL?

We used the abbreviation PLL in this sentence since we compared all sequences retrieved from *Verticillium* and that are identified as putative Pectin lyase or Pectate lyase. PLL (Pectin lyase-like) is a generic term that includes both PLs (Pectate lyases) and PNLs (Pectin Lyases) [3]. In absence of fine biochemical characterization, we indeed do not know the specificity of each of the isoforms. Therefore, to mention all *Verticillium*'s sequences, PLL (PL and/or PNL) appears suitable. These abbreviations are mentioned in the introduction part.

- What's the abbreviation of aa?

aa abbreviation refers to amino acids. As this was not clear we have changed all aa abbreviations with the words amino acids.

- In section "2.2. Fungal strain and growth", is the shaken condition of 80 rpm suitable for the cultivation?

We indeed used 80 rpm for shaking condition. It is enough and suitable for developing this fungal strain.

- Line 128, *V. dahliae* PelB? What's the purpose of the SignalP-5.0 Server in this work?

SignalP-5.0 was used in this study to identify the putative signal peptide as mentioned, lines 112-113 of the revised manuscript. Thanks to this bioinformatic analysis, we later removed the nucleotides encoding amino acids related to signal peptide in order to (i) avoid any problems of protein secretion, since the vector used for heterologous expression already possess a sequence encoding a yeast signal peptide, and (ii) for producing a lyase without signal peptide since the mature enzymes working in the cell wall are known to be free of their signal peptide.

- How do the VdPelB mutants generate by expression in *P. pastoris*? The method of the generation of mutants is not clear. Should it first prepare in *E. coli*? Should each mutant be confirmed by DNA sequencing?

The cloning procedure for VdPelB and its mutants was followed as mentioned in EasySelect™ Pichia Expression Kit, Invitrogen. VdPelB mutants were generated using the specific mutation primers as followed: VdPelB DNA was amplified by VdPelB-native primers and gel purified. To generate the mutants, purified DNA was used as a template in a PCR reaction with VdPelB-native forward and for example VdPelB-G125R reverse primer (primer carrying mutation in the nucleotides for Gly). A second PCR reaction was carried with VdPelB-G125R forward primer (primer carrying mutation in the nucleotides for Gly) and VdPelB-native reverse primer. The

DNA fragments were gel purified and the third PCR reaction was carried out where we have annealed the two DNA fragment into one with G125R mutation. In this third PCR reaction only VdPelB-native forward and reverse primers were used. As the primers carried the restriction enzymes site (Pst1 and Not1) DNA was digested by specific enzymes, gel purified and ligated to the pPICZalphaB expression vector.

This vector was used to transform the *E.coli* cells which were used to obtain sufficient quantities of vector for *Pichia* transformation. Before *Pichia* transformation we have sent the vector for sequencing and after confirming that our vector indeed has a desired amino acid mutation we transformed *Pichia*. As this part was not sufficiently detailed in the manuscript, we added in the 2.3 section of the Ms some additional explanations.

- Section 2.8. Digestion of commercial pectins and released OGs profiling, the conditions for the separation of OGs should be clear. What's the flow rate?

The conditions used for LC-MS OG profiling were already described in a previous paper (Voxeur et al 2019) and further detailed in Safran et al 2021, both references being cited in the current manuscript. However, since reviewer #1 requires additional information related to the method with for instance the flow rate used, we added some elements in the 2.8 section of the Ms.

- For MD simulations of VdPelB protein and complex with a fully non-methyl esterified polygalacturonate decasaccharide or with a fully methylesterified polygalacturonate decasaccharide, should it first conduct the docking analysis? It is suggested to add docking studies to this work.

We thank the reviewer for the comment. With all its limitations, docking remains an effective technique to explore the binding of small molecule compounds to macromolecular targets. Nevertheless, this is more difficult to apply for big molecule such as decassacharide.

- Line 223, nPT? nVT? I think they should be NPT and NVT. Please check them through this submission.

We thank the reviewer for the comment and have now changed the capitalisation of "n" in the description of the ensembles.

- Section 3.2. Cloning, expression, and purification of VdPelB, some text could be moved to the method part.

As suggested by reviewer #1, some information was moved from section 3.2 to 2.3 of the method part. As a consequence, the title of section 3.2 was slightly changed and is now "Expression and purification of VdPelB".

- Section 3.2 can be merged with section 3.1.

We do not think that merging of the sections 3.1 and 3.2 improves the flow and the structure of the Ms. Consequently, and according to the previous comment, we simplified the section 3.2 but we did not merge the sections as suggested.

- Line 293, it is not clear to show the "poly-histidine tag".

We agree with the reviewer #1, poly-histidine tag is not crystal-clear denomination. Thus, we changed throughout the Ms by writing 6xHIS tag. The nucleotide encoding the 6XHIS tag are located in the sequence of the expression vector, pPICZalphaB. Thus, during the translation of the mRNA, this tag is fused at the C-terminus of VdPelB sequence to produce a tagged protein, which ease purification using IMAC and Western blot analysis with anti6xHIS antibody. The VdPelB mutants show the same tag since they were produced with the same expression vector.

- Does the putative VdPelB contain signal peptide?

As identified by bioinformatic analysis, VdPelB indeed contains a signal peptide, However, the *Pichia*-expressed VdPelB (native and mutated versions) do not contain any signal peptide, since, the signal peptide introduced by the expression vector, pPICZalphaB is cleaved during the enzyme secretion in culture media.

- In the method part, NetNGlyc 1.0 Server is used to analyze the glycosylation sites of VdPelB. However, no such result is discussed.

Indeed, we did not investigate in depth the N-glycosylation. However, we have used the NetNGlyc 1.0 Server to assess the presence of putative N-glycosylation sites in VdPelB.

Following the reviewer comment we have removed the NetNGlyc 1.0 Server from the method part, as no N-glycosylation of the protein was identified in the crystal structure.

- It claims that "the presence of 19 putative O-glycosylation sites, as predicted by NetOGlyc 4.0 Server.", and VdPelB is expressed in *P. pastoris* that glycosylation may easily be observed. There should be more evidence for this result. Could the VdPelB expressed by *P. pastoris* be stained using PAS?

As mentioned above for N-glycosylation, the predicted O-glycosylation of VdPelB first assessed using NetOGlyc 4.0 Server. The presence of putative O-glycosylation was further hypothesized after obtaining the SDS-PAGE which shows multiple bands which are likely to correspond to multiple glycosylated isoforms. However, we believe that PAS staining is not necessary as VdPelB was indeed confirmed as being O-glycosylated when analysing the crystal structure of the protein. This is discussed in section 3.2 and section 3.3 of the Ms.

- It is also concluded that "VdPelB had an apparent molecular mass of ~38 kDa". This is just an estimation, and it is suggested to show the MS data of VdPelB expressed by *P. pastoris*.

We did not analyze the secreted VdPelB protein by proteomic because (i) we previously sequenced the cDNA inserted in the expression vector used for heterologous expression, (ii) we revealed VdPelB on SDS-PAGE at the proper size using western blot with anti-6xHIS antibodies (since our protein is fused with 6xHIS tag, also used for purification), and (iii) we detected PL activity for our secreted/purified protein, knowing that none pectate/pectin lyases were identified in *Pichia pastoris*. Consequently, this activity comes from the secreted/purified protein of interest (VdPelB). Moreover, we obtained crystal structure of VdPelB from the purified extract that only contain pectate lyase, ultimately showing that we worked with the proper enzyme.

- Line 368, groove?

We thank the reviewer for seeing this misspelling. It is indeed groove and we changed it in the Ms.

- Table 2 could be moved to SI.

As suggested by the reviewer #1, we moved the table 2 in the SI, which is now table S3.

- The graphical abstract and Fig.S2, it may show that VdPelB is a dimer form. It is suggested to confirm this result by SEC or non-denaturing SDS-PAGE.

This comment is particularly relevant, thanks to the reviewer#1. However, it is not a dimer but simply two VdPelB molecules that closely crystallized in the same asymmetric unit (smallest portion of a crystal that provides the symmetry of the space group). Thus, this only relates to the crystallization conditions. Consequently, we did not check if a dimer can exist in native condition by SEC or non-denaturing SDS-PAGE.

- Is the G125 site close to active sites of VdPelB? What's the distance?

The C α of the G125 is 6.28 Å apart from the Ca²⁺ ion. However, the G125R mutant depending on the rotamer conformation show distances between 3 and 6 Å between the NH groups of arginine and Ca²⁺.

- It claims that "G125R mutant showed increased activity on PGA and switch in pH optimum from 8 to 9", does it show additional salt bridges around the pocket VdPelB of the mutant from MD analysis?

In the VdPelB-G125R, arginine has multiple possible rotamers, as it is surrounded mostly with glycine residues, making different conformation possible. While the exact mechanism of switch in pH optimum is not clear we think that arginine with high pKa which can interact in strong hydrogen bonding and complex electrostatic interactions within the active site, could change the optimal pH by acting on the protonation state of amino acids.

Regarding the salt bridges, by examining the structure there is a possibility that G125R makes a salt bridge contact between the NH groups and D122, the closest amino acid as the distance is between 3 and 6 Å.

- It claims that "G125R mutant showed increased activity on PGA and switch in pH optimum from 8 to 9", and it may be reasonable for the improvement of activity by the G125R mutant. How does the optimum

pH of VdPelB change from 8 to 9 only introduced by a single mutant? There should be more confirmations and citations.

We agree with the reviewer #1 that we did not elaborate sufficiently on how only one mutation in G125 could change the optimal pH. We thank the reviewer for the observation and are happy to dwell more into the observed differences, although MD simulations were not conducted on mutants, the observation on the WT dynamics informed experiments on potential mutations. While arginine holds obvious important differences with glycine, with a sidechain that contains both charged and hydrogen-bond donor/acceptor moieties, the differences observed in the activity of the mutated enzyme from pH 8 to 9 could be rationalised within the protonation behaviour of R125 sidechain. From pH 8 to 9, the population of an arginine partially solvent-exposure would change considerably, with numerous molecules now losing the charge. This would reduce the salt-bridging ability of the residue, in favour of h-bond accepting abilities. The effect of this change on the dynamics of the substrate and enzymatic activity is so far unknown, and holds an interesting question regarding the interplay between strong substrate-enzyme interactions along the binding groove, and weaker multivalent h-bond interactions that could facilitate processivity balancing sliding and dissociation rates. While this question is beyond the scope of this paper, we acknowledge that it could certainly be a topic for future investigation. We have added in the Ms additional explanations and literature citations, in total four papers, where a shift is observed when mutating a single amino acid in different types of enzymes.

- Fig.4 is hard to discern, please change the color or pattern of each figure, as well as Fig.S9.

We thank the reviewer for suggesting changes in the graphical representations. Indeed, colours can improve figures. We did modifications with additional colours for figure 4 as well as other figures that were previously only black, grey and white-coloured.

- The major concern is the biochemical characterization of VdPelB, and this submission does not present the normal biochemical characterization of VdPelB.

Indeed, the biochemical characterization could be completed with other analysis. However, in the current manuscript, we only focused on the main biochemical features of VdPelB such as substrate specificity, optimal temperature and pH for activity, Ca²⁺ dependency to correlate with protein structure and molecular dynamics simulation. Following the reviewer's suggestion we have determined VdPelB and VdPelB-G125R, Km (2.7 versus 4.8 mg.ml⁻¹), Vmax (79.1 versus 184.8 nmol of GalA.min⁻¹.µg⁻¹) and kcat (40.5 versus 70.9 s⁻¹). Additional data would indeed be interesting but we felt that it would not particularly improve our understanding of the mode of action of VdPelB in relation with the structure and the amino acids of importance for tuning enzyme's activity.

- Could an enzyme be characterized only by optimum temperature and pH?

It is true we might extend the biochemical characterization, but, as mentioned above, our multidisciplinary study, focused on the key parameters that we can correlate with structure and molecular dynamics. In addition, for temperature we focused on conditions relevant of the physiological conditions *in planta* (e.g. range of temperature for activity, which is moderated like that observed in fungi and plants).

- For the optimum temperature of VdPelB, the variables should be expanded. It should also select temperatures above 45°C and temperatures below 25°C.

Thanks for this comment. We did not initially assay the activity at temperatures below 25°C and above 45°C to stay in the physiological range. However, as requested by reviewers 1 and 2, we expanded the temperature range from 20 to 70°C for VdPelB and VdPelB-G125R and the data are presented in Fig. S8. While VdPelB shows higher activity on 20°C both enzymes start to lose activity at 60 and 70°C.

- Please re-confirm the pH scope of Tris-HCl, and it usually shares a good ability for buffer usage ranging from 7.0 to 9.2. It should select another kind of buffer for the optimum pH of VdPelB when the pH is above 9.5. Please check it carefully.

As pectins are not easily solubilized in the Glycine-OH buffer usually used for pH values above 9.5, we used the Tris-HCl buffer for assays up to pH10.0 as pectin solubility in this buffer is better. It is true that it is not the optimum buffer for these pH values, but it was the best way to assay the activity for pH values above 9.5.

- It is recommended to show the results of different ions on the activities of VdPelB for biochemical characterization.

We agree with the reviewer#1, that the biochemical characterization of VdPelB is not as complete as it could be, with numerous experiments that could be conducted. However, as mentioned above, our initial aim was to relate the structure of the enzymes to some key biochemical and dynamical characteristics. However, we now included some additional results that could be of interest for a broader panel of scientists. Thus, we added in the Ms some additional data (Km, Vmax, kcat and broader temperature optimum.).

- It should add the pH stability and thermal stability of VdPelB for the biochemical characterization.

We agree with the reviewer #1. While we did not add pH stability and thermal stability of VdPelB for the biochemical characterization new data regarding the Km, Vmax, kcat and broader temperature optimum are available.

- For the biochemical characterization of VdPelB and its mutant, Ca²⁺ should be added to the buffer system.

Ca²⁺ was added in the buffer for both native and mutants isoforms of VdPelB. We added this information in all figure legends and specified this in the method section.

- Could Ca²⁺ affect the secondary structure of VdPelB? It should supply the CD data with or without Ca²⁺ addition.

This is an interesting comment. While we don't exactly know if Ca²⁺ affects the secondary structure we can observe on the Fig. S7 that our enzyme is well folded and active at low Ca²⁺ concentration. Binding of Ca²⁺ could affect protein structure mostly the position of the amino acid sidechains in the active site as no other calcium binding site is seen on the VdPelB structure.

- For the MD results, the free binding energy of the complexes should be analyzed.

We thank the reviewer for the comment. However, we note that what the reviewer is pointing at it is something that suffers of considerable methodological limitations due to the nature of the investigated system. The understanding of the binding-free energy from simulations can more easily be achieved for small-molecule compounds bound to protein targets (and even that is not granted at a reasonable level of accuracy), which have much lower degrees of freedom compared to a carbohydrate oligomer. Due to the numerous degrees of freedom of HG chains and the large substrate-enzyme binding interface in carbohydrate binding enzymes, a collective variable that would allow a meaningful investigation of binding free energy with robust MD simulation methods is still unknown and an investigation of binding free energies would first require finding what are the relevant degrees of freedom for HB unbinding.

This make a different and purely computational project. On the other hand, we also notice that the different possible methylesterification and acetylation states of each monomer along a HG oligomer, call for a combinatorial investigation after the identification of the collective variable best describing dissociation. We also consider that dissociation of the enzyme from a oligosaccharide does not necessarily grant (whenever it could become methodologically achievable) identity with dissociation from a longer HG chains as most likely found in experiments. For this reason, we would like the reviewer to consider that the assessment of accurate binding free energies is beyond the scope of this work and could be pursued in future investigations.

- The method of LC-MS/MS should be included.

We initially did not develop in detail the method used for LC-MS/MS since it was already described in Voxeur et al 2019 as well as Safran et al 2021, both cited in our current manuscript. We however added some additional elements in the Material and Methods section 2.8.

- The model of LC-MS/MS should be marked in Fig. S11 & Fig.S12.

Thank you for this suggestion. We have used the ACQUITY UPLC Protein BEH size exclusion chromatography (SEC) column (125 Å, 1.7 µm, 4.6 X 300 mm; Waters) for OG separation. MS detection were performed using an ACQUITY UPLC H-Class system coupled to a SYNAPT G2-Si-Q- TOF hybrid quadrupole time-of-flight instrument (Waters) equipped with an electrospray

ionization (ESI) source (Z-spray) and an additional sprayer for the reference compound (lock spray). Samples were analysed by ESI-high-resolution MS (HRMS) and MS/MS in negative ionization mode. Data acquisition and processing were performed with MASSLYNX software (v.4.1; Waters). This data is now added to the M&M section 2.8 and in Fig. S11 & Fig.S12 caption.

- In addition, do not start sentences with abbreviations. Please check and revise them carefully.

We thank reviewer #1 for this comment. We changed the text, notably by adding "The" or "pectate lyase" before VdPelB when starting a new sentence.

- The discussion and conclusion leave much to be desired, and conclusions should be improved carefully.

We thank reviewer#1 for his comment and the need for improving the discussion and conclusion. As suggested, we modified accordingly the manuscript.

- The typescript of this text suffers from a number of problems. Please check them carefully.

We did the modifications for spelling problems identified following the reviewer's comments.

Reviewer #2:

"The structural, dynamical and biochemical characterizations of *Verticillium dahlia* pectate lyase, VdPelB, highlight its specificities."

Josip Safran, Vanessa Ung, Julie Bouckaert, Olivier Habrylo, Roland Molinié, Jean-Xavier Fontaine, Adrien Lemaire, Aline Voxeur, Serge Pilard, Corinne Pau-Roblot, Davide Mercadante, Jérôme Pelloux, Fabien Seneschal

The manuscript describes the pectate lyase, VdPelB, from *Verticillium dahlia* in terms of its structure, biochemical properties as well as the dynamics of its substrate interactions. The authors very methodically describe the biochemical properties and specificities of the enzyme in terms of its structure and amino acid composition. They have used mutants to clearly explain the observed properties of the wild type enzyme. It is a well-designed study, executed very methodically, and represented well in the manuscript. It is indeed an extensive study on the enzyme and does shed light on the pathogenicity determinants and could prove useful in designing inhibiting pathogenicity.

I have a few minor points that, if addressed, would greatly improve the manuscript. They are as follows:

1. The manuscript lacks statistical analysis. Some statistical analysis while comparing the activities in the manuscript would make the authors' arguments much stronger. They can just provide the P values for each comparison. For example, when they state that the G125R mutant has higher activity than the wild type enzyme, a P value there would make it more appropriate. Please incorporate statistical analysis.

We thank reviewer#2 for this relevant comment. We have consequently statistically analyzed data for all figures where bar plots are presented. The significant differences thus appear as *, ** and * marks, according to the significance. Moreover, information about statistical test are indicated in the method part as well as in the figure legends.**

2. The authors have mentioned performing homology modelling in the methods section, but nothing is mentioned about that anywhere later in the manuscript. If it has not been used further, it could be removed from the manuscript.

We have indeed mentioned homology modelling as it is a required step when solving the crystal structure. After crystal diffraction, the electron densities map is not sufficient to obtain the protein structure and we need to use a homology model to solve the phase problem in the molecular replacement step of structure solving. We have added the explanation in section 2.1.

3. Page 6, Line 141: "large beamlike crystals" What do the authors mean exactly? They can simply mention the dimensions of the crystals that they obtained and used for data collection.

We thank the reviewer#2 for this comment. We have included the crystal size (120 µm x 30 µm) into the manuscript.

4. Page 7: Sections 2.8 and 2.9 are the same; they have been duplicated. Please correct it.

Thanks for this comment. Indeed, we did not see that this section was duplicated. We consequently removed one of the duplicates.

5. Page 17, Figure 3: the color boxes legend on the figure reads "methyesterified" instead of "methylesterified", missing the l. Please correct this.

We corrected this spelling error.

6. The temperature dependence graph (Figure S8) does not show much difference in activity between the different temperatures studied. Have the authors gone beyond 45oC? If yes, and they show significantly lower values, it would be better to show those values in the plot.

As suggested also by the first reviewer we increased the temperature range (20 to 70°C) for activity and changed the Fig. 4 in consequence.

7. Figure S1: For the mutants, the ladder should be shown for each gel. The authors should run a new gel with the ladder and all the purified wild type and mutants in the same gel and provide that gel picture. This gel is not convincing without the side by side ladder on the same gel.

We agree with the reviewer #2. Thus, to simplify the Figure S1, we did a new SDS-PAGE with all version of the VdPelB and the ladder on the same gel. You can now see it on the new Fig S1.

8. Page 19, Lines 464-465: The first sentence of section 3.8 requires grammatical correction.

We thank the reviewer #2 for highlighting this spelling problem in the sentence. We did the modification in the manuscript.

9. Page 19, Line 473: "the activity of G125R mutant was increased by circa 50% at pH9 and pH10". This statement of increase in activity by 50% is not a correct representation of the data. They should consider stating the fold increase, such as " it was doubled".

We agree the sentence is not perfectly consistent with the data. We modified it in the manuscript as suggested by reviewer#2.

10. Page 20, Line 495: Delete "were"

We did the modification as suggested.

11. Page 20, line 503: "of AsPel, which act as well as an endo-PL" needs correction.

Thanks for this comment. We indeed changed the sentence to be clearer in our statement.

12. Page 25, line 557: delete "of" from "digestion products of showed that VdPelB" This field is optional. If you have any additional suggestions beyond those relevant to the questions above, please number and list them here.

We modified the text as suggested by reviewer#2

Reviewer #3:

In this work, the authors conducted a detailed analysis of *Verticillium dahliae*, starting from the bacterium's physiological structure, and explored its biological composition and secondary structure simulation through chemical means. As a phytopathogenic pathogen, this work provides some powerful ideas for the study of *Verticillium dahliae*. Especially for the design of antibacterial materials, it has certain inspiration for its microbial targeting property. Therefore, we believe that the starting point of this work is of extraordinary significance. The paper is concise and clear, the topic is prominent, and the subject matter fully satisfies the journal's publication requirements. Furthermore, I recommend publishing it after a few minor revisions. My detailed comments are listed below.

1. It is recommended that the authors add a chapter to the main text to specifically introduce the characteristics of "*Verticillium dahliae*", including appearance, metabolism, pathogenicity, etc. with a simple schematic.

We thank reviewer #3 for his suggestion and we have indeed added some supplementary information in the introduction (lines 91-95). However, we did not include all information related to the appearance, metabolism, pathogenicity as suggested, as our work is mainly focused on the enzymes that are secreted from the *Verticillium dahliae*, rather than on the fungus per se.

2. The author preliminarily verified the pathogenic mechanism of the pathogen in this work, and this conclusion is very reliable, but the author did not propose a solution for how to kill or inhibit the pathogen. I hope the author can give some treatment plans for the bacteria based on the conclusions.

Yes, indeed we did not include any suggestion on how to kill or inhibit the pathogen as it was not the initial scope of this manuscript. We were indeed focusing on the enzymes that are produced by Verticillium and not on the fungus itself. While the reviewer #3 question is interesting we won't be able to address it in the current Ms. However, we suggested in the conclusion that the OG that differed between sensitive and resistant flax cultivars could be of interest for defining strategies to improve plants' resistance to pathogens.

3. The author revealed the relationship between pectinase and pathogenic bacteria, and hoped that the author could briefly prospect the application of pectinase in inhibiting the persecution of pathogenic bacteria.

We are not sure to understand what reviewer#3 refers to as we did not work with pathogenic bacteria.

Reviewer #4:

This field is optional. If you have any additional suggestions beyond those relevant to the questions above, please number and list them here.

Literature

- [1] R.D. Scavetta, S.R. Herron, A.T. Hotchkiss, N. Kita, N.T. Keen, J.A.E. Benen, H.C.M. Kester, J. Visser, F. Journak, Structure of a plant cell wall fragment complexed to pectate lyase C, *Plant Cell*. 11 (1999) 1081–1092. <https://doi.org/10.1105/tpc.11.6.1081>.
- [2] N. Kita, C.M. Boyd, M.R. Garrett, F. Journak, N.T. Keen, Differential Effect of Site-directed Mutations in pelC on Pectate Lyase Activity, Plant Tissue Maceration, and Elicitor Activity, *J. Biol. Chem.* 271 (1996) 26529–26535. <https://doi.org/10.1074/jbc.271.43.26529>.
- [3] O. Mayans, M. Scott, I. Connerton, T. Gravesen, J. Benen, J. Visser, R. Pickersgill, J. Jenkins, Two crystal structures of pectin lyase A from *Aspergillus* reveal a pH driven conformational change and striking divergence in the substrate-binding clefts of pectin and pectate lyases, *Structure*. 5 (1997) 677–689. [https://doi.org/10.1016/S0969-2126\(97\)00222-0](https://doi.org/10.1016/S0969-2126(97)00222-0).



Click here to access/download

Supplementary Material

20221228_Ms_VdPeIB_Supplementary materials
caption_revision.pptx



Declaration of interests

The authors declare that they have no known competing financial interests or personal relationships that could have appeared to influence the work reported in this paper.

The authors declare the following financial interests/personal relationships which may be considered as potential competing interests:

Safran Josip reports financial support was provided by Conseil Régional Hauts-de-France. Safran Josip reports financial support was provided by Fonds européen de développement régional.